

**A Comparison Between Surface Electromyography and Acceleromyography for Virtual
Upper Extremity Spasticity Assessments in Stroke Patients**

by

Valerie Nadeau

A thesis submitted in partial fulfillment of the requirements for the degree of

Master of Science

in

Rehabilitation Science

Faculty of Rehabilitation Medicine

University of Alberta

© Valerie Nadeau, 2024

Abstract of Thesis

Background: Many elements currently hinder the accessibility to spasticity assessments, such as living rurally or limited mobility. Without access to appropriate care for the assessment and management of spasticity, a patient's quality of life may be compromised. Electromyography (sEMG) is a potential technique for objective and virtual evaluations of spasticity because of its capacity to extract useful biomechanical information about spasticity. However, there is a need to identify a suitable alternative to sEMG because of its electrical interference and other obstacles that could affect the signal quality if it is misused in a telehealth setting. Acceleromyography (AMG) is a promising alternative sensor due to its ease of use and the potential to overcome barriers to virtual spasticity assessments. It remains to be seen whether the AMG sensor is similar to the sEMG in terms of the information it can give regarding muscle activity for spasticity assessments.

Objectives: The study intends to investigate whether the sEMG and AMG sensors are comparable in gathering information on muscle activity to give clinicians information on muscular spasticity in a virtual environment in the upper extremities. The purpose of this study is to simultaneously compare the biomechanical data that sEMG can acquire regarding muscle activity during active and passive motions to that of AMG for those with and without muscle spasticity.

Methods: The literature review section of the thesis is covered in the second chapter to determine which significant barriers sEMG currently has in telehealth and if these have been overcome. The initial search allowed for assessing the obstacles to virtual sEMG discovered thus

far and how researchers have come up with solutions to overcome them. Furthermore, the design process of the portable device, which is based on Daniel Gillespie's earlier device, the TONE device, is described in depth in Chapter 3. The device was designed based on what clinicians currently need for spasticity assessments with the goal of providing clinically relevant data. In addition, using the portable device designed to compare these two sensors simultaneously, chapter 4 used a muscle fatigue and reliability tests on a population of participants without spasticity to determine if these gave similar information on the ability to pick up slow and fast fibres. Upper extremity patients with spasticity after a stroke were the intended population for this study. Once it was concluded that the two sensors were comparable in their ability to pick up slow and fast fibres, their signals were compared using the affected and non-affected arms on patients with spasticity during active and passive movements to determine if they obtained similar characteristics that could be used to assess muscle spasticity.

Results: Due to the large volumes of data that sEMG requires to process and its high bandwidth requirement, the most frequently mentioned barrier in the literature review was the unreliability of real-time data. Cybersecurity and poor user-friendliness were two further significant barriers. Few articles offer ways to improve inadequate real-time data, which suggests that no approaches have been effectively used. Prior training before virtual assessments was a common strategy used in the studies to address barriers to usability. Using the designed portable device in chapter 3 to compare the simultaneous data obtained from sEMG and AMG, it was discovered that AMG's ability to identify slow and fast fibres is similar to that of sEMG. Additionally, sEMG and AMG were comparable in the way they could identify and distinguish particular spasticity characteristics in the affected arm of individuals with spasticity after a stroke. Among these were

the low signal-to-noise ratio and the lack of fast fibres in power spectra during active movements.

Conclusion: Based on its capacity to provide information on muscle contractions and its lack of barriers, the research suggests that AMG is an excellent alternative to sEMG. However, to provide healthcare professionals with adequate insight into the severity of spasticity and to enable them to establish appropriate treatment and care plans, it is crucial to emphasize the need for future research. This research should focus on enabling the development of a new, standardized method for conducting these assessments, thereby engaging healthcare professionals in the ongoing research process.

Preface

This thesis is the original work of Valerie Nadeau. The research conducted for this thesis received ethics approval from the University of Alberta Research Ethics Board, Project Name “Development and clinical validation of remote assessment for post-stroke spasticity,” Pro00129191, 4/3/2023.

The materials in this thesis are original research conducted at the Rehabilitation Robotics Lab at the University of Alberta and the Glenrose Rehabilitation Hospital. The research study was led by supervisor Dr. Martin Ferguson-Pell. The device developed in this thesis was designed, developed and programmed by Dr. Martin Ferguson-Pell with the assistance of Yousef Moussa. The device was designed based on the previous device (TONE device) by Daniel Gillespie, a prior Ph.D. student in Rehabilitation Sciences at the University of Alberta. Valerie Nadeau designed the research protocols for all three study portions with the assistance of Dr. Martin Ferguson-Pell. The data collection and analysis in Chapter 4 contain original work by Valerie Nadeau. Dr. Martin Ferguson-Pell assisted with writing the MATLAB code necessary for the data analysis portion of the thesis.

Chapter 2 of this thesis has been previously published in the Telemedicine and eHealth Journal as “Identifying and Overcoming the Barriers to Virtual Electromyography Assessments: A Scoping Review” Telemedicine and e-Health Journal, vol. 30, issue 2, 354-363. Secondary authors of this paper include Emmanuella Osuji, MSc; Martin Ferguson-Pell, PhD and Liz Dennett, MLIS. I was responsible for creating the original draft, review and editing; methodology; validation; formal analysis; investigation. E.O. contributed to methodology;

validation; investigation. M.F-P. contributed to review and editing; conceptualization; and supervision. L.D. contributed to review and editing; methodology; resources.

The content in chapters 1, 3, 4 and 5 are original work of Valerie Nadeau and have not been previously published.

Since the thesis is based on independent manuscripts, there may be some repetition in the introduction sections of these chapters.

Dedication

This thesis is dedicated to my parents and brother, who have always supported me through all my milestones, big or small. I would not be where I am today without them.

Acknowledgements

I would like to acknowledge the people who have contributed significantly to making this research successful.

First, I would like to thank my supervisor, Dr. Martin Ferguson-Pell, who made all this possible. I could not have asked for a better supervisor who has offered me tremendous support. Whether it be the countless hours spent getting the technology to work adequately or helping me finalize my thesis, he was always there, no matter the support I required! His encouragement, patience, and mentorship made this a great learning experience. Dr. Martin Ferguson-Pell was an excellent teacher throughout my master's degree, from whom I have learned many skills as a researcher with him as my supervisor.

I would also like to thank my committee members, Dr. Jessica D'Amico and Dr. Lalith Satkunam, for all the time and efforts they put into ensuring I was able to collect enough data on patients with spasticity at the Glenrose Rehabilitation Hospital to meet my thesis timeline requirements. Additionally, they have given me excellent advice, feedback, and guidance, ensuring that I get a more holistic view of my research.

I would also like to thank Yousef Moussa for his assistance in building the different versions of the portable device used in this study using printer circuit boards. Executing this was a challenging task, and I thank Yousef for his hard work and determination.

Furthermore, I would like to thank Khilesh Jairamdas, who helped design the real-time data dashboard. Khilesh was always there to help if I had any questions. I really appreciate all his hard work and assistance.

Also, I would like to thank Jordan Gainor and Zhiyuan (Mike) Yang, who spent countless hours helping me prepare for my data collection and also helped me collect data at the Glenrose Rehabilitation Hospital. They always offered help when I needed it, and the data collection process would only have gone as smoothly with their assistance.

Additionally, I would like to thank everyone at the Rehabilitation Robotics Lab for not only never hesitating to volunteer to help me with any part of my study, whether that be testing out the device to help ensure it runs smoothly before data collection or helping me collect meaningful data, but also for always encouraging me through it all.

I would also like to thank NSERC CREATE in Sensory-Motor Adaptive Rehabilitation Technologies (SMART) for funding this project (NSERC ID number 436403993).

Lastly, an immense thank you to all the students, patients, and participants who volunteered to take part in this research study. My research would not have been possible without you.

Table of Contents

<i>Abstract of Thesis</i>	<i>ii</i>
<i>Preface</i>	<i>v</i>
<i>Dedication</i>	<i>vii</i>
<i>Acknowledgements</i>	<i>viii</i>
<i>List of Tables</i>	<i>xiii</i>
<i>List of Figures</i>	<i>xiv</i>
<i>List of Abbreviations</i>	<i>xvi</i>
<i>Chapter 1. Introduction</i>	<i>1</i>
<i>1.1 Background on Stroke and Spasticity</i>	<i>1</i>
<i>1.2 Physiology of Muscle Contractions</i>	<i>2</i>
<i>1.2.1 Types of Muscle Contractions</i>	<i>4</i>
<i>1.2.2 Active and Passive Movements</i>	<i>5</i>
<i>1.3 Pathophysiology of Spasticity</i>	<i>5</i>
<i>1.4 Current In-Person Spasticity Assessments</i>	<i>6</i>
<i>1.4.1 Scales to Measure Spasticity</i>	<i>7</i>
<i>1.5 The Need for Objective Measurements</i>	<i>9</i>
<i>1.6 The Need for Virtual Spasticity Assessments</i>	<i>10</i>
<i>1.7 Surface Electromyography for Objective and Virtual Spasticity Assessments</i>	<i>12</i>
<i>1.7.1 Signal Origin</i>	<i>13</i>
<i>1.7.2 Barriers to sEMG</i>	<i>13</i>
<i>1.8 Acoustic (Mechano-) Myography as an Alternative</i>	<i>14</i>
<i>1.8.1 Types of Acoustic (Mechano-) Myography</i>	<i>15</i>
<i>1.8.2 Appropriate Transducer for Virtual Spasticity Assessments</i>	<i>16</i>
<i>1.9 Research Statement, Questions and Objectives</i>	<i>16</i>
<i>1.10 Relevance of Research</i>	<i>17</i>
<i>1.11 Structure of the Thesis</i>	<i>18</i>
<i>Chapter 2. Identifying and Overcoming the Barriers to Virtual EMG Assessments: A Scoping Review</i>	<i>19</i>
<i>2.1 Abstract</i>	<i>19</i>
<i>2.2 Introduction</i>	<i>20</i>
<i>2.3 Methods</i>	<i>21</i>
<i>2.3.1 Search Strategy</i>	<i>21</i>
<i>2.3.2 Inclusion and Exclusion Criteria</i>	<i>22</i>
<i>2.3.3 Study/Source of Evidence Selection</i>	<i>23</i>
<i>2.3.4 Data Extraction</i>	<i>23</i>

2.4 Results.....	24
2.4.1 Article Characteristics.....	25
2.4.2 Barriers to Conduction sEMG Assessments Virtually	28
2.4.3 Overcoming Barriers to Conducting sEMG Assessments Virtually	30
2.5 Discussion.....	34
2.5.1 Barriers to Virtual sEMG Assessments.....	35
2.5.2 Overcoming the Barriers to Virtual sEMG Assessments	37
2.6 Strengths and Limitations.....	39
2.7 Conclusion.....	41
Chapter 3. Development of a Portable Device for Virtual Spasticity Assessments	43
3.1 Introduction.....	43
3.2 Clinical Context.....	46
3.2.1 sEMG, Goniometer and Force Sensor to Replace the MAS or MTS	46
3.2.2 AMG Sensor as an Alternative to sEMG	48
3.3 Objectives of the Development of the Device	50
3.3.1 Real-Time Data	50
3.3.2 Raw Data Storage on an SD card.....	50
3.3.3 AMG as an Alternative Sensor	51
3.4 Device Development.....	51
3.4.1 Hardware Development	51
3.4.2 Firmware Development.....	56
3.4.3 Dashboard Interface	57
3.5 Discussion.....	59
3.6 Conclusion.....	61
Chapter 4. Comparison of EMG and AMG Using a Portable Device Designed for Virtual Spasticity Assessments	62
4.1 Introduction.....	62
4.1.1 Slow and Fast Fiber Types	63
4.1.2 Muscle Fibre Type Changes in a Spastic Muscle	63
4.1.3 sEMG Slow and Fast Fibre Detections on Power Spectra.....	64
4.1.4 Acoustic (Mechano-) Myography Sensors as an Alternative to sEMG	65
4.1.5 Purpose and Objectives	66
4.2 Methodology.....	68
4.2.1 Optimal Sensor Placement Location	68
4.2.2 Muscle Fatigue Test.....	70
4.2.3 Reliability Test.....	73
4.2.4 Test on Patients With Post-stroke Spasticity.....	75
4.3 Results.....	77
4.3.1 Muscle Fatigue Test.....	77
4.3.2 Reliability Test.....	83

4.3.3 Test on Patients With Post-stroke Spasticity	84
4.4 Discussion.....	90
4.4.1 Muscle Fatigue Test	90
4.4.2 Reliability Test	93
4.4.3 Test on Patients With Post-stroke Spasticity	95
4.5 Limitations.....	97
4.6 Conclusion.....	98
Chapter 5. Thesis Discussion and Conclusion	99
5.1 Summary of Findings	99
5.2 Implications of Findings.....	104
5.3 Conclusion.....	106
References	108
Appendices.....	125
Appendix 1. Ethics Approval	125
Appendix 2. Search Strategy.....	125
Appendix 3. Component Parts of Designed Portable Device	126
Appendix 4. Arduino Firmware Code for Designed Portable Device	127
Appendix 5. MATLAB Code for Power Spectra	152
Appendix 6. MATLAB Code for Rectified Data	157
Appendix 7. MATLAB Code for Signal-to-noise Ratio	161

List of Tables

<i>Table 1. Summary of the parameters use to evaluate spasticity when using the MAS.....</i>	<i>8</i>
<i>Table 2. Summary of the parameters use to evaluate spasticity when using the MTS.</i>	<i>9</i>
<i>Table 3. Country in which the study was conducted in the included texts.</i>	<i>27</i>
<i>Table 4. Description of the study setting.</i>	<i>27</i>
<i>Table 5. Types of participants.</i>	<i>27</i>
<i>Table 6. Barriers to virtual EMG assessments.</i>	<i>30</i>
<i>Table 7. Ways to overcome barriers in virtual EMG assessments.</i>	<i>34</i>
<i>Table 8. Summary of the significance values for each different test of the repeated measures ANOVA.....</i>	<i>80</i>
<i>Table 9. Summary of the coefficient of variation for each different test.....</i>	<i>84</i>
<i>Table 10. Summary of participant characteristics.</i>	<i>86</i>
<i>Table 11. Summary of the slow and fast fiber frequency of sEMG for the affected and non-affected arm of each participant.....</i>	<i>86</i>
<i>Table 12. Summary of the slow and fast fiber frequency of AMG for the affected and non-affected arm of each participant.....</i>	<i>86</i>
<i>Table 13. Summary of the signal to noise ratios of sEMG for the affected and non-affected arm of each participant.....</i>	<i>87</i>
<i>Table 14. Summary of the signal to noise ratios of AMG for the affected and non-affected arm of each participant.....</i>	<i>87</i>

List of Figures

<i>Figure 1. Preferred Reporting System for Systematic Reviews and Meta-Analysis diagram of the screening process.....</i>	<i>25</i>
<i>Figure 2. Number of published articles per year in the included texts.....</i>	<i>28</i>
<i>Figure 3. Overview of the portable device and its component parts.</i>	<i>52</i>
<i>Figure 4. Overview of the inside of the force sensor. The arrows show the two sensors used on the board (SEN-10245) and the signal conditioning board (MIKROE-4658 by MicroElektronika (Belgrade).</i>	<i>53</i>
<i>Figure 5. Side view of the force sensors. Two plexiglass sheets, sealed with regular caulking silicon, contained the two sensors inside.....</i>	<i>53</i>
<i>Figure 6. Summary of the steps in which the wearable device sends data to be received on the SD card and the Dashboard wirelessly in circuit 1. The orange boxes indicate the receiving and transmitting sequence. The blue boxes indicate the end device for collecting and obtaining data.</i>	<i>55</i>
<i>Figure 7. Summary of the steps in which the sEMG and AMG sensor data were transmitted to the microcontrollers.....</i>	<i>56</i>
<i>Figure 8. Representation of the real-time data available and shown by the Dashboard.....</i>	<i>59</i>
<i>Figure 9. Rectified sEMG and AMG against time during isometric contraction for a MVC in the lower bicep.</i>	<i>69</i>
<i>Figure 10. Rectified sEMG and AMG against time during isometric contraction for a MVC in the upper bicep.</i>	<i>70</i>
<i>Figure 11. Demonstration of how the frequency and amplitude values were recorded using MATLAB for the sEMG power spectrum.</i>	<i>73</i>
<i>Figure 12. Demonstration of how the frequency and amplitude values were recorded using MATLAB for the AMG power spectrum.....</i>	<i>73</i>
<i>Figure 13. Mean sEMG amplitude ratios over five epochs while the muscle is being fatigued in a sample of 10 participants. The contraction was divided into five equal epochs.....</i>	<i>80</i>
<i>Figure 14. Mean sEMG frequency ratios over five epochs while the muscle is being fatigued in a sample of 10 participants. The contraction was divided into five equal epochs.....</i>	<i>81</i>
<i>Figure 15. Mean AMG amplitude ratios over five epochs while the muscle is being fatigued in a sample of 10 participants. The contraction was divided into five equal epochs.....</i>	<i>81</i>
<i>Figure 16. Mean AMG frequency ratios over five epochs while the muscle is being fatigued in a sample of 10 participants. The contraction was divided into five equal epochs.....</i>	<i>82</i>
<i>Figure 17. Side-by-side comparison of the linear regression for the frequency ratio change per epoch for the sample of all 10 participants for both the sEMG and AMG sensors.....</i>	<i>82</i>

Figure 18. Side-by-side comparison of the linear regression for the amplitude ratio change per epoch for the sample of all 10 participants for both the sEMG and AMG sensors.....83

Figure 19. Rectified amplitude of the affected arm of the first participant. The top graph represents the sEMG signal and bottom graph represents the AMG signal.....87

Figure 20. Rectified amplitude of the non-affected arm of the first participant. The top graph represents the sEMG signal and bottom graph represents the AMG signal.....88

Figure 21. Rectified amplitude of the affected arm of the second participant. The top graph represents the sEMG signal and bottom graph represents the AMG signal.....88

Figure 22. Rectified amplitude of the non-affected arm of the second participant. The top graph represents the sEMG signal and bottom graph represents the AMG signal.....89

Figure 23. Rectified amplitude of the affected arm of the third participant. The top graph represents the sEMG signal and bottom graph represents the AMG signal.....89

Figure 24. Rectified amplitude of the non-affected arm of the third participant. The top graph represents the sEMG signal and bottom graph represents the AMG signal.....90

List of Abbreviations

ACh – Acetylcholine

AMG – Acceleromyography

ANOVA – Analysis of variance

ATP – Adenosine Triphosphate

Ca²⁺ – Calcium

dB – Decibel

EMG – Electromyography

FMS – Fugl-Meyer Scale

Hz – Hertz

ICC – Intraclass Correlation Coefficient

IoT – Internet of Things

IMU – Inertial Measurement Unit

LMC – Leap Motion Controller

Li-ion – Lithium-ion

MAS – Modified Ashworth Scale

mHealth – Mobile Health

MMG – Acoustic (Mechano-) Myography

MTS – Modified Tardieu Scale

mV – Millivolts

MVC – Maximal Voluntary Contraction

PRISMA – Preferred Reporting Items for Systematic Reviews and Meta-Analyses

SELinux – Security-enhanced Linux

sEMG – Surface Electromyography

SPSS – Statistical Package for Social Sciences

TONE – Telerehabilitation Objective Neuromuscular Evaluation

UMN – Upper Motor Neuron

VPN – Virtual Private Network

Chapter 1. Introduction

1.1 Background on Stroke and Spasticity

A stroke is an acute or neurological deficit due to vascular injury from an infarction or hemorrhage in the central nervous system. Many factors contribute to an increased risk of having a stroke, one of which is hypertension (Murphy & Werring, 2020). The vast majority of strokes are ischemic, which occurs when there is a blockage in a blood vessel that reduces the supply of blood to a part of the brain. Some strokes are also due to intracerebral hemorrhages, which occur when a hematoma forms in the brain (Rajashekar & Liang, 2024). Stroke has become a considerable health challenge worldwide and is said to be a leading cause of death and physical disabilities in adults in middle to high-income countries. In 2019, 12.2 million reported incident cases and 101 million reported prevalent stroke cases were reported. Studies have found that globally, stroke is the second leading cause of death and accounts for 11.6% of deaths. Stroke was also found to be the third leading cause of disability in 2019 (GBD 2019 Stroke Collaborators, 2021). Studies have shown that 80% of those who have had a stroke will have some motor impairment initially, one of which is spasticity (Sommerfeld et al., 2004). Spasticity is a complication that occurs after an individual has had a stroke. It can be classified as a neuromuscular physical disability (Milligan et al., 2019). Spasticity is very common among stroke survivors, and studies have shown that spasticity has an incidence rate between 17 to 43% in stroke survivors who were followed up for 3 to 12 months (Zeng et al., 2020).

While spasticity is relatively easy to recognize, defining it in the literature has been proven difficult. A commonly used definition to define spasticity is one by Lance, who describes it as “a motor disorder characterized by a velocity-dependent increase in tonic stretch reflexes

with exaggerated tendon jerks, resulting from hyperexcitability of the stretch reflex” (Lance, 1990; Trompetto et al., 2014). While this definition has been widely used, it has been challenged by other scholars. Many have proposed different definitions and descriptions. However, the definitions currently proposed in the literature all have the general consensus that spasticity is associated with a hyperexcitable spinal reflex (Li & Francisco, 2015). The Upper Motor Neuron (UMN) syndrome is the most significant consequence of spasticity. The UMN syndrome is divided into "positive" and “negative” UMN signs. "Positive" signs represent an excess in muscle tone and stretch reflex. Excess in muscle tone or stretch reflex is defined as the amount of tension or resistance to lengthening while the muscle is at rest (Li & Francisco, 2015; van den Noort et al., 2009). “Positive” signs also include flexor and extensor spasms, brisk tendon jerks, and a catch. A catch is a sudden resistance to rapid movement due to fast movements triggering a strong involuntary contraction. On the other hand, there are also "negative" UMN signs, including weakness, impaired coordination and motor control (Li & Francisco, 2015; van den Noort et al., 2009).

Data collected in 2020 concluded that 2.1 per 100,000 Albertans were hospitalized with a stroke every year, which accounts for a significant portion of our population (Ganesh et al., 2022). The prevalence of patients with a stroke that will develop spasticity is 42%, with severe spasticity being 15.6% of these cases (Harb & Kishner, 2024). Therefore, this is a very prevalent portion of the population that requires further investigation.

1.2 Physiology of Muscle Contractions

Many nerves innervate muscle fibres called motoneurons. A motor unit consists of a single motoneuron and the muscle fibre in which it innervates. Different muscles with a variety of functions will have a different amount of muscle fibre units.

A contraction in the skeletal muscle occurs in the synapse between the motoneuron and muscle fibre, called the neuromuscular junction (Pham & Puckett, 2024). The motoneuron will initially receive a propagation of action potentials, which causes its presynaptic membrane to depolarize and open voltage-gated calcium (Ca^{2+} channels). The flow of Ca^{2+} causes acetylcholine (ACh) to be released in the neuromuscular junction. Once the ACh reaches the neuromuscular junction, it diffuses towards the postsynaptic membrane at the side of the muscle fibre (Pham & Puckett, 2024). ACh binds to specific receptors called nicotine receptors on the postsynaptic membrane, which causes a depolarization of the postsynaptic membrane of the muscle fibre. Thus, this creates an action potential in the muscle fibre (Pham & Puckett, 2024).

A mechanism then occurs, called excitation-contraction coupling, to allow the conversion of the action potential into a muscle fibre contraction. The action potential in the muscle fibre membrane travels into T-tubules found in the muscle fibre membrane called the sarcolemma, which allows the propagation of the action potential inside the muscle fibre. When the action potential depolarizes T-tubules, their receptors (dihydropyridine receptors) will have a conformational change, causing them to mechanically interact with receptors (ryanodine receptors) on the sarcoplasmic reticulum (Pham & Puckett, 2024). Consequently, the interaction causes Ca^{2+} to be released from the sarcoplasmic reticulum in the muscle fibre.

A skeletal muscle is composed of units called myofibrils. Myofibrils are divided lengthwise into segments called sarcomeres, and a Z-line separates each sarcomere at either end. Sarcomeres contain two different kinds of myofilaments: actin and myosin (Pham & Puckett,

2024). Actin myofilaments are thin filaments, and myosin is a thicker myofilament that contains troponin and tropomyosin complexes. The release of Ca^{2+} ions causes it to bind to the troponin. Consequently, the binding of Ca^{2+} causes a conformational change, which displaces the tropomyosin complex, allowing actin to bind to the myosin-binding sites (Pham & Puckett, 2024).

Thus, the following events allow for a cross-bridge cycle. Once actin can bind to its myosin-binding site, the thin and thick filaments can slide past each other and generate a muscle contraction by shrinking the entire sarcomere and bringing the Z-lines closer to each other (Pham & Puckett, 2024). At the start of this cycle, myosin is bonded to actin, but no adenosine triphosphate (ATP) is bonded to myosin. Once the ATP binds to the myosin filament, it allows for a conformational change that decreases myosin's affinity for the actin filament. Thus, the two filaments unbind (Pham & Puckett, 2024).

Once the muscle has contracted, muscle relaxation can occur once the Ca^{2+} is accumulated in the sarcoplasmic reticulum by the Ca^{2+} ATPase pump, causing calcium to unbind to troponin (Pham & Puckett, 2024).

1.2.1 Types of Muscle Contractions

Muscle contractions can be divided into four types. These include isometric, isotonic, concentric and eccentric contractions.

An isometric contraction occurs when muscle tension occurs without a change in muscle length. In this case, the joints or limbs do not move, and no motion occurs (Hrywniak et al., 2021). For example, this contraction can occur when an individual pushes upwards against a resistance or immovable object (Padulo et al., 2013).

An isotonic contraction occurs when a constant muscle tension is developed while shortening or lengthening a muscle. There are two types of isotonic contractions: concentric and eccentric. Concentric contraction causes the muscle to shorten, generating a force (Hryvniak et al., 2021). On the other hand, in eccentric contractions, the muscle lengthens when there is a greater opposing force (Padulo et al., 2013).

1.2.2 Active and Passive Movements

Two common movements are used to generate a contraction: active and passive. Passive movements occur when the limb or body is manipulated without the intentional effort of the person being tested. The limb or body can be manipulated by a therapist, researcher, or another external person who moves the tested limb or body to generate a contraction (Trinity & Richardson, 2019). On the other hand, active movements are when the person being tested moves their limb or body independently without assistance (Holzgreve et al., 2020).

1.3 Pathophysiology of Spasticity

Researchers have found that the exaggerated stretch reflex in those with spasticity can be due to the excitability or overactivation of muscle spindles. A stroke may cause damage to the pyramidal tract, a group of efferent nerve fibres in which a signal is carried from the cerebral cortex to the brainstem or spinal cord. Thus, this is believed to cause an exaggerated stretch reflex and an abnormal muscle tone (Kuo & Hu, 2018). Hence, when a limb is passively stretched, this would cause more activation of spindle afferents. Another reason for the exaggerated stretch reflex could be alpha-motoneurons' activation (Kuo & Hu, 2018). These motor neurones innervate muscle fibres and are the principal way skeletal muscle contractions are generated (Zayia & Tadi, 2024). In summary, researchers have stipulated that spasticity is

due to the abnormal activation of spindles, which are processed by the spinal cord (Kuo & Hu, 2018).

In other words, spasticity is caused by damage to upper motor neurones, which prevents the brain and spinal cord from communicating with each other, resulting in spinal reflex disinhibition (Kuo & Hu, 2018). Spinal reflex disinhibition occurs when there is a failure to suppress incoming signals (Marshall et al., 2023). Passive stretching of the muscle causes the sensory input of the muscle spindles through afferent fibres to the spinal cord and the alpha-motoneurons to be even more activated than usual. Also, spinal interneurons may lose their influence on the central nervous system (Kuo & Hu, 2018). The disruption of these influences could lead to reduced inhibition of the antagonist muscle and increased action potential in neurones, leading to increased muscle activation (Kuo & Hu, 2018).

Researchers have also explained how spasticity affects a muscle's mechanical properties. Spasticity can reduce the number of sarcomeres in a muscle and increase the amount of connective tissue (Kuo & Hu, 2018). This change might cause pulling forces to transmit impulses to muscle spindles more frequently, increasing the muscle spindles' sensor input and consequently increasing spasticity (Kuo & Hu, 2018).

1.4 Current In-Person Spasticity Assessments

Post-stroke spasticity creates barriers to community participation (Francisco et al., 2021). It often leads to joint immobility and many other complications, including interference with daily living activities such as hygiene, walking, eating, and toileting (Rivelis et al., 2024).

For health-related conditions, such as spasticity after a stroke, the Canadian Stroke Best Practice advised timely and appropriate assessments for extremity spasticity (Teasell et al.,

2020). Detecting, assessing and managing post-stroke spasticity earlier can prevent complications and improve function, thus increasing independence for these individuals (Kuo & Hu, 2018).

Currently, in-person assessments require gaining a detailed patient history and performing a physical examination. Detailed history involves gaining information on the duration and severity of spasticity. It also allows one to acquire baseline information regarding current medication taken, additional diseases, the muscle groups affected, and pain (Balci, 2018). On the other hand, muscle tone and tendon reflexes are observed during the physical examination. While evaluating muscle tone, the patient is asked to remain in the supine position for the lower and upper extremities to allow the clinician to assess various pathological reflexes, muscle strength and passive and active joint range of motion (Balci, 2018).

1.4.1 Scales to Measure Spasticity

Many clinical scales are currently used in practice to evaluate spasticity. The Modified Ashworth Scale (MAS) is the most commonly used and well-known scale in practice (Balci, 2018). MAS measures increased muscle tone during passive stretch using a 6-point scale, where a grade of 4 indicates the affected parts are rigid during flexion and extension (Table 1). The preference for MAS by clinicians stems from its ability to be used and applied easily in a clinical environment and its ability not to require additional tools when used by the clinician. The drawback of this scale is that it cannot measure spasticity factors other than tone disorders (Balci, 2018).

Another commonly used scale to evaluate spasticity is the Modified Tardieu Scale (MTS), which assesses spasticity during passive motions. In this case, passive stretches are

performed at a lower or higher speed when the extremity segment falls with gravity. V1 indicates that it is as slow as possible, and V3 indicates it is as fast as possible (Balci, 2018). MTS also grades the muscle reaction quality from 0 to 5, where a grade of 5 indicates the joint cannot be moved (Table 2).

Lastly, the Fugl-Meyer Scale (FMS) is occasionally used to evaluate the sense of touch, pain, and joint position of the hand, wrist and posture (Balci, 2018).

Table 1. Summary of the parameters use to evaluate spasticity when using the MAS.

0	No tone increase
1	Slight increase in tone and presence of catch-and-release at the end of a range of motion
1+	Slight increase in tone and catch-and-release which is followed by minimal resistance for the remainder of the range of motion
2	Muscle tone is increased in most of the range of motion but joints or affected parts are still easily movable
3	Considerable increase in tone, passive movement becomes very difficult
4	Affected parts are rigid during flexion and extension

Table 2. Summary of the parameters use to evaluate spasticity when using the MTS.

Muscle reaction quality	
0-	No resistance throughout the passive movements
1-	Slight resistance during the passive movements with no clear catch at a specific angle
2-	Clear catch at a specific angle, which interrupts passive movements, with the affected part relaxing after
3-	Fatigable and weak clonus for less than 10 seconds when passive stretch continues at a specific angle
4-	Unfatigable and strong clonus that lasts longer than 10 seconds when passive stretch continues at a specific angle
5-	Immobile joint
Stretching speed	
V1	As slow as possible or slower than the affected limbs natural drop due to gravity
V2	Normal speed of the limb falling due to gravity
V3	As fast as possible or faster than the affected limbs natural drop due to gravity

1.5 The Need for Objective Measurements

Currently, there are no reliable criteria for spasticity assessments, and clinicians often have to depend on the perception of the patient or their caregiver's change in muscle tone. This may hinder their ability to prescribe adequate treatments as clinicians are relying on the biased perception of patients and caregivers (Skalsky, 2017).

Clinicians rely on scales, such as the MAS or MTS, to decide a patient's course of treatment (i.e., surgical interventions and medications) (Skalsky, 2017). These assessments rely on intuition and experience (Puzi et al., 2020). Thus, many researchers have stated that there is a problem with using these scales for these assessments due to their lack of objectivity (Skalsky, 2017). Furthermore, these scales have been found to have poor inter and intra-rater reliability.

One of the reasons for the poor inter and intra-rater reliability is that the speed at which the clinician stretches the affected limb may change between clinicians. Consequently, this may change the grade seen on the scales, as the results depend on the subjectivity of speed (Balci, 2018; Harb & Kishner, 2024).

Most of these scales' current criticism comes from the fact that they do not permit differentiation between many other factors that can cause an exaggerated stretch reflex and increase in muscle tone. The scales, specifically the MAS, can also not differentiate features that distinguish spasticity from other tonus disorders (Balci, 2018; Harb & Kishner, 2024). Researchers have found that these scales also do not provide sufficient information regarding which muscles contribute to spastic movements (Ahmad Puzi et al., 2017).

Sloot et al. suggested that objective assessments will improve clinical decision-making to permit better spasticity management through surgical interventions and medication. Hence, this will prevent risks such as unnecessary surgical interventions or medication titration when subjective measurement scales are used (Balci, 2018; Harb & Kishner, 2024).

1.6 The Need for Virtual Spasticity Assessments

The quality of life of a patient who has had a stroke may be hindered without access to proper care to assess and manage this spasticity. Telehealth services or virtual assessments for spasticity may allow for timely, objective evaluations and improve access to care. Current in-person assessments are often used to determine a proper course of treatment, one of which is receiving botulinum toxin injections, commonly required for patients with spasticity, once every 3 to 4 months (Levy et al., 2023). Botulinum toxin injections can help improve and reduce a patient's muscle tone and facilitate basic limb function. Consequently, these assessments determine if these injections are required to improve a patient's quality of life and independence

(Shaw et al., 2011). However, a patient may come in for their assessments, which may determine that they do not require or are not eligible for botulinum toxin injections at this time (Levy et al., 2023). Therefore, they may make an unnecessary and challenging trip.

Patients who have spasticity have been found to have trouble accessing healthcare for two main reasons. The first reason is that their limited mobility often requires specialized transportation, which requires thoughtful planning and associated costs (Verduzco-Gutierrez et al., 2020). Thus, this may require extensive patient preparation to ensure they have the proper accommodations to get to their appointments. Before getting to their appointments, they may need to ensure they have accessible transportation and have scheduled time for caregiver assistance (Valdez et al., 2021). Current public spaces are also challenging for those with limited mobility to navigate. Many public spaces are not equipped with power doors or elevators and have steep curb cuts, which may make it difficult for patients to access certain parts of these spaces to get to and from their appointments (Valdez et al., 2021). Secondly, many patients who have spasticity also have other underlying health conditions. Therefore, it is advantageous to minimize needless exposure to crowded clinics and hospitals (Verduzco-Gutierrez et al., 2020). In addition, those who live in rural areas frequently lack access to in-person healthcare services because of the expense of commuting to a clinic or hospital in a city (Valdez et al., 2021).

A virtual spasticity assessment to determine a patient's spasticity management and treatment plan may improve the accessibility of spasticity assessments. Therefore, virtual health assessments are becoming increasingly important. There is a need to develop an advanced objective spasticity assessment that can be used virtually.

1.7 Surface Electromyography for Objective and Virtual Spasticity Assessments

Currently, some objective assessments have been researched to assess spasticity through biomechanical methods that could be conducted in a telehealth setting. These include isokinetic dynamometers or a pendulum test to assess the resistance to change of passive ranges of motion at different angles and speeds.

However, the most investigated is surface electromyography (sEMG). sEMG is a way of monitoring muscle activity by recording the electrical signal produced during a muscle contraction (Ladegaard, 2002). It uses electrodes that are applied to the surface of the skin, unlike intramuscular EMG, which uses wires or needles placed into the muscle (Merletti & Farina, 2009; Mills, 2005).

sEMG is currently used in several research applications to study the pathophysiology of spasticity. Researchers have previously used sEMG to determine the spastic response of certain muscle groups during active or passive movements. Using the sensors, clinicians can obtain information on motor unit discharges in spasticity patients (Yu et al., 2020).

Previous studies have also found that in patients with spasticity, there is an increase in the amplitude and frequency domains during a stretch reflex. Involuntary muscle contractions from spasticity are also represented in sEMG spatial distribution (Xie et al., 2020). Consequently, the literature has suggested that sEMG can be a valuable tool for evaluating spasticity by extracting its time and frequency domains (Yu et al., 2020).

Certain researchers have already concluded that using time-domain features, such as root mean square, and frequency-domain features, such as mean power frequency, in sEMG has been correlated with the MAS (Yu et al., 2020). sEMG researchers have found a positive correlation

between increased sEMG amplitude in spasticity patients and a high grade on the MAS (Huber et al., 2022).

sEMG's ability to gain valuable biomechanical data regarding spasticity from its time and frequency domain makes it a promising tool for objective spasticity assessments. On the other hand, sEMG also has the potential to be used in a telehealth setting (Constantinescu et al., 2018). In recent years, various EMG assessments have been developed to be conducted virtually (Elbaz et al., 2021).

1.7.1 Signal Origin

When sEMG electrodes are placed on the skin's surface, they can determine action potentials. When a depolarization-repolarization process occurs, the action potential travels to the surface of the muscle fibre. The depolarizing of the membrane is propagated down the muscle fibre and can be recorded by the electrodes (Turker & Sze, 2013). Once the sEMG electrode comes in contact with the action potential, it presents a bipolar signal to the sEMG differential amplifiers. This is because these electrodes measure the difference between two points during the propagation of the action potential. In summary, since sEMG signals are superpositions of several action potentials, they give us a window into the electrical signals present in many muscle fibres (Turker & Sze, 2013).

EMG signals are said to have an amplitude signal that ranges peak to peak from 0 to 10 mV and has a frequency range from 0 to 500 Hz (Nazmi et al., 2016).

1.7.2 Barriers to sEMG

While sEMG electrodes have been reliably used for post-stroke muscle spasticity assessments, many barriers prevent them from being easily used in a telehealth setting.

One of the most significant practical barriers to using sEMG in a telehealth setting is that it requires skin preparation before the electrode is placed to prevent any artifacts (Turker & Sze, 2013). The skin must be properly cleaned and dried before the electrode is placed on the skin to record muscle activity. This involves using rubbing alcohol, ensuring the skin is not flaky, oily or dry, and ensuring any excess body hair is shaved before application. Preparing the skin is done to reduce the electrical impedance of the skin-electrode interface preventing noise in the sEMG signals (Turker & Sze, 2013).

Another barrier to sEMG use is that precise electrode placement is required to produce an accurate sEMG signal. Two strategies are used to ensure proper electrode placement. The first is to ensure proper electrode contact with the skin, and the second is to minimize skin impedance (Turker & Sze, 2013). This barrier is especially present if dynamic movements are present during sEMG recording. For accurate sEMG measurements to be picked up by the electrode, it is essential to ensure the electrode is positioned on the muscle's longitudinal midline, between two motor points or between a motor point and a tendon insertion. Furthermore, the electrode's longitudinal axis must parallel to the muscle fibre's length (Turker & Sze, 2013).

1.8 Acoustic (Mechano-) Myography as an Alternative

Due to the electrical interference of sEMG and other barriers that may hinder the signal quality if it is misused, there is a need to find a suitable alternative if it is to be used in a telehealth setting without the presence of a specialist (Uwamahoro et al., 2021). An alternative to sEMG for muscle spasticity assessments virtually could be acoustic (mechano-) myography (MMG). MMG records mechanical events during a contraction (Ibitoye et al., 2014; Roberts & Gabaldón, 2008). Researchers have found that MMG provides information regarding muscle

contraction features and fibre-type composition (Uwamahoro et al., 2021). MMG signals are detected when changes in the muscle fibre diameter occur due to motor unit activation (Carr et al., 2018). Researchers have stipulated that the signal is generated by the muscle's lateral movements during contractions or relaxations when it moves towards or away from the Z line. Furthermore, the muscles' resonant frequency may also generate the signal through lateral oscillations. Lastly, dimensional changes in the active muscle fibres may also create a signal (Beck et al., 2005).

The sensor may be a suitable alternative to sEMG for virtual spasticity assessments as it does not present the same barriers. However, it has not yet been well studied to determine if it can convey the same information regarding muscle contractions and spasticity.

One of the most significant advantages of MMG is that it does not require any skin preparation beforehand and is less sensitive to where the sensor is placed on the muscle (Woodward et al., 2019). The acoustic signal from the muscle also has a much lower frequency range of 0 to 40 Hz when compared to EMG, reducing the bandwidth requirement when real-time data is transmitted to the remote specialist clinician (Tarata, 2003). Therefore, MMG is much more user-friendly when used in a telehealth setting without the knowledge of an expert clinician present.

1.8.1 Types of Acoustic (Mechano-) Myography

There are various types of MMG transducers. These include hydrophones, condenser microphones, piezoelectric sensors and accelerometers, to name a few. The most commonly used MMG transducers are condenser microphones and accelerometers (Beck et al., 2005).

Microphones pick up sound waves through the skin when the muscle contracts, causing a

diaphragm to oscillate, which is then detected electronically. On the other hand, vibration propagating through the skin's surface during a muscular contraction generates skin excursion, which accelerometers record (AlMohimeed & Ono, 2020; Linderman et al., 2023).

1.8.2 Appropriate Transducer for Virtual Spasticity Assessments

For this research, an accelerometer was chosen. The decision to use an acceleromyography sensor (AMG) was made because they are simple to calibrate, inexpensive and less susceptible to environmental noise, making an ideal alternative to sEMG for virtual spasticity assessments (Campbell et al., 2017). Previous studies have found that accelerometers have the most reliable signal acquisition and detection during voluntary muscle contraction. Researchers have also found it has a better signal-to-noise ratio than other MMG transducer types (Talib et al., 2018). An AMG is a lightweight design with great signal acquisition and is readily available, making it an excellent candidate for virtual spasticity assessments and a promising alternative to sEMG.

1.9 Research Statement, Questions and Objectives

It is not yet evident in the literature whether or not the AMG sensor is comparable to the sEMG in terms of the data it can collect and the information it can provide to clinicians for spasticity assessments. Therefore, the proposed research will examine how sEMG compares to AMG in the biomechanical data it can obtain for quantitative information on muscle activity during active and passive movements. The research will focus on upper extremity spasticity. The reasoning is based on a study by Lundström et al., which determined that spasticity is more frequently prominent in the upper limbs. Urban et al. also confirmed this in their research, where their findings found more frequent spasticity in the upper extremity muscles (Kuo & Hu, 2018).

Thus, the study aims to determine whether or not the sEMG and AMG sensors are comparable in collecting data to provide clinicians with information on muscle spasticity in a virtual environment in the upper extremities.

The following research questions will be addressed:

- a) Is AMG comparable to sEMG in the ways it can detect slow and fast fibre changes in the frequency domain?
- b) How much does quantitative physiological information collected from sEMG during passive and active movements in the upper extremities compare to the AMG sensor?
- c) Are sEMG and AMG comparable in their ability to detect spasticity in the upper extremities of post-stroke patients?

1.10 Relevance of Research

The proposed research will allow enhanced virtual healthcare protocols for spasticity assessments. It will support the selection of the most practical sensors to provide clinicians with information on a patient's spasticity. This is crucial to our current health care system, which has a significant need for such a protocol as there is a large barrier in how stroke spasticity patients access these assessments. Stroke spasticity patients have physical limitations, which may significantly affect their mobility. Consequently, accessing in-person appointments is only sometimes feasible and sometimes requires a caregiver. For example, travel is expensive, time-consuming and often hazardous for rural patients. The proposed research will allow for a basis in future research to develop a protocol healthcare clinicians can follow for objective virtual stroke spasticity assessments. This study is a step toward more accessible assessments and treatments for spasticity after stroke, essential to these patients' quality of life and independence.

1.11 Structure of the Thesis

The thesis is divided into three chapters. The first chapter consists of the literature review. It evaluates current barriers to virtual sEMG found in the literature and how researchers have developed strategies to overcome these barriers so that the sensors can be used more adequately in a telehealth setting.

Chapter 2 details the process of adapting a portable device based on a previous device, the TONE device, by Daniel Gillespie, a former Ph.D. student in Rehabilitation Sciences at the University of Alberta. The goal of this portable device was to record both raw sEMG and AMG sensors simultaneously, synchronized with an electrical goniometer to record elbow angle and angular velocity, be easy to use, and transmit adequate clinically relevant information to the remote clinician.

Chapter 3 highlights the clinical study done to compare the two different sensors, sEMG and AMG, and determine which is the best suited for remote spasticity assessments in stroke patients. It demonstrates if the two sensors give comparable information for these assessments. Finally, the last chapter of the thesis is an overall discussion of the findings of this research. It includes future research suggestions on how clinicians and patients can move forward to make virtual spasticity assessments a reality.

Chapter 2. Identifying and Overcoming the Barriers to Virtual EMG Assessments: A Scoping Review

2.1 Abstract

Introduction: Electromyography (EMG) assessments have been conducted virtually more frequently in recent years, leading researchers to explore the barriers to EMG assessments in a telehealth setting and how to overcome them.

Methods: A scoping review was conducted according to the methodology described by Arksey and O'Malley. A comprehensive search using controlled vocabulary and keywords for two concepts, EMG and telehealth, was conducted using Medline and EMBASE on February 7, 2022. Two independent reviewers screened titles, abstracts, and full-text articles. Two reviewers also extracted the data and described the findings in a descriptive analysis.

Results: A total of 248 articles were screened during the abstract and title review, of which 64 full texts were screened for eligibility. Of these, 15 publications met the inclusion criteria. Most articles were published in 2018 or later (66.7%). The most frequently mentioned barrier to conducting a virtual EMG assessment was poor data and signal transmission (53.3%). Another frequently mentioned barrier was poor patient usability (33.3%). Solutions most frequently reported related to patient usability (33.3%). These included interactive instructions and video chat to monitor and provide the patient with technical support.

Conclusion: The last 4 years have seen an increase in articles published on EMGs' use in telehealth to monitor or diagnose patients. Further research is required to determine if the proposed solutions have improved clinical outcomes for the patient.

2.2 Introduction

Electromyography (EMG), which has been introduced into routine clinical practice since the 1950s, is a useful method of physiological monitoring of muscle activity (Ladegaard, 2002). It is an important diagnostic and monitoring tool in health care due to its crucial role in many biomedical and clinical applications. These applications include but are not limited to medical research, rehabilitation, and biomechanics (Heaffey et al., 2015). There are several clinical assessments that utilize EMG. For example, EMG is useful in clinical practice as it is used to diagnose muscle and nerve disorders such as peripheral neuropathy and carpal tunnel syndrome (Lee et al., 1999).

EMG has traditionally been used for in-person clinical assessments. Recently, there has been an increased need and demand for virtual health care, in part, brought on by COVID- 19 and also because of recognized inequities in access to care for patients in rural and remote settings. Telemedicine allows the delivery of care through internet-based services, and in the last few years, EMG assessments have begun to be conducted virtually (Elbaz et al., 2021). When used appropriately, telehealth has the potential to save health care dollars while simultaneously saving travel time and out-of-pocket costs for patients (Arksey & O'Malley, 2005). While telehealth has provided many advantages in the health care field, the use of EMG in telemedicine is recent and has been shown to have some constraints and limited use in practice (Arksey & O'Malley, 2005).

The barriers to using EMG virtually and recommendations for overcoming these have been reported in the literature; however, to the best of our knowledge, a scoping review is yet to be conducted to assess and summarize these barriers.

This scoping review aims to determine if there are any clinical or technical barriers to conducting

EMG assessments virtually and how they are used in a virtual health context. In addition, this review summarizes solutions that have been recommended to address barriers to using EMG as part of a virtual care assessment.

The population of interest for this scoping review includes all patients who underwent virtual EMG assessments.

2.3 Methods

This scoping review used the methodology guided by Arksey and O'Malley (Tricco et al., 2018). However, in this case, only two data-bases were searched. This article adheres to Preferred Reporting Items for Systematic Reviews and Meta-Analyses (PRISMA) for scoping reviews (*Covidence Systematic Review Software*, n.d.).

2.3.1 Search Strategy

The search was conducted on February 7, 2022. Two electronic databases were used: Medline (1946-present through Ovid) and EMBASE (1946-present through Ovid). The search strategy used controlled vocabulary and free text terms to highlight the following concepts and objectives mentioned in the research question: (1) electromyography and (2) tele-health. Telehealth includes any general term for remote health (e.g., telerehab, telemedicine, m-health). Studies were limited to English, and news articles, editorials, and veterinary studies were removed from the results. The Medline search strategy can be found in the Appendix. All sources were checked to be peer-reviewed to maintain the accuracy of the results.

2.3.2 Inclusion and Exclusion Criteria

Articles were included if they discussed the use of EMG assessments in telehealth or conducted remotely. This included but was not limited to wearable EMG devices and EMG virtual health applications (i.e., migraine, dysphagia, stroke, spinal cord injuries, and pain monitoring). Articles were only included if authors or investigators discussed the limitations of EMG assessments and/or how to overcome the barriers of conducting EMG assessments virtually. This included but was not limited to the transmission of the data virtually, the quality of the signal, the usability of the device, data storage, safety and patient confidentiality, and user-friendliness. The included article types were scientific peer-reviewed articles obtained from the electronic database search. All articles published during or after 2006 were included due to the rapid advancement of technology and the limited knowledge of telehealth and EMG assessments before 2006. Article settings that were included had to consider a virtual or remote setting during EMG assessments. Article interventions had to consider an EMG application that was used to assess or monitor a patient remotely. Article outcomes had to consider barriers or how to overcome barriers of remote EMG. Finally, articles had to consider a population that needed to use EMG to measure any sort of muscle activity due to neuromuscular disorders.

Articles were excluded if they were not written in the English language due to feasibility. Articles were also excluded if they only included clinical EMG applications that did not consider their applications in a virtual setting. Books, newspaper articles, theses, dissertations, and conference abstracts were also excluded due to feasibility.

Finally, articles were excluded if they only described applications of EMG use virtually without considering any barriers to these assessments and/or how to overcome certain barriers to the data collection method.

2.3.3 Study/Source of Evidence Selection

All citations were uploaded into Covidence[®], and duplicates were removed (*Covidence Systematic Review Software*, n.d.). Title and abstracts were screened and assessed by two independent reviewers against the inclusion and exclusion criteria. Next, two independent reviewers ordered full-text publications of all relevant titles and abstracts and screened against the inclusion and exclusion criteria. Finally, the reasons for excluding specific sources during the full-text that did not meet the inclusion and exclusion criteria were recorded. If any disagreements occurred between the reviewers during any stage of the selection process, these disagreements were resolved through a discussion-based meeting.

2.3.4 Data Extraction

One reviewer determined which variables would be extracted and created a data extraction form before the literature review. The data extraction process was done using Covidence by two independent reviewers who used the same form. Any disagreements that occurred between reviewers were resolved through a discussion-based meeting. Extracted data included general article information and characteristics (year of publication, the country where the study was conducted, the purpose of the study, and the setting). It also included key findings

related to the clinical and technical barriers of EMG used virtually and how these were overcome. The key findings also included restrictions to the scope of professional practice that could affect virtual EMG assessments.

Results were synthesized by grouping the articles according to the types of barriers they presented and the proposed solutions for these barriers (if any). These were then each summarized. Finally, details for the evidence obtained in this review were presented through tables and graphs and a narrative summary.

2.4 Results

A total of 249 articles were imported into Covidence for screening in the initial search, with 1 duplicate removed. A total of 248 articles were screened for the title and abstract review. After the title and abstract screening, 184 articles were excluded, and 64 articles were obtained for a full-text review screening. Then, 49 articles were excluded based on the full-text screening because the study design (9 publications), setting (4 publications), population (1 publication), interventions (16 publications), or outcomes (18 publications) were not relevant to the scoping review. One publication was excluded because it had not been peer-reviewed. A total of 15 articles were deemed relevant and included in the scoping review (Figure 1).

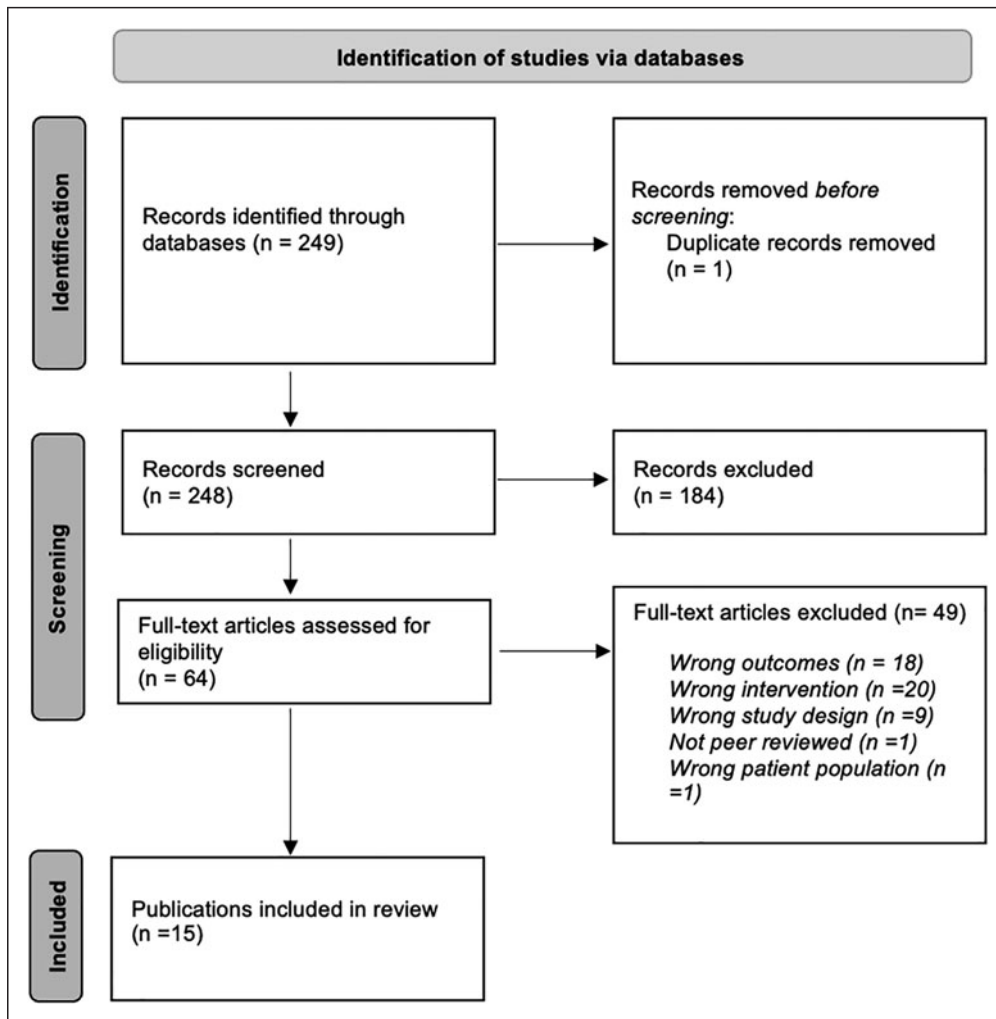


Figure 1. Preferred Reporting System for Systematic Reviews and Meta-Analysis diagram of the screening process.

2.4.1 Article Characteristics

A total of 15 articles were identified. The number of articles published concerning EMG and its virtual application and assessment has significantly increased over time, with a significant upward trend starting between the years 2018 and 2022 (Figure 2).

The articles in the included texts were conducted in 11 different countries, most in the United States and Italy (20.0% each). The countries in which the articles were conducted are found in Table 3.

Most articles investigated the use of a wearable EMG sensor for EMG data monitoring and assessments (33.3%) (Berger et al., 2006; Ingvaldsen et al., 2021; Kantarcigil et al., 2020; Kishimoto et al., 2009; Sethi et al., 2020; Zhao et al., 2020). Some articles looked at algorithms for the compression of EMG signals to improve remote data transmission (20.0%) (Ahamed et al., 2013; Constantinescu et al., 2018; Dinashi et al., 2022). Some articles also compared the wireless portable EMGs to those typically used clinically to evaluate their strengths and weaknesses (20.0%) (Badawi et al., 2020; Palumbo, Ielpo, et al., 2021; Rogante et al., 2010). A few articles focused on studying the remote-based EMG sensor placement for the highest signal accuracy and comparing it to a research-grade (or clinically used) sensor (13.3%) (Hassan et al., 2020; Marin-Pardo et al., 2021). Finally, a few articles focused on cloud-based systems for remote real-time information and data, unreliable real-time data (13.3%) (Hassan et al., 2020; Palumbo, Vizza, et al., 2021).

Most of the articles were conducted in a laboratory setting (60.0%). Laboratory setting studies were done to design a specific device (i.e., wearable) for ease of use in a virtual setting. Two studies were done in a remote clinical setting (13.3%). Clinical setting encompassed both clinic-to-clinic and clinic-to-home models. The clinic-to-clinic model is when the patient is at a remote clinic with a clinical assistant and the specialist is located in a virtual setting. The clinic-to-home model is when the patient is at home and the specialist is located in a virtual setting. The articles did not mention which model was used. Finally, one study was conducted in a laboratory and then described a case study in a remote clinical setting (6.7%). In addition, two articles were reviews (13.3%), and one described a system (6.7%). Most studies were conducted with healthy participants (7 of 12 articles, 58.3%). The settings and the types of participants are presented in Tables 4 and 5, respectively.

Table 3. Country in which the study was conducted in the included texts.

Country	Number of articles	Percentage
United States	3	20.0%
Italy	3	20.0%
Malaysia	1	6.7%
Egypt	1	6.7%
Brazil	1	6.7%
Canada	1	6.7%
Iran	1	6.7%
Pakistan	1	6.7%
Norway	1	6.7%
Japan	1	6.7%
China	1	6.7%

Table 4. Description of the study setting.

Description	Number of Articles	Percentage
Laboratory	9	60.0%
Clinical	2	13.3%
Laboratory and clinical (case study)	1	6.7%
Neither; reviews (one of which was a scoping review)	2	13.3%
Neither; description of a system	1	6.7%

Table 5. Types of participants.

Description ^a		
Healthy participants	7	58.3%
Head and neck cancer survivors (vs. healthy participants)	1	8.3%
1 stroke patient (case study) and healthy participants	1	8.3%
Stroke patients	1	8.3%
Amyotrophic lateral sclerosis patients	1	8.3%
Migraine patients	1	8.3%

^a from 12 articles; 2 articles were reviews, and 1 article was a simulation exercise

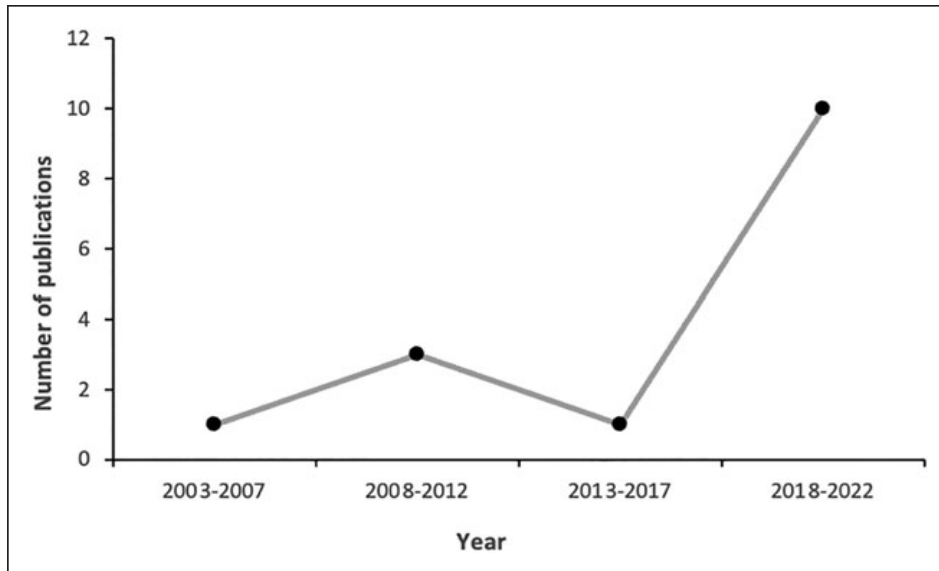


Figure 2. Number of published articles per year in the included texts.

2.4.2 Barriers to Conduction sEMG Assessments Virtually

Several barriers to conducting EMG assessments virtually were identified in the included articles. The most common barrier was related to the delayed or unreliable real-time data of EMG signals in telemedicine due to high bandwidth consumption and the large amounts of data to be processed (80%) (Constantinescu et al., 2018; Hassan et al., 2020; Kishimoto et al., 2009; Marin-Pardo et al., 2021; Palumbo, Ielpo, et al., 2021; Palumbo, Vizza, et al., 2021; Zhao et al., 2020). Some articles also mentioned that wireless EMG systems have high power consumption and low energy efficiency (13.3%) (Palumbo, Ielpo, et al., 2021; Palumbo, Vizza, et al., 2021). Cybersecurity issues to ensure data confidentiality were also raised as a concern (13.3%) (Hassan et al., 2020; Palumbo, Ielpo, et al., 2021).

The second most common barrier mentioned in the articles was poor patient usability or user-friendliness in the clinic- to-home model (40.0%) (Badawi et al., 2020;

Hassan et al., 2020; Kantarcigil et al., 2020; Palumbo, Ielpo, et al., 2021; Sethi et al., 2020). In this model of virtual EMG use, the patient is expected to apply the electrodes on their own. Because of the bulky equipment, the patients found it difficult to attach the electrodes to themselves without the clinician's intervention. One article described that the surface EMG electrodes they used were too rigid and lacked flexibility, preventing their use as a wearable technology. One article mentioned that EMG electrodes required the electrodes to be at the exact anatomical location to obtain accurate recordings. Another article mentioned that there was variability in the sensor location across sessions. It was also difficult for the patient to pair the EMG sensor system to the application on the computer due to technological difficulties. One article mentioned that the system required a minimum level of computer knowledge to set up and utilize. Barriers to virtual EMG assessments are summarized in Table 6.

Table 6. Barriers to virtual EMG assessments.

Barriers	Number of articles	Percentage
Delayed or unreliable real-time data	12	80%
Poor patient usability or poor user-friendliness	6	40.0%
High power consumption and low energy efficiency for battery-based systems	2	13.3%
Cybersecurity	2	13.3%

2.4.3 Overcoming Barriers to Conducting sEMG Assessments Virtually

The articles described various solutions by which the identified barriers could be managed to address the issues related to conducting EMG assessments virtually.

Patient usability and user-friendliness. All articles that identified issues related to poor patient usability or user-friendliness proposed a solution for this barrier (33.3%) (Hassan et al., 2020; Kantarcigil et al., 2020; Rogante et al., 2010; Sethi et al., 2020; Zhao et al., 2020). Improvements in patient usability were recommended through more interactive instructions on how to operate the EMG independently. For example, two articles suggested adding tips and techniques progressively throughout the sessions (Hassan et al., 2020; Kantarcigil et al., 2020). Another article included an options menu for the software, which contained additional options for user support (Rogante et al., 2010). In some articles, a regular video chat between the clinician and patient would occur to monitor the patient and provide technical support. This ensured that the electrodes were placed correctly and that the EMG data were obtained accurately (Hassan et al., 2020; Rogante et al., 2010). Another solution proposed regarding the bulkiness and rigidity of the system was to use an ultrathin wearable EMG electrode (20.0%) (Hassan et al., 2020; Kishimoto et al., 2009; Zhao et al., 2020). One article described one such system made of a

polyimide film in a honeycomb layout to allow for better flexibility and breathability over extended periods of time. It is important to note that usability will vary depending on the location. For example, in a clinic-to-clinic model where the EMG data are collected from a remote clinic and sent to a specialist in another location, usability may not be as large of an issue due to available help from a clinician on site. However, if the patient is being tested from home or a clinic-to-home model, it may be more challenging for a clinician to assist the patient in using the software or where to place electrodes, for example.

Real-time data. To address the reliability of real-time data, several articles described various EMG systems being developed and validated to address this (20%) (Hassan et al., 2020; Palumbo, Ielpo, et al., 2021; Palumbo, Vizza, et al., 2021). It is important to consider that the EMG system does not contain any significant data above 200 Hz when it is used clinically. These data are used for comparing of the muscle or power spectra to identify fast or slow fibers.

Data transfer latency could be managed through Fog computing architecture (6.7%) (Palumbo, Vizza, et al., 2021). Fog computing architecture is when a series of nodes will process the data in real-time when they receive it from an IoT device. The nodes will then send information to the cloud periodically (Palumbo, Vizza, et al., 2021). Consequently, this will allow to distill the results, allowing less data to be transferred, reducing transmission delay. Cloud-based systems have been reported to have data transfer delays (latency). Delays increase with an increase in the number of sensors used since the cloud server must deal with the data from all the sensors at once (Palumbo, Vizza, et al., 2021). Fog-computing architecture has been proposed as an option to minimize the delay and improve efficiency. It uses fog devices (nodes) as an extra data processing step that groups sensor data and then transfers it to the cloud server. This decreases

the amount of individual sensor data transferred to the cloud server (Palumbo, Vizza, et al., 2021).

Signal transmission could be improved with new methods of signal compression techniques (13.3%) (Ahamed et al., 2013; Constantinescu et al., 2018). For example, using discrete wavelet transform or deep convolutional autoencoders could reduce the size of the data without losing important information. These methods would be useful for minimizing data storage or removing irrelevant information within the data for better and faster data processing (Ahamed et al., 2013; Constantinescu et al., 2018). However, it is important to note that signal transmission speed will depend on the clinician's goal and what they are trying to assess. Raw data transmission that is postprocessed transfers much larger amounts of data than if edge or fog computing is used (i.e., where the amount of data that is transmitted is much lower as it has already been processed). Edge or fog computing would allow to reduce the latency of the data being transmitted.

Bandpass filtering, a technique that allows frequencies within a specific range and rejects frequencies outside that range, was proposed in three articles (20.0%) (Berger et al., 2006; Hassan et al., 2020; Kishimoto et al., 2009). The bandpass filter in one article had a bandwidth of 20–500 Hz and a notch filter of 60 Hz. However, while the two other articles used bandpass filtering, the type of bandpass filter used was not mentioned.

One article mentioned a dynamic bit allocation scheme which is a process for better utilization of the system's memory space so that the data adjust itself to the available memory capacity (6.7%) (Constantinescu et al., 2018).

Power consumption. A wearable system's most significant power demand is its wireless

transmission. One study presented a novel EMG system that provided more power using a dual 9-V battery. One review article also suggested the use of dual 9-V batteries, passive electrodes with a battery for power supply on the sensor, or rechargeable Li-ion batteries to provide more power than the normal amount that needs to be consumed (13.3%) (Palumbo, Ielpo, et al., 2021; Palumbo, Vizza, et al., 2021).

Security. While two articles mentioned that cybersecurity was an important consideration in telehealth, only one provided ways to ensure data privacy. Enhanced security was proposed through monitoring data in real-time, firewalls, anti-distributed denial of service (DDoS), Security Enhanced Linux (SELinux), and VPN (6.6%) (Rogante et al., 2010). Anti-DDoS is used to prevent malicious attempts to make the system unavailable to users. SELinux is an access control program that enforces security on a system. It has mechanisms that separate system integrity and data confidentiality (multilevel security). VPN can also be used for increased security as it provides privacy and anonymity for online users through encryption (Rogante et al., 2010).

Solutions to overcoming barriers to virtual EMG assessments are summarized in Table 7.

Table 7. Ways to overcome barriers in virtual EMG assessments.

Barriers	Solutions	Number of articles	Percentage
Patient usability and user-friendliness	More interactive instructions (e.g., video chats, progressive tips)	5	33.3%
Reliability of real-time data	Novel systems being developed	3	20.0%
Bulkiness and rigidity of system	Use of ultra-thin wearable EMG electrode	3	20.0%
Signal quality	Bandpass filtering	3	20.0%
High power consumption	Use of dual 9-V batteries, passive electrodes or rechargeable Li-ion batteries for dual power supply	2	13.3%
Signal transmission	Signal compression: new algorithm methods	2	13.3%
Bandwidth availability	Dynamic bit allocation scheme	1	6.7%
Cybersecurity	Better security through monitoring data in real-time, firewalls, anti-DDoS, SELinux and VPN	1	6.7%
Latency in real-time data transmission	Use of Fog computing architecture	1	6.7%

2.5 Discussion

This scoping review identified 15 published articles relevant to the research questions. While the scoping review considered articles published since 2006, most were published in the last 4 years. Technological advancements in society, in general, may explain this increase in articles. Alternatively, it may be due to the pursuit of technology development in more recent years to make telehealth a more frequent and feasible application to use. The COVID-19 pandemic has required physicians and other health care providers to adapt their means to

deliver health care quickly through the use of online tools and digital and virtual applications. Statistics have shown that in April 2020, almost half of the physicians in the United States started to use telehealth, up from 18% in 2018. One could assume that similar data could be seen globally (Xu et al., 2021).

The two countries with the most publications were Italy and the United States. Most of the remainder of the publications included in the scoping review was also from developed countries (Canada, Norway, and Japan), for a total of 60% of the articles published in developed countries (United Nation, 2014). This is consistent with studies that have shown that more programs have been attributed to telehealth in more developed countries. In 2019, it was estimated that the market for telehealth in the United States reached 43.4 billion dollars, with an annual growth rate of 17.7%. However, less effort has been put into telehealth in developing countries due to a smaller return on investment, a limited health care budget, and challenges due to limited technological infrastructure (Combi et al., 2016). Future research should explore the differences in barriers between developed and developing countries and how the availability of the technology, research funding, and socioeconomic factors influence the differences between the two.

2.5.1 Barriers to Virtual sEMG Assessments

The review revealed that the most common barrier to virtual EMG assessment reported in the literature was related to information technological infrastructure. The review characterized this as poor reliability of real-time data to remote locations and explained by the substantial amount of data collected. This barrier was reported in more than 50% of the studies. A significant concern was that poor reliability of real-time data could lead to wrong or delayed

diagnosis due to the inaccessibility of the data. When high volumes of data are being processed, transmitting data to a remote cloud server can cause high latency and network utilization.

Consequently, this may mean improper care for the patient and needless patient suffering.

Most commercial EMG systems use at least a 1000 Hz sampling rate. However, clinical data are typically in the range of 10 to 200 Hz range. Higher sampling rates provide an advantage to represent the amplitude of the EMG signal accurately. Nyquist theorem requires a minimum sampling rate that is at least twice the signal maximum frequency but also suggests that higher sampling rates give a better representation of the amplitude of the signal being sampled. A higher sampling rate will avoid missing essential data and better represent the amplitude envelope of your data. However, as mentioned, this creates high volumes of data processed and may cause this delay. It is also important to consider that there are two approaches you can use to transmit data. You can transmit data synchronously or asynchronously. Delay in asynchronous data is dependent on the duration of the measurement being made.

Phones, laptops, and tablets were used to measure EMG remotely in the study, all of which use different transmission paths. Most mobile and computing systems have the processing power necessary to transmit EMG data. Two approaches are widely used for wireless communication and were reported in the articles used in the scoping review. One approach is to use Bluetooth operating at 2.4 GHz and the other is ZigBee protocol operating at 902 MHz. Everyday microcontrollers are capable of communicating with both Bluetooth and ZigBee protocols. It is important to note that these different transmission paths may cause variations in the reliability of the real-time data being received remotely.

Some publications included wearable EMG devices as a rehabilitative intervention for neurological conditions (i.e., stroke). Wearable devices specifically are said to generate

substantial amounts of data. Unfortunately, health care systems may have inefficient databases to store or analyze a large capacity of information. Therefore, further technological advancements are required to address data collection and storage before these devices can efficiently be adopted (Aldekhyyel et al., 2021; Shah & Tomljenovic-Berube, 2021).

The second most reported barrier was poor patient usability or user-friendliness, reported in 40% of the articles, and unreliable real-time data, reported in 20% of the studies. The review reported that patients had difficulty attaching the EMG sensor to themselves or connecting the sensor to an application to self-monitor. Patient independence during the collection of EMG data remotely was challenging to achieve. This was primarily due to a lack of training before using the equipment. There is the risk that EMG data collection application without the direct involvement of the health care practitioner can lead to incorrect or incomplete data collection. These findings are consistent with what has previously been found in the literature regarding data collection obtained remotely with any medical devices in that usability is also a barrier, specifically for patients with any cognitive disability or low dexterity (Aldekhyyel et al., 2021; Shah & Tomljenovic-Berube, 2021). Elderly patients may also have difficulty reading the instructions to understand how to use the EMG device (Aldekhyyel et al., 2021; Shah & Tomljenovic-Berube, 2021). It is important to note that these barriers would only occur when data are being collected remotely or from the home to the clinic. In a clinic-to-clinic setting, the bandwidth of the clinic to acquire faster real-time data could easily be changed, and direct access to a clinician for assistance would improve user-friendliness.

2.5.2 Overcoming the Barriers to Virtual sEMG Assessments

Various solutions to overcome the barriers were proposed in the published articles. Patient usability was one of the most frequently mentioned barriers in the studies and, not surprisingly,

was the barrier in which most studies suggested ways to overcome this problem. This demonstrated that most studies focused on improving EMG virtual assessments centered around the patient's skill requirements. One solution to this barrier was increasing patient confidence and independence through prior training before use and technical support through regular videoconferencing. Another solution was implementing specific tips and techniques to collect EMG data independently, which was added progressively in certain applications for the specific concerns that participants brought forward. Some articles even proposed increasing patient engagement with their clinician by suggesting that clinicians remotely intervene directly with the software collecting EMG data using remote desktop features of the videoconferencing system.

User-friendliness was also mentioned in the articles, further highlighting that patient needs seem to be a priority in ensuring the success of virtual EMG assessments. This finding was expected because in telehealth providing exceptional patient usability and user-friendliness are essential to effective patient engagement and ensuring a positive patient experience. This aligns with the International Organization for Standardization definition of usability as “the extent a specific user can use a particular product or device to achieve goals of efficiency and satisfaction” (Aldekhyyel et al., 2021).

Telehealth will only be made possible if patients are willing to participate. Most individuals will choose the most convenient option when choosing between in-person or virtual health care. Therefore, to improve telehealth and its popularity, most articles tended to focus on improving the ease of use for the patient. One option is to design how EMG data are collected (i.e., user-friendly software and hardware) tailored to individual users' needs. As such, this could significantly improve patient participation and adherence (Aldekhyyel et al., 2021).

Poor reliability of real-time data was the most common barrier identified in the articles, yet very few articles proposed solutions to overcome this. This demonstrates a knowledge gap in the current literature. While studies raised this as a significant barrier that needs to be overcome to allow data to be transmitted efficiently without consuming a large amount of bandwidth, solutions have not yet been applied successfully.

Access to real-time data is important in certain clinical situations, such as obtaining a rapid result for immediate treatment or trying to synchronize a real-time assessment by video. Several articles described various EMG systems being developed and validated to address data reliability or to ensure that there is no delay in transmission in real-time. However, none suggested a hybrid approach where the preprocessed data would be sent in real-time and raw data asynchronously.

2.6 Strengths and Limitations

This scoping review identified articles of interest using two researchers who followed appropriate literature screening and study selection techniques. Data were extracted upon identifying relevant articles using a data extraction form designed a priori. The findings were grouped into similar themes. Disagreements between the reviewers were resolved by discussing and reaching a consensus.

Some limitations of the scoping review are worth noting. To start, the scoping review did not appraise the quality of the articles. Even if the goal of this scoping review was to identify the barriers and solutions of virtual EMG reported in the literature, and assessing the quality is usually not a component of a scoping review, quality assessments should be strongly considered before these findings are applied to

improving future virtual EMG assessments for patient diagnosis and monitoring. In terms of limitations regarding the quality of the scoping review, the search was limited to two databases and only articles published in English were included. This may have led to missed studies, causing biased results as it narrowed down the search and the variety of articles obtained.

Furthermore, 40% of the articles were from the United States or Italy, with only one publication (6.7%) in Canada. This may limit the generalizability of the findings to the countries of origin. A study done by Man et al. indicated a publication bias where articles were most likely to be published in high-ranking journals according to their English proficiency and the amount of funds available for research. This may directly impact the number of articles published by developing countries (Man et al., 2003).

Third, a broad search was conducted for any application involving virtual EMG assessments. Barriers to conducting EMG assessments may vary according to the condition being diagnosed or monitored. In addition, different conditions may have different needs and impairments, which would reflect specific barriers. For example, patients suffering from low dexterity due to stroke may have a more specific set of barriers, such as difficulty placing the electrodes (Agha et al., 2013). However, a broader inclusion was used to get a bigger picture of general barriers to virtual EMG assessments as there is still not much research on the subject and, therefore, limited search results. Furthermore, another limitation involves the increasing popularity of the telehealth field, which means that, as technology advances, other barriers may emerge according to such advances. It is important to acknowledge that the scoping review may only be

relevant for a few years as the technology becomes more sophisticated, the identified barriers are removed or mitigated, and others are created.

In addition, the EMG electrode was not placed in the same area for each study reviewed. Multiple layers of muscle affect its ability to detect deeper muscle activity. Using EMG is significantly compromised as there is cross talk between different muscles. There can also be two or three different muscles that are all firing and contributing to the signal. Therefore, muscle bundles can be tricky. Consequently, the quality of the signal does vary according to where it is located.

Finally, it is safe to assume that the time or length of the EMG data collected varied per article, although this was not specific. This may have created a considerable difference in bandwidth consumption and real-time data per study. Bandwidth consumption may also vary dependent on the number of EMG channels used in the articles. Most articles used one EMG channel, but some used up to four. This may create a larger bandwidth consumption for those that use more channels, creating a large barrier to virtual EMG use.

2.7 Conclusion

In conclusion, as technology progresses, more and more health care practitioners are using telehealth as a means to monitor and diagnose patients.

According to the published articles, the most commonly identified barriers to using virtual EMGs were poor patient usability of the device and signal and data transmission issues. This was followed by barriers which included high power consumption of battery-based systems and issues with cybersecurity.

Most articles solved the barrier of patient usability by adding very precise and interactive

instructions that would make it easier to follow remotely. To have more accurate real-time data, many articles proposed to include fog computing architecture to allow the periodic transmission of information. Signal compression techniques and bandpass filtering were also proposed. Furthermore, the high-power consumption of battery-based systems was overcome by changing the battery to dual 9-V or Li-ion batteries. Finally, articles suggested using firewalls, anti-DDoS, SELinux, and VPN for better cybersecurity.

Various solutions were proposed; however, further research is required to determine if these solutions have resulted in enhanced use of virtual EMGs and improved clinical outcomes for the patient. Future studies should also consider how to overcome data security in EMG virtual assessments, as there was limited information found during the review.

The results of the scoping review may be helpful to clinicians wishing to offer virtual EMG assessments. It may be used to improve clinical practice by developing best practices for using EMG virtually. It may lead to engineering research to improve virtual EMG. With constant advances in the technology used for telehealth, it is a question of time before many of the barriers to using EMG virtually become issues of the past.

Chapter 3. Development of a Portable Device for Virtual Spasticity Assessments

3.1 Introduction

Spasticity, which is a commonly seen complication in those suffering from neurological conditions such as stroke, spinal cord injuries, multiple sclerosis, cerebral palsy and traumatic brain injuries, usually requires a consultation with a specialist (Yee et al., 2023). Timely spasticity assessments and management are needed as the lack of proper assessments could result in the loss of joint range of motion, preventing or decreasing limb use of the affected limb. Thus, this may reduce the quality of life of the affected individual (Chang et al., 2013).

In-person health care assessments for patients who live in rural or remote communities are often inaccessible due to the travel costs to a specialist clinic or hospital in a city. They may also be inaccessible or challenging for patients due to their physical limitations or the need to be accompanied by a caregiver. These are considerable barriers for how patients access their treatments, and spasticity assessments need to be more accessible (Haleem et al., 2021). Virtual health technologies are an innovative option for offering rehabilitation services. In recent years, healthcare professionals have been able to provide specialized care and treatment plans by connecting virtually with patients, regardless of their geographical location or any in-person restrictions preventing them from easily accessing a clinic (e.g. limited mobility) (Haleem et al., 2021).

One of the many challenges of virtual health assessments for those suffering from spasticity is that there needs to be a way to replace information gathered with the current hands-on assessments clinicians use.

Current spasticity assessments require a clinician to subjectively "feel" for the "catch" and identify the responsible muscles while performing a series of movements to see if the patient requires Botulinum toxin injections (Peng et al., 2011). A "catch" in spasticity refers to involuntary contraction due to more rapid movement (van den Noort et al., 2009). The way the clinician evaluates the "catch" involves the Modified Ashworth Scale (MAS), which is used to measure increased muscle tone based on perceived resistance and elbow joint range of resistance during a passive stretch on a 6-point scale, where 4 means the affected limb is rigid to passive extension or flexion (Harb & Kishner, 2024; Yu et al., 2020). Another commonly used assessment is the Modified Tardieu Scale (MTS), which evaluates the velocity of a passive stretch graded on a scale from V1, which means it is as slow as possible, or V3, which implies it is as fast as possible. It grades the muscle reaction from 0 to 5, where 5 considers the joint immobile (Rivelis et al., 2024).

Many researchers have also questioned the validity of these scales as they are subjective. There is currently no objective way of measuring spasticity, making it difficult to assess this virtually without the presence of specialized clinicians (Skalsky, 2017). Consequently, research is needed to develop virtual tools for optimal, efficient, and convenient care.

Thus, a portable device using biomechanical data to inform clinicians about spasticity could be developed to address the barriers of virtual and objective spasticity assessments. This would make these virtual assessments feasible and improve their overall accuracy.

The Rehabilitation Robotics Lab at the University of Alberta developed a portable device based on the knowledge of what clinicians require during spasticity assessments. The device was based on a previous device built in the Rehabilitation Robotics Lab, the TONE device, by Ph.D. student Daniel Gillespie, whose objective was to develop a device that enables clinicians to evaluate biomechanical and neurophysiological data that allows them to understand spasticity objectively (Gillespie, 2023). The previous TONE device only recorded rectified sEMG data, while the device developed for this study recorded sEMG and AMG at the recommended 1000 Hz sampling rate used for routine assessments.

The device's intended use would be achievable with a hub-and-spoke clinic-to-clinic model. In this case, the patient being assessed in a remote clinic has a staff member or assistant with limited knowledge of spasticity to perform the assessment using tools that transmit relevant data under the guidance of specialists via videoconferencing.

In this paper, we report further development of TONE by considering whether acoustic (mechano-) myography (MMG) could replace the use of surface electromyography (sEMG) previously used in the original TONE device to monitor muscle activity when performing either the Modified Ashworth or Tardieu protocols. By doing so, MMG's relatively low bandwidth

requirements and user-friendliness can be adopted to accommodate real-world rural clinical settings.

This paper will discuss the design approaches and objectives used to create a portable device based on the TONE device. It will incorporate both an MMG and sEMG sensor to enable synchronous comparison for research purposes.

3.2 Clinical Context

3.2.1 sEMG, Goniometer and Force Sensor to Replace the MAS or MTS

To conduct spasticity assessments, clinicians rely on the MAS or MTS to evaluate muscle spasticity by “feeling” for a change in tone and a “catch.” Researchers recognize the limitations of the MAS or MTS, which relies on the clinician's subjective judgement and does not consider spasticity's velocity dependency. To build a device virtually, however, we need to find tools suitable for conducting these assessments virtually and giving clinicians information similar to their gold-standard test (Yu et al., 2020).

Electromyography. Muscle activity can be physiologically monitored with EMG, as it can record the electrical activity in response to a nerve stimulating the muscle during a contraction (Ladegaard, 2002). There are currently two methods for measuring EMG: intramuscular EMG and surface EMG. Intramuscular EMG employs electrodes made of typically 50-micron diameter stainless steel wires placed into a muscle guided by a hollow needle. In contrast, surface EMG is a non-invasive method using electrodes applied to the skin (Merletti & Farina, 2009; Mills, 2005). One benefit is the ability to use sEMG in various telehealth settings, increasing its accessibility for patients who require virtual spasticity assessments (Constantinescu et al., 2018).

sEMG may also be a helpful tool for evaluating spasticity specifically. sEMG is currently used and known for being able to investigate the pathophysiology that composes spasticity. More specifically, Yu et al. found that sEMG signals can inform researchers or clinicians about a patient suffering from spasticity's motor unit spontaneous discharges. Research has also shown that patients with spasticity have an increase in the amplitude of sEMG signals during passive stretch (Yu et al., 2020). Therefore, studies have shown that sEMG can allow us to gain information about muscle tone and “catch” through objective data. In current clinical applications, sEMG is used to assess gait for patients who have experienced a stroke. The electrodes can identify which muscles become activated during the gait cycle (Fujita et al., 2021). Consequently, current research has demonstrated that sEMG could be an excellent alternative for spasticity assessments to give clinicians similar hands-on information to the MAS or MTS.

Force sensors. Force sensors also help to overcome the lack of “feel” in virtual assessments that clinicians use to indicate when a “catch” occurs during a spastic contraction, permitting a more objective value to replace the MAS or MTS in a virtual setting. The “catch” in muscle spasticity gives clinicians a cue for the presence of increased muscle tone (Rosales et al., 2011).

Goniometers. A goniometer measures joint angles and monitors angular velocity during limb extension and flexion. It has been used clinically to assess spasticity, allowing clinicians to precisely measure the “catch's” joint angle during passive stretch. Goniometers provide very valuable information when conducting spasticity assessments virtually (van den Noort et al., 2009).

In conclusion, combining these tools can potentially improve the access and accuracy of spasticity assessments. Based on this research, a portable device that includes muscle activity sensors, force sensors, and a goniometer can be a suitable alternative to the MAS or MTS currently used in practice as it gives adequate and comparable measurements.

3.2.2 AMG Sensor as an Alternative to sEMG

Although sEMG can give us information about muscle tone and “catch” for spasticity assessment, it has several constraints in practice if used virtually. Before using sEMG, the skin must be prepared to provide good electrical contact. This entails surface preparation using an alcohol swab and often shaving to remove hair. Proper skin contact is necessary to lower the skin’s electrical resistance and improve the consistency of the sEMG signal (Türker, 1993). sEMG also has a minimum bandwidth requirement of 57.6kB for one EMG channel. If sampling rates are lower to accommodate limited available bandwidth, this may result in inaccurate data (Türker, 1993).

On the other hand, acoustic (mechano-) myography (MMG) has the potential to be a more user-friendly sensor as no skin preparation is required and bandwidth requirements are much lower. The AMG bandwidth requirement is found in the region of 4.8kB. Thus, this makes it readily available in most rural communities with internet or cell phone access. MMG can also be used without prior skin preparation or minimal skin contact (Ibitoye et al., 2014). MMG, therefore, has the potential to be more practical in settings where expert sEMG clinicians are not available.

Due to research done on the advantages of MMG sensors as opposed to sEMG, which has barriers when used in a telehealth setting, the revised version of the TONE system was designed to provide synchronous data from both an sEMG and an MMG sensor. Consequently, this would allow further research on how these two sensors may be comparable to evaluate muscle spasticity.

MMG transducers convert the vibrations generated by the muscle contraction into a signal. The sensors record the vibration of muscle fibres as they slide past each other during a contraction. MMG signals can be detected as a sound wave transmitted from the muscle through the soft tissues to the sensor or a physical vibration generated at the skin's surface. Thus, MMG records the mechanical events that occur during a contraction, whereas EMG monitors the electrical events of a contraction (Ibitoye et al., 2014; Roberts & Gabaldón, 2008). Microphones and accelerometers are two well-known MMG transducers that convert vibrations into signals. Microphones detect sound waves generated when a diaphragm sensor couples with the skin. The diaphragm is displaced by the vibrations generated by the sound waves, which produce an electrical signal because the minute displacement of the skin is associated with pressure waves generated by the contractions. On the other hand, accelerometers can detect this motion (AlMohimeed & Ono, 2020).

For this study, an ADXL 355 accelerometer was chosen as this type of MMG transducer as it is readily available, can be easily taped to the skin and is less sensitive to environmental sounds that can create artifacts (Campbell et al., 2017). Previous studies have also shown that accelerometers have a better signal-to-noise ratio compared to the other MMG transducer types (Talib et al., 2018). We used a tri-axial accelerometer on this device but only recorded data from

the axis perpendicular to the skin. Consequently, the portable device will compare the sEMG and acceleromyography (AMG) sensors.

3.3 Objectives of the Development of the Device

Based on the current clinical needs of spasticity assessments, the revised version of the TONE device includes a sEMG sensor, an AMG sensor, a force sensor and a goniometer having the following specifications:

3.3.1 Real-Time Data

The device should be able to display the real-time rectified sEMG sensor, force, and goniometer signal. Real-time data is a convenient way for the clinician to gain insight into a diagnosis and treatments during the assessment without any post-processing of the data required and match the signal generated by the sensors with visual observations. This would allow a more convenient use of the clinician's time and the opportunity to intervene early if necessary.

3.3.2 Raw Data Storage on an SD card

Second, the data obtained during these assessments should be stored on an SD card to enable comparison of the sensors' spectral signals by post-processing the raw data. Currently, the literature states that an sEMG signal's power spectrum allows visualization of the magnitude of the frequency components that represent the signal. Its composition relays information about the patterns of muscle activity influenced by muscle fibre types (fast and slow twitch), muscle fibre fatigue, motor unit firing rates, and the summation of different action potentials at the site where the electrode is placed (Fuglsang-Frederiksen & Rønager, 1988).

3.3.3 AMG as an Alternative Sensor

Lastly, an AMG sensor was added to find a more practical sensor to use in a telehealth setting, especially where bandwidth and clinical expertise are limited.

3.4 Device Development

3.4.1 Hardware Development

The device was built on two printed circuit boards. The first incorporated the AMG, wearable force sensor, and goniometer sensors, with the hardware built to send the data wirelessly to the Dashboard or store the raw data on the SD card. The second board contained an amplifier circuit for the sEMG electrodes (Figure 3).

The specific components of each sensor were the following:

- 1. *sEMG*:** The sEMG electrode used was an early version of the Delsys differential sEMG active electrode with an integral pre-amplifier and a 500 Hz low pass filter to avoid aliasing. The sensing surface of these electrodes is two 10 mm diameter stainless steel discs separated by a 20 mm stainless steel bar providing the ground.
- 2. *AMG*:** The AMG sensors used are 3D analog accelerometers. Therefore, they are sensitive to orientation relative to gravity. The AMG sensor is an ADXL 355 accelerometer (+-3g range). This range was chosen to avoid the orientation and movement of the sensor relative to gravity, causing it to saturate.

3. **Goniometer.** The goniometer is an electrical potentiometer.

4. **Force sensor.** The force sensor was designed specifically for this system according to the specifications provided by clinician colleagues. It can be worn on the hand of the clinician to take force measurements while the patient pushes up onto the force resistance to pick up the “catch” in patients with spasticity adequately. The force sensor incorporated two SEN-10245 force sensors. The signal conditioning circuit used for the force sensor was MIKROE-4658 by MicroEleletronika (Belgrade). The sensor was made using RTV silicon between two sheets of plexiglass. This allows the creation of a soft interface layer to the sensor material (Figure 4, 5).

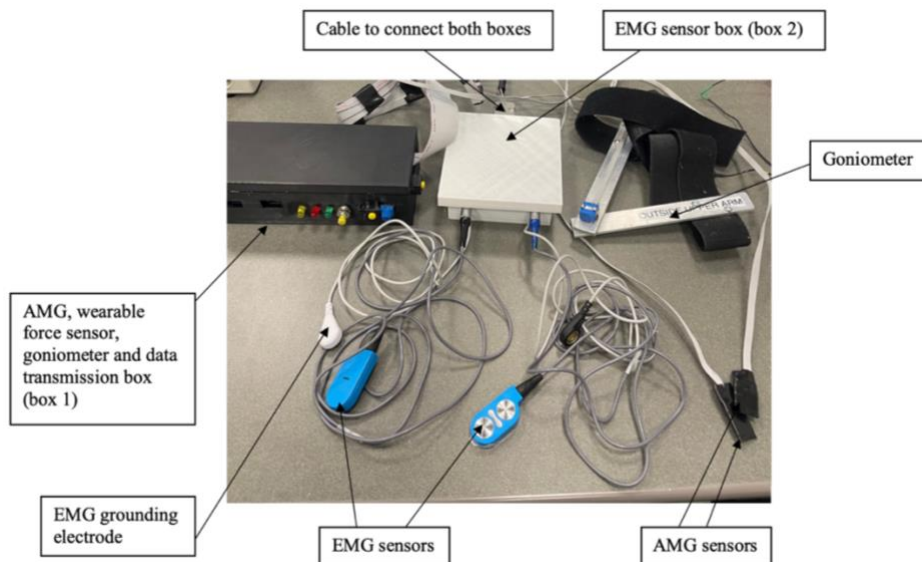


Figure 3. Overview of the portable device and its component parts.

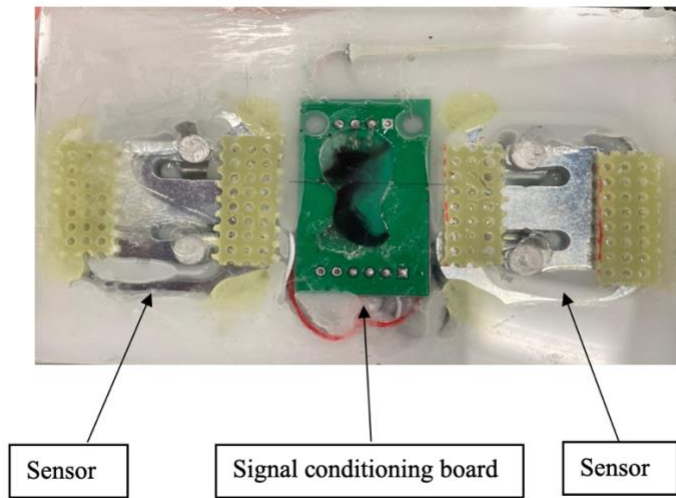


Figure 4. Overview of the inside of the force sensor. The arrows show the two sensors used on the board (SEN-10245) and the signal conditioning board (MIKROE-4658 by MicroElelektronika (Belgrade)).



Figure 5. Side view of the force sensors. Two plexiglass sheets, sealed with regular caulking silicon, contained the two sensors inside.

The Arduino programming language was utilized to obtain the data from a Feather M0 microcontroller (Adafruit, NY).

The portable device has one microcontroller that transmits data to the Dashboard via an XBee S1 802.15.4 module (Digi, Hopkins MN), receives it from a second microcontroller and XBee module, and stores the data on the SD card.

Circuit 1 comprised two Feather Adaloggers to allow raw data storage on the SD card. The SD card data stores elapsed time, raw sEMG and raw AMG data. The first Adalogger (A) allows storing high-frequency sEMG and AMG data on the SD card at a high sampling rate for precise data acquisition. On the other hand, the second Adalogger (B) permits transmitting the real-time data (i.e., rectified sEMG, force and goniometer data) to a Dashboard found on a laptop using the Xbee wireless transmission system. Adalogger B runs an independent program that shares the same analog inputs as Adalogger A. Consequently, it can sample more slowly to transmit data wirelessly using the Xbee transmitter to the laptop's Dashboard. The Xbee wireless transmitter also transmits the sEMG, force, and goniometer angle to the Dashboard (Figure 6).

Circuit 2 incorporated the sEMG electrode connections, the EMG signal processing amplifiers, the firmware, which included real-time rectification of the raw EMG signal and an XBee wireless transmitter that incorporated the rectified EMG, goniometer and force data. The EMG electrodes' pre-amplifier signals were further amplified, and an offset of about 1.6v was used to accommodate the bipolar nature of EMG and AMG by setting a trimmer to ensure the full sEMG signal was recorded. The inputs in this circuit were for two sEMG sensors and a force sensor pad.

Both the sEMG and AMG sensors were signal-conditioned through separate amplifiers. Once amplified, they input the microcontroller's AD converter channels. For the sEMG, the signal was connected to the AD converter channels of the SD card microcontroller and the Dashboard microcontroller. For the AMG, the signal was only recorded by the SD card microcontroller (Figure 7).

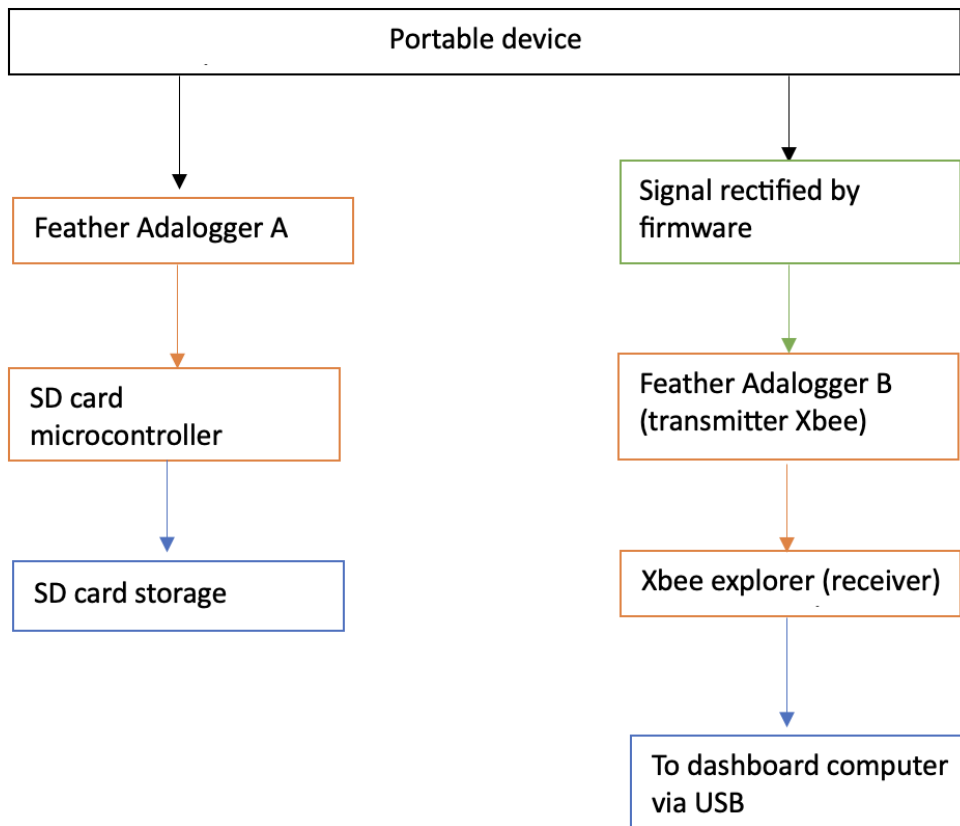


Figure 6. Summary of the steps in which the wearable device sends data to be received on the SD card and the Dashboard wirelessly in circuit 1. The orange boxes indicate the receiving and transmitting sequence. The blue boxes indicate the end device for collecting and obtaining data.

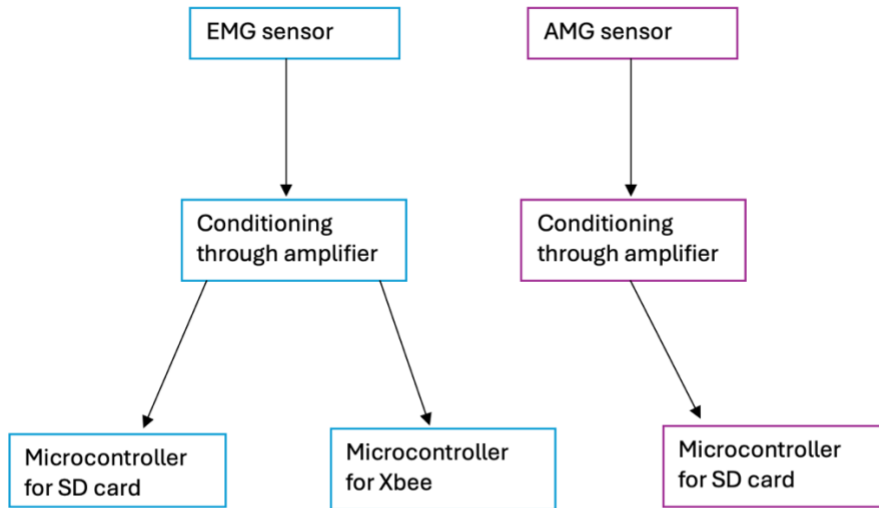


Figure 7. Summary of the steps in which the sEMG and AMG sensor data were transmitted to the microcontrollers.

3.4.2 Firmware Development

The device's firmware used the Arduino programming language (Adafruit: Ivrea, Italy). The sampling rate used a low-pass filter at 500 Hz and was sampled at a little over 1000 Hz on both microcontrollers. The data sent to the Xbees was transmitted at a 57600 baud rate.

Calibrations. The force sensor was calibrated with a force gauge. The force was placed on a flat surface, and the force gauge was applied with increased force over 5 data points. The calibration curve was plotted in Excel with the output force values (x-axis) against the force gauge values in Newton (y-axis). The linear equation from this plot was added to the programming software. Also, AMG sensor was calibrated by moving it according to three axes relative to reflect the x, y and z axes. The data obtained during the test was then plotted in Excel to ensure all three axes

were reflected. Furthermore, goniometer was calibrated to ensure its angle matched the set angles of a retractor. It was placed on a flat surface, and the retractor was placed on top of the goniometer. The protractor and goniometer were moved at 20-, 40-, 60-, and 80-degree angles according to the angle of the retractor. The calibration curve was then plotted in Excel with the goniometer values on the x-axis against the values of the retractor on the y-axis. The equation from the plot was added to the programming software.

Rectified sEMG. The Arduino programming software was used to rectify the sEMG signal on the microcontroller before the data was transmitted to the Dashboard or stored on the SD card. Consequently, this reduced the bandwidth requirements for wireless transmission to the Dashboard. While designing the device, the smoothing done with the microcontroller intended to use a conservative approach to prevent essential features that are needed to quantify spasticity from being eliminated. Since this device is designed for research purposes and to determine these features, a more conservative approach was taken until the research could confirm the necessary parameters.

3.4.3 Dashboard Interface

A dashboard interface was included to enable the signals generated to be transmitted over Zoom using screen sharing. The Dashboard allows the integration of all the information needed for clinicians to make informative decisions on a patient's spasticity. Furthermore, once data is observed in real-time, the information obtained is saved as an Excel sheet. The information provided by the Dashboard includes the rectified sEMG signals and the force applied to gain information on muscle tone and the “catch” of a patient with spasticity. It also consists of a

goniometer to give information on the angular velocity of the “catch” during extension and flexion.

The Dashboard was developed in C++ with Visual Studios (Microsoft: Redmond, WA). The goal was to read the data transmitted from the sensor system to an Xbee wireless receiver plugged into a desktop or laptop computer through a USB port. The serial data is encoded in packets by the Feather microcontroller, transmitted by the sensor system, received by an XBee receiver and then passed out by the dashboard software to be displayed in real-time on the dashboard application on the Windows-based computer. Force, goniometer, and sEMG readings were collected each time the loop was executed at 500 Hz. Raw EMG signals were averaged, creating an array of 10 values. This array was updated each time the loop was executed. Thus, average sEMG data was outputted to a wireless transmitter at about $1/10^{\text{th}}$ of the sampling rate. The sampling rate was chosen to ensure that the Dashboard was synchronized with the device and that there was no significant visible lag. The sEMG signal transmitted to the Dashboard was in rectified form as the bandwidth of the wireless system and the processing time of the simple dashboard software did not permit raw sEMG transmission at the sampling rate employed by the sensor system's microcontroller, which was four channels at 1.2kHz. The data file saved by the Dashboard was post-processed after it had been transmitted to the Dashboard using a 3rd order low-pass Butterworth filter with a cut-off frequency of 0.5 Hz. Each parameter was appropriately scaled and plotted against time (Figure 8).

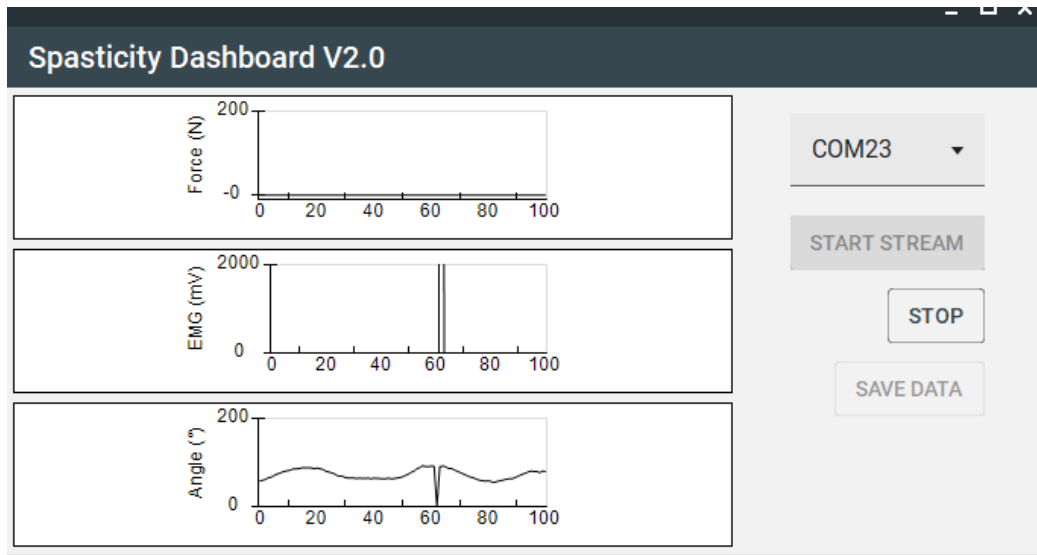


Figure 8. Representation of the real-time data available and shown by the Dashboard.

3.5 Discussion

The device allows researchers to evaluate whether goniometers, force sensors, and sEMG or AMG sensors give adequate information and can substitute for the currently used in-person assessment using the MAS or MTS. The intended use of this device is to research the most optimal way to conduct spasticity assessments using these tools for those who require them remotely.

A next generation device could incorporate many additional things to make it more clinically relevant. First, future studies would need to look into how clinicians could capture various ranges of motions, such as flexion or extension, to evaluate spasticity. One potential solution to this problem is for researchers to look into the incorporation of an Inertial Measurement Unit (IMU) sensor and how data could be incorporated in real-time. IMU sensors are nine-axis sensors that contain a three-axis accelerometer, gyroscope, and magnetometer. Thus, these sensors can measure linear acceleration, angular speeds and magnetic fields.

Currently, a standard procedure is used for joint angle measurements by an IMU sensor, as seen in studies similar to the one conducted by Seel et al., which proposed a strategy for joint measurements during gait analysis using an IMU sensor (Yi et al., 2021). Researchers would have to explore if this can be applied to a telehealth setting to give real-time, reliable data.

Currently evaluated using the MTS, joint angles can give clinicians an idea of the angle and angular velocity when the “catch” occurs, which can help indicate the severity of a patient's spasticity (Fujimura et al., 2022). Some clinicians may be required to evaluate particular joints that this device cannot target with the goniometer, such as hand spasticity or smaller extremities due to their small size. Measuring the joint angle of smaller joints, such as hands and fingers, may require the development of different computer applications or sensors to allow these assessments to occur virtually (Matsunaga et al., 2023). Heung et al. and other researchers have proposed a device that can estimate finger joint stiffness using a soft actuator, a type of robotic glove that is soft, flexible and portable. However, researchers are still determining if stiffness estimation is friendly for telehealth since it uses marker-based joint angle measurements (Matsunaga et al., 2023). Therefore, this may make the initial setup potentially difficult for these assessments. Other researchers have proposed the leap motion controller (LMC) as a replacement for this technology, a markerless hand and joint tracking device. Still, its accuracy has not been proven adequate for rehabilitation (Matsunaga et al., 2023). Future studies should look into a device or sensor that can seamlessly collect accurate information on joint angle and stiffness for the hand and finger joint that is user-friendly and easy to use in a virtual setting.

Furthermore, while some studies have performed sEMG muscle activity analysis for hand muscles or much smaller joints, such as sEMG applications for grasping objects, it is uncertain if this sensor could be used for spastic movements and if AMG is a suitable alternative (Jarque-Bou et al., 2021). The validity of this device for different joints and extremities would need to be studied individually to determine an appropriate protocol.

3.6 Conclusion

The portable device is intended to be used for future research to see if it provides the information required to facilitate virtual spasticity assessments. The device offers real-time data of important measurement tools that could potentially allow clinicians to make informed decisions during a patient spasticity assessment. This is an excellent device for research proposes to enable researchers to see if it is feasible. For example, future studies that would like to know if sEMG and AMG are comparable for virtual spasticity assessments. Consequently, this allows for more accessible spasticity assessments where patients are not required to travel to an in-person clinic. Furthermore, it allows for more objective, quantifiable ways to measure spasticity. The combination of wireless data transmission through a visual dashboard and high-frequency data acquisition makes it a valuable tool for physiotherapists, physicians and researchers.

Chapter 4. Comparison of EMG and AMG Using a Portable Device Designed for Virtual Spasticity Assessments

4.1 Introduction

Spasticity is a common condition for those suffering from neurological conditions. This condition requires timely assessments and management to prevent the decreased use of the affected individual's limbs (Chang et al., 2013). The Modified Ashworth Scale (MAS) is used to conduct these assessments. MAS is a 5-point scale to evaluate muscle tone based on the resistance of an individual's affected limb during passive stretch (Harb & Kishner, 2024). However, these assessments must be conducted in person. In-person spasticity assessments may be challenging for those who live in rural communities due to the associated cost and length of travel. It may also be a challenge for those who have physical limitations. Thus, there are significant barriers to how patients with spasticity access these essential assessments.

Many researchers have studied how to conduct these assessments virtually efficiently. Some have suggested robotic-assisted methods for the autonomous evaluation of spasticity, while others have used surface electromyography (sEMG) to determine involuntary muscle activity due to spasticity (de-la-Torre et al., 2024; Guo et al., 2022; Xie et al., 2020). Many have stated that sEMG is a helpful tool to determine spasticity characteristics as it demonstrates muscle fibre characteristics for a spastic muscle through increased amplitude and fibre type detection.

4.1.1 Slow and Fast Fiber Types

Observing muscle fibre recruitment is an excellent way to study what occurs during muscle contractions. There are three major types of muscle fibres: slow twitch or type I fibres, fast twitch/intermediate or type IIa fibres, and fast twitch or type IIb fibres. These fibre types have different endurance capacities.

Slow twitch fibres have a high endurance and a slow contraction speed, which is why they are referred to as having an oxidative metabolism. These fibres have a higher concentration of myoglobin, consequently allowing them to have an increased ability to transport oxygen (Soames, 1993). Thus, they can undergo sustained use during a muscle contraction as they produce more energy, but their force production is usually relatively low, making them better for aerobic activities.

On the other hand, fast-twitch type IIb fibres will undergo fatigue at a much faster rate but will produce a much larger force (Melhorn, 1999). Therefore, they are well suited for short or fast activity bursts that require less oxygen than slow fibres. There are two different types of fast fibres. Fast-twitch type IIa fibres have an oxidative metabolism and glycolytic properties; thus, they can fatigue less quickly than type IIb fibres and generate a stronger force than slow-twitch fibres (Melhorn, 1999).

4.1.2 Muscle Fibre Type Changes in a Spastic Muscle

For those with spasticity, the histopathology of spastic muscles shows slow fibres are predominant, whereas there is a deficiency in fast fibres (Gorgey & Dudley, 2008; Ito et al., 1996). The reason is that fast fibre types are more vulnerable than slow fibre types to microtraumatic damage (Olsson et al., 2006).

4.1.3 sEMG Slow and Fast Fibre Detections on Power Spectra

Power spectra allow us to convey information about the patterns of muscle activity. This includes motor activity influenced by motor unit potentials, muscle fibre fatigue and motor unit firing rates (Fuglsang-Frederiksen & Rønager, 1988; Lievens et al., 2020; Vukova et al., 2008).

Previous studies have found that lower frequency components of power spectra are associated with slow muscle fibres, and higher frequency components represent fast muscle fibre activity (Grimby & Hannerz, 1977). Fatigue-induced changes alter the frequency content of power spectra for sEMG. In this case, we see an increase in low-frequency content. Researchers have found that these differences develop much quicker in fast fibres than in slow fibres (Fuglsang-Frederiksen & Rønager, 1988; Vukova et al., 2008). The literature has indicated that since sEMG shows the electrical activity of a muscle, it needs to adapt to the loss of fast-fibre motor neuron activity during a sustained contract by replacing them with slow-fibre motor neurons. Thus, slow and fast fibres are seen in the sEMG power spectrum and can be used to evaluate muscle fatigue and, potentially, muscle spasticity by observing the concentration of fast fibres (Fuglsang-Frederiksen & Rønager, 1988; Vukova et al., 2008).

However, it has been found that sEMG has some constraints if used in a telehealth setting, making it an unideal candidate for virtual spasticity assessments. The most considerable constraint is its ease of use. Since the skin must be cleansed before its use, and sEMG requires good skin contact, this may lead to inaccurate data collection if these steps are not followed adequately (Türker, 1993). There is also a very high bandwidth requirement when using sEMG. Consequently, large amounts of processed data may lead to slow or delayed real-time data, which clinicians must access for timely spasticity assessments (Türker, 1993).

4.1.4 Acoustic (Mechano-) Myography Sensors as an Alternative to sEMG

Acoustic (mechano-) myography sensors (MMG) have feature extraction capabilities similar to sEMG devices, including time and frequency domain feature extractions. However, it does not have some of the barriers sEMG presents (Krueger et al., 2014). It can be used without skin preparation and with minimal skin contact. It requires a much lower bandwidth requirement. Thus, this sensor is more user-friendly and has the potential to be used without an expert clinician present, delivering faster, more reliable real-time data (Krueger et al., 2014).

Researchers have concluded that using MMG frequency domains to generate power spectra may give insight into the firing rates of motor units. It has been speculated that MMG power spectra also contain information regarding slow and fast fibres. Previous investigators have suggested that the high-frequency components between 15 and 60 Hz in an MMG give us information on fast twitch motor units. Below 15 Hz, the power spectrum of an MMG could provide information about slow-twitch motor units (Beck et al., 2007). However, researchers are still determining, due to the nature of MMG and its ability to reflect the mechanical output of the muscle instead of its electrical activity, if it is less sensitive to detecting frequency components of muscle activity. Thus, further research is required to confirm these speculations (Woodward et al., 2019).

Currently, two commonly used MMG sensors have been studied extensively in the literature. The first is microphones, which can detect skin displacements during a contraction. The second type of MMG sensor is the accelerometer sensor, which detects skin surface displacements when muscles contract and thus can measure the acceleration of the x, y and z axes (AlMohimeed & Ono, 2020). These are commonly referred to as acceleromyography sensors (AMG). For the purpose of this research, an AMG is the type MMG sensor used due to

its lightweight design, low signal-to-noise ratio, and reliability in terms of the signal it can pick up (Talib et al., 2018).

4.1.5 Purpose and Objectives

This paper aims to explore if the sEMG and AMG sensors are comparable in the way they are able to detect features that occur while the muscle contracts. A portable device was designed at the Rehabilitation Robotics Lab at the University of Alberta based on the previous TONE device designed by Daniel Gillespie, a former PhD Rehabilitation science student. The device offers real-time, and stored sEMG and biomechanical data obtained from electronic goniometers and force sensors. It also includes the data from an AMG sensor. Daniel Gillespie had already compared how the biomechanical data of goniometers, force sensors and sEMG is manifested under spastic conditions (Gillespie, 2023). However, it has not yet been determined if AMG could be substituted for sEMG as a sensor to evaluate muscle spasticity.

Therefore, the first part of the study involved a muscle fatigue test to determine if similar information about muscle fibers can be picked up by the AMG sensor. Hence, this will allow us to conclude if slow and fast fibers are recruited on an AMG power spectrum, similar to what is observed on an sEMG sensor, by observing if similar shifts to lower frequency are observed during muscle fatigue.

To determine if AMG could pick up slow and fast fibers the following research question was addressed:

Do the trends in the characteristics of the power spectra for sEMG and AMG differ in detecting a significant change in slow and fast fibre ratios generated by inducing muscle fatigue?

The research question will be answered using the following hypotheses:

Null hypothesis: There is no significant change in the ratio of slow to fast muscle fibre recruitment represented by the frequency peaks in their power spectra with muscle fatigue.

Alternative hypothesis: There is a significant change in the ratio of slow to fast muscle fibre recruitment represented by the frequency peaks in their power spectra with muscle fatigue.

The second part of the study involved testing the consistency (variance) of sEMG and AMG in obtaining the slow-to-fast fibre ratios represented by the peaks in the power spectra between participants when conducting an isometric contraction repeatedly.

Since it was established that the AMG and sEMG sensors represented slow and fast fibre recruitment, a pilot study was conducted on 3 participants to determine if sEMG and AMG sensors could pick up characteristics of muscle spasticity when comparing the affected and the non-affected arm during active and passive movements. A passive stretch exercise was used to evaluate the passive movement as the literature has already established that sEMG can detect spasticity through increased rectified amplitude (Nazmi et al., 2016). Therefore, this exercise would allow us to determine if AMG can pick up spasticity characteristics through a rectified amplitude change similar to sEMG. Furthermore, the active movement to determine spasticity characteristics was chosen as an isometric contraction during this test. Studies have found that sEMG signals recorded under isometric conditions are commonly used clinically to classify muscle fatigue and neuromuscular diseases. Thus, the third part of the study aimed to see if accurate and quantifiable data could be obtained to evaluate and see signs of muscle spasticity,

specifically in the time and frequency domain, and if the data was comparable between both sensors.

4.2 Methodology

4.2.1 Optimal Sensor Placement Location

A pilot test was conducted to ensure the optimal location for the sEMG and AMG sensors on the upper extremities, allowing for the best data and optimal comparison between both sensors.

The sensor was placed on the upper bicep, lower bicep, and forearm muscle belly. A single participant was asked to perform an isometric contraction by putting their arms under a table at 90 degrees and pushing upwards onto the resistance to generate a maximum voluntary contraction (MVC). They were asked to hold this contraction for 5 seconds.

The raw data was plotted and rectified using MATLAB. The data was filtered using a second-order Butterworth filter. For the sEMG, the filter had a low-pass filter of 5 Hz and a high-pass filter of 0.05 Hz. On the other hand, the AMG sensor had a low-pass filter of 2 Hz and a high-pass filter of 0.1 Hz.

The results showed that the upper biceps give a more distinct signal for sEMG with an amplitude of about 225 mV for the upper bicep, whereas the lower bicep only has an amplitude of over 150 mV (Figure 9, Figure 10). On the other hand, the raw AMG signal appears to be less sensitive to position. It is important to note that we assumed the contraction strength stayed

relatively the same. In conclusion, this test confirmed that an adequate signal is more likely on the muscle belly upper bicep and this position was chosen for the measurements taken in this study.

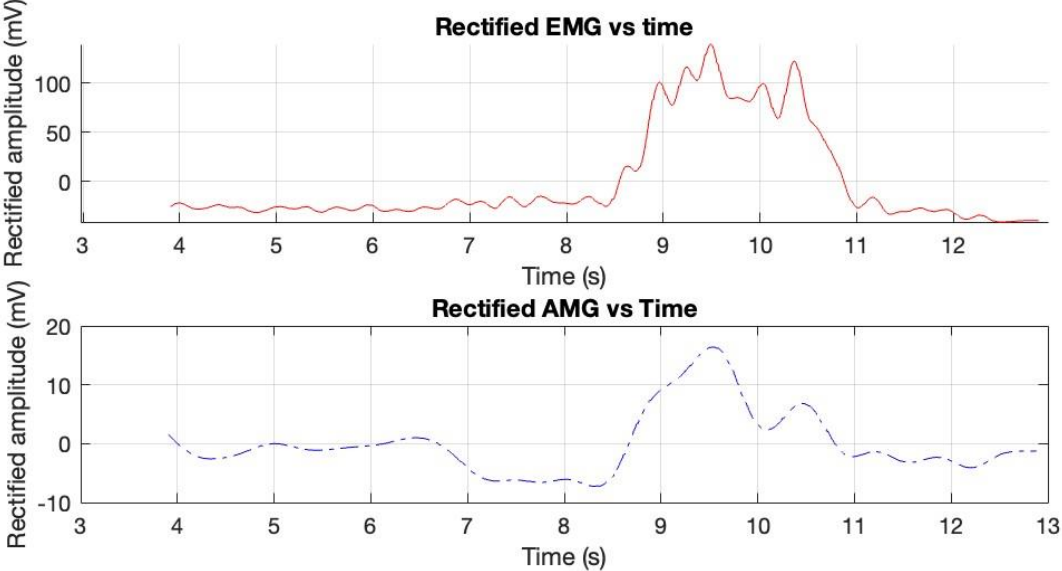


Figure 9. Rectified sEMG and AMG against time during isometric contraction for a MVC in the lower bicep.

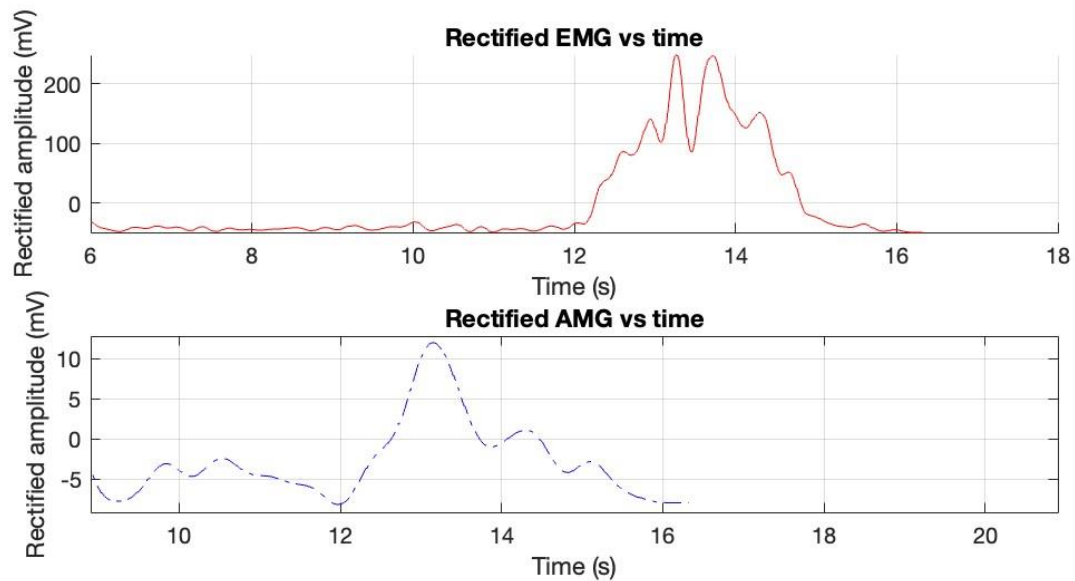


Figure 10. Rectified sEMG and AMG against time during isometric contraction for a MVC in the upper bicep.

4.2.2 Muscle Fatigue Test

Participant recruitment. The Rehabilitation Robotics Lab at the University of Alberta in Edmonton, Alberta, was the study's recruitment, advertising, and data-gathering site. This study recruited and included 10 participants.

Inclusion criteria. The study's participants were required to be older than 18 to be included. They must comprehend the instructions, which may be achieved by alternative means or by using a translation in case language is an obstacle. Participants must have a complete upper limb range of motion and show no signs of spasticity or prior diagnosis.

Exclusion criteria. Participants with a history of central nervous system injury or additional diagnoses were not eligible to participate in this study.

Experimental protocol. The sEMG and AMG sensors were positioned to record data simultaneously in the muscular belly of the biceps brachii. Alcohol wipes were used to prepare the skin before placing the sEMG sensors. An EMG sensor grounding pad was also placed on the elbow. The electrodes on the bicep were held in place, allowing optimal skin contact with pro-wrap.

During the data collection, participants were instructed to sit in a chair with their joint angles maintained at 90 degrees. They rested their arms on a stool to retain their joint angles at this position.

For data collection, participants were instructed to push upward against a fixed resistance without moving their arms, performing an isometric contraction. In this instance, a table in front of them served as the resistance by placing their hands under the table when they pushed upwards. They were instructed to press as hard as possible against the resistance to execute their MVC. Participants were asked to hold their MVC until they felt tired and could no longer hold the contraction. While holding their MVC, they were timed for the time it took to feel fatigued.

Data analysis. Using a MATLAB program written for this study, a frequency analysis based on Fast Fourier Transforms (FFT) of the data was used to generate a power spectrum for each of sEMG and AMG signals. The peaks in the spectrum were associated with those reported in the literature for the recruitment of slow and fast fibre of sEMG. The amplitudes and frequencies of these peaks were calculated as ratios as muscle fatigue set in. The sEMG and AMG data Excel sheet was divided into five equal epochs in the contraction burst, representing the progression of muscle fatigue. The greatest fatigue was anticipated to occur at the end of the contraction or the

highest epoch number. A linear regression was plotted to determine if the frequency and amplitude ratios change as muscle fatigue progresses, and the epoch number grew was used to confirm this.

The MATLAB program was used to generate the power spectra for the five epochs for sEMG and AMG, and data was then plotted as a power spectrum. sEMG and AMG were plotted at a sampling frequency of 1258 Hz and filtered using a 2nd-order Butterworth filter. The two peaks were identified once these were plotted as a power spectrum. The two peaks for sEMG represent slow fibres at the lower frequencies and fast fibres at the higher frequencies. The amplitude and frequency of both peaks were recorded using MATLAB, which was used to select the two peaks and find the maximum values of each peak (Figure 11, Figure 12). Once recorded, the slow-to-fast fibre ratio was calculated for the frequency and amplitude.

Once slow-to-fast fibre ratios (low-frequency peak 1 to high-frequency peak 2) were calculated, both the amplitude and frequency ratios for each epoch per participant were transferred to SPSS for analysis. A repeated measures ANOVA was conducted for both sensors for the amplitude and the frequency ratios of the different epochs for the sample of 10 participants.

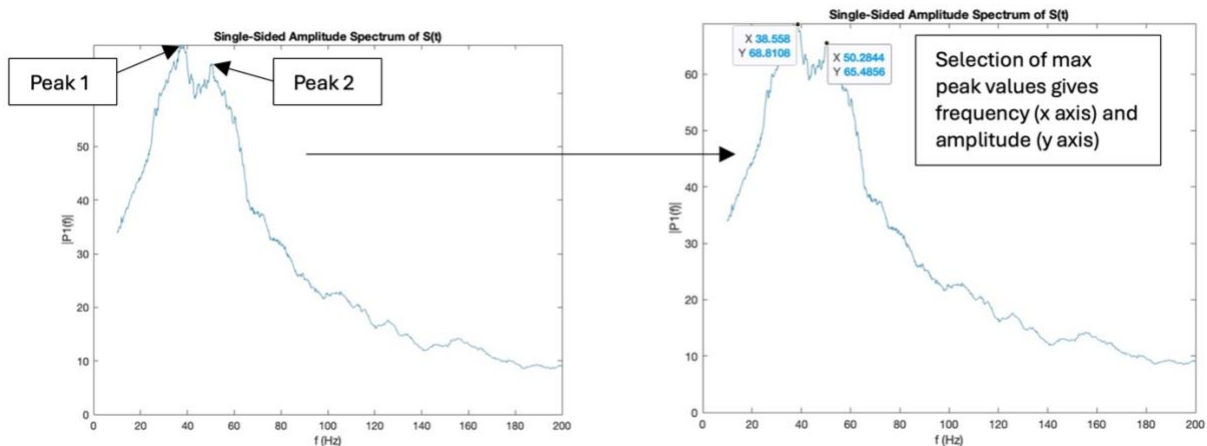


Figure 11. Demonstration of how the frequency and amplitude values were recorded using MATLAB for the sEMG power spectrum.

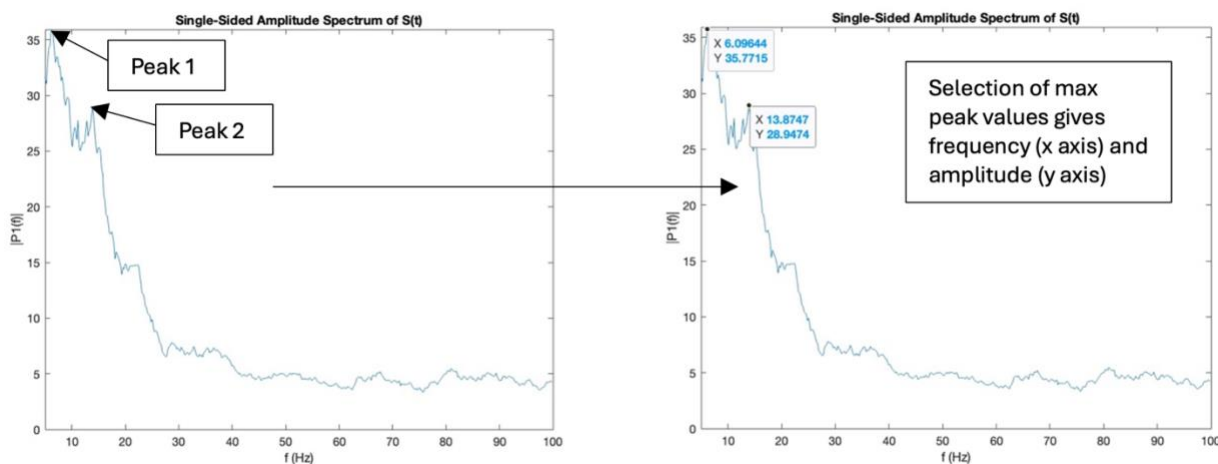


Figure 12. Demonstration of how the frequency and amplitude values were recorded using MATLAB for the AMG power spectrum.

4.2.3 Reliability Test

Participant recruitment. The study data collection location, recruitment, and advertising occurred at the Rehabilitation Robotics Lab at the University of Alberta in Edmonton, Alberta.

Ten participants were recruited and included in this study.

Inclusion criteria. The participants in this study had to be over 18 years old. They were also required to understand the instructions through a translator if language was a barrier or through other means. Participants were required to have a full range of motion in the upper limbs with no previous diagnosis or indication of spasticity.

Exclusion criteria. Participants were excluded from the study if they had an additional diagnosis or previous injury to the central nervous system.

Experimental protocol. The sEMG and AMG sensors were placed on the muscle belly of the biceps brachii EMG to record data simultaneously. Before applying the sEMG sensors, the skin was prepped using alcohol wipes. A grounding pad for the EMG sensor was also placed on the elbow. Pro-wrap was used to hold the electrodes on the bicep and allow for good skin contact. During data collection, participants were asked to sit on a chair and maintain their joint angle at 90 degrees with the help of a stool placed beside them.

Participants were first asked to perform an isometric contraction for data collection by pushing upwards onto a stable resistance without moving the arm. In this case, the resistance was underneath a table in front of them. They were asked to perform their MVC by pushing as hard as they could on the resistance. The participant was asked to hold this contraction for 5 seconds. Participants repeated this isometric contraction five times at MVC.

Data analysis. The slow-to-fast fibre ratio for sEMG amplitude and frequency and AMG

amplitude and frequency were collected for all 10 participants. This was done through their power spectra generated on MATLAB, using the same methodology as the muscle fatigue test in chapter 4.2.2. The mean and standard deviation between subjects were calculated for both sensors using the ratios.

Consequently, this allowed us to see how reliable the two sensors were in detecting the slow and fast fibres by calculating the percentage of the coefficient of variation using the following formula:

$$\frac{\text{standard deviation}}{\text{mean}} \times 100$$

4.2.4 Test on Patients With Post-stroke Spasticity

Participant recruitment. The study data collection location, recruitment, and advertising occurred at the Glenrose Rehabilitation Hospital in Edmonton, Alberta. Three post-stroke spasticity participants were recruited and included in this study. The sample size was chosen as a proof-of-concept study to get a baseline idea of how sEMG and AMG would be used to evaluate spasticity in stroke patients and determine a suitable protocol for future studies.

Inclusion criteria. The participant must be over 18. Participants would be included if they had a hemorrhage or ischemic stroke producing an upper motor syndrome resulting in documented problems of spasticity in the upper limbs. Also, the participant had to communicate effectively, with the help of a third person, completing answers on their behalf when required.

Exclusion criteria. Participants were excluded if they had causes of spasticity other than stroke

(e.g. multiple sclerosis, spinal cord injury, etc.). Participants were also excluded if they presented with dementia, confusion, delirium or significant cognitive impairment. Furthermore, those with generalized disorders of muscle activity (e.g. myasthenia gravis, Lambert-Eaton syndrome, amyotrophic lateral sclerosis) or any other significant peripheral neuromuscular dysfunction were excluded.

Experimental protocol. Similarly to the other two studies, the sEMG and AMG sensors were placed on the muscle belly of the biceps brachii to record data simultaneously. The same skin preparation measures were taken to ensure good skin contact and limited skin impedance of the sEMG sensor.

Participants were asked to sit down while a research assistant helped maintain their joint angle at 90 degrees.

Participants were first asked to perform a series of movements using their non-affected arm. They were first asked to push upwards onto the research assistant's hand, which acted as a resistance to generate an isometric contraction at MVC. They repeated this exercise 5 times. Participants were then asked to relax their arms, and with the help of the research assistant, their arm was passively extended five times.

Participants were asked to repeat these two sets of movements one more time using their affected arm with the help of the research assistant.

Data analysis. Data was analyzed using MATLAB for a single trial. Power spectra for the isometric contractions of the affected and non-affected arms for sEMG and AMG were generated on MATLAB using the same methods and parameters as the muscle fatigue test in chapter

4.2.2.5. MATLAB was also used to generate a signal-to-noise ratio for sEMG and AMG. This was done by taking the root mean square of the sensor at baseline and then the root mean square of the contraction.

The root mean square formula is the following:

$$\sqrt{\frac{1}{n}\sum x^2}$$

Where n is the number of measurements and x represents each value.

Then, the signal-to-noise ratio was calculated by dividing the root mean square of the contraction by the root mean square of the baseline to the signal-to-noise ratio.

To calculate the signal-to-noise ratio in decibels (dB), the following formula was used:

$$20 \times \log_{10} \left(\frac{\text{root mean square of contraction}}{\text{root mean square of baseline}} \right)$$

For the passive stretch movement, data for the sEMG and AMG of the affected and non-affected arms was rectified using MATLAB. The data was plotted at a sampling frequency of 1258 Hz and filtered using a 2nd-order Butterworth.

4.3 Results

4.3.1 Muscle Fatigue Test

The study included 10 participants, four males and six females, with an average age of 25 ± 5 . Slow and fast fibre ratios for the amplitude and frequency of the sEMG and AMG were calculated per epoch per participant.

Mean amplitude and frequency plot. The mean amplitude and frequency ratios for both sEMG and AMG for each epoch were plotted against participant number. The results demonstrated that mean sEMG and AMG frequency and amplitude ratios tend to increase as the epoch number increases when observed between participants (Figure 13, Figure 14, Figure 15, Figure 16).

Linear regression. A linear regression was plotted to represent the frequency and amplitude ratio changes as the epoch number increased for both sensors. The results indicated that the linear regression of the frequency ratio with change in epoch number appeared to indicate a moderate correlation for sEMG and a strong correlation for AMG based on Chan et al. interpretation of Pearson's correlation coefficient (Akoglu, 2018). In this case, sEMG has an R^2 value of 0.5 or an R-value of 0.7, and AMG has an R^2 value of 0.6 and an R-value of 0.8 (Figure 17). Chan et al. have indicated that a correlation coefficient of 0.7 indicates a moderate correction, and 0.8 is a very strong correlation (Akoglu, 2018). For the results regarding the linear regression of the amplitude ratio with a change in epoch number, the correlation coefficient for sEMG remained the same. In contrast, the AMG correlation coefficient appeared weaker than those for frequency ratios. sEMG had an R^2 value of 0.4 and an R-value of 0.7. Meanwhile, AMG had an R^2 value of 0.5 and an R-value of 0.7 (Figure 18). Thus, both sEMG and AMG had a moderate correlation of the amplitude ratio change with epoch number.

Repeated measures ANOVA. A repeated measures ANOVA was conducted on SPSS to address the following hypotheses:

Null hypothesis: There is no significant change in the ratio of slow to fast muscle fibre recruitment represented by the frequency peaks in their power spectra with muscle fatigue.

Alternative hypothesis: There is a significant change in the ratio of slow to fast muscle fibre recruitment represented by the frequency peaks in their power spectra with muscle fatigue.

The repeated measures ANOVA was done as four separate tests, which are listed as follows:

- sEMG amplitude ratios for each epoch
- sEMG frequency ratios for each epoch
- AMG amplitude ratios for each epoch
- AMG frequency ratios for each epoch

All epoch ratios for each of the four tests were tested to ensure they were normality distributed using the Kolmogorov-Smirnov and Shapiro-Wilk tests. It was also confirmed that no outliers existed in the dataset for each epoch ratio for the different tests. Lastly, if sphericity was found in the dataset, the Wilks' Lambda test was used to determine significance. Sphericity was found in all tests except for the AMG amplitude ratios test, in which the Greenhouse-Geisser correction was used to assess significance. An alpha or significance level of 0.05 (95% confidence level) was used. The results of each test are summarized in Table 8.

Based on the results obtained during the repeated measures ANOVA, we can conclude that since the $p < 0.05$ in all cases, we have statistically significant effects between the slow and fast fibre ratios for either the amplitude or frequency of both sensors during various epochs

between participants. Therefore, we reject the null hypothesis for all tests. Consequently, we can conclude that we observe a significant difference between slow and fast fibre frequency and amplitude ratios for both sensors through muscle fatigue.

Table 8. Summary of the significance values for each different test of the repeated measures ANOVA.

Test type	Significance value
sEMG amplitude ratios	0.004*
sEMG frequency ratios	0.001*
AMG amplitude ratios	<0.001*
AMG frequency ratios	0.004*

**Indicates a significant result at a confidence level of 95%*

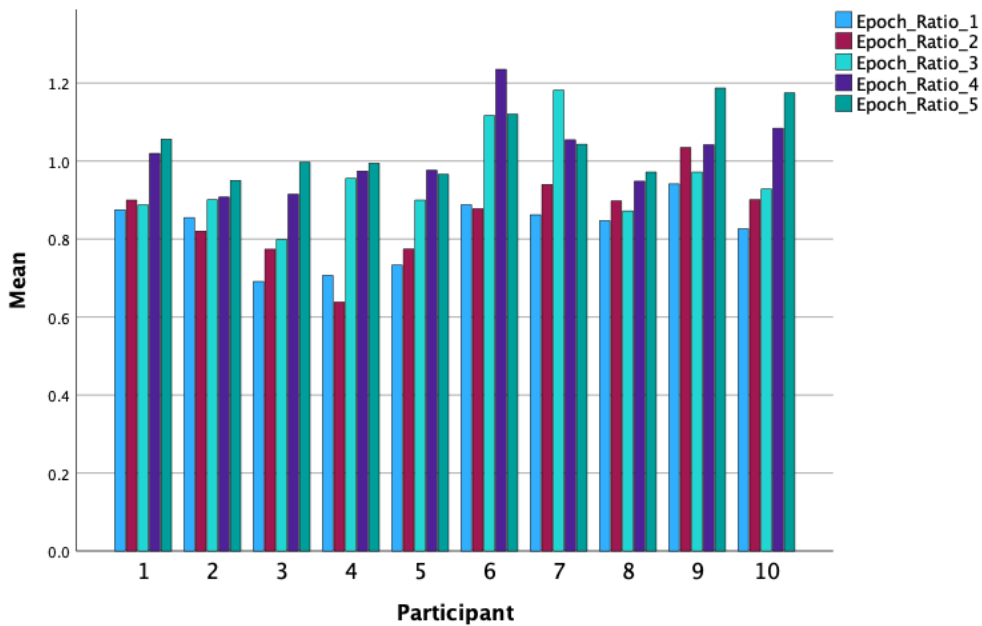


Figure 13. Mean sEMG amplitude ratios over five epochs while the muscle is being fatigued in a sample of 10 participants. The contraction was divided into five equal epochs.

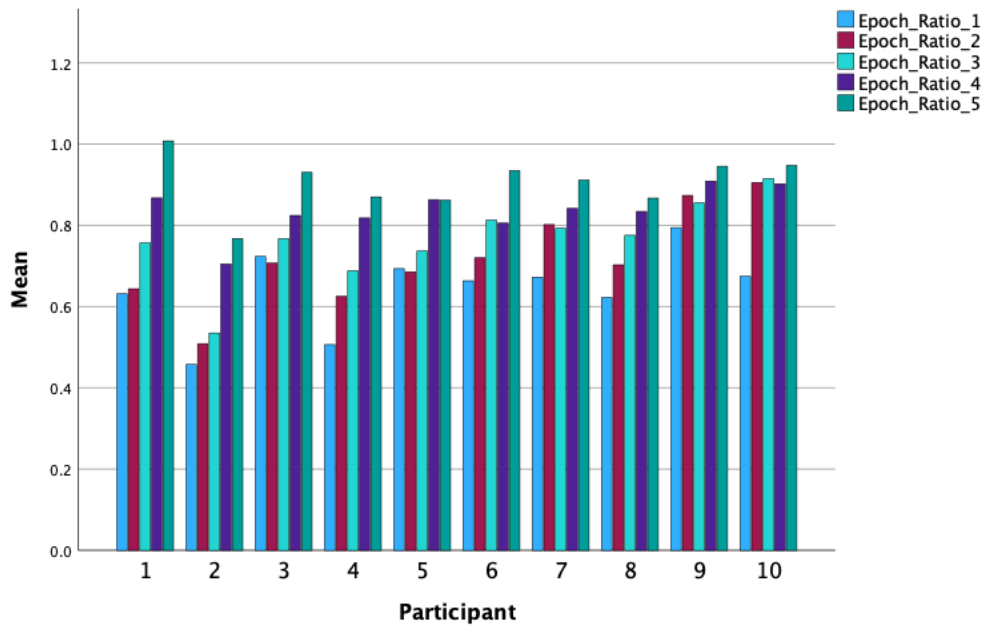


Figure 14. Mean sEMG frequency ratios over five epochs while the muscle is being fatigued in a sample of 10 participants. The contraction was divided into five equal epochs.

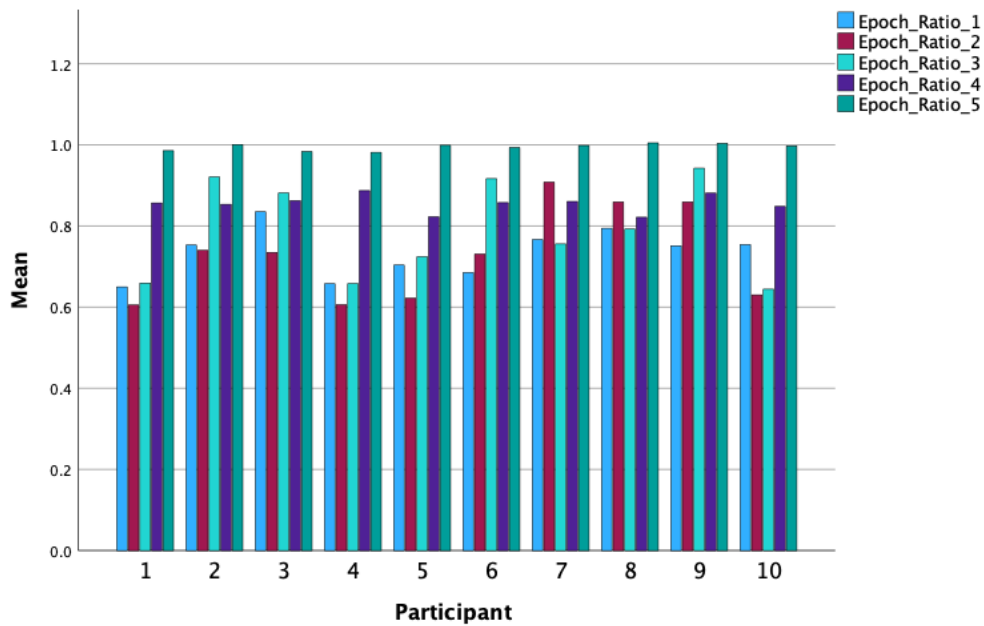


Figure 15. Mean AMG amplitude ratios over five epochs while the muscle is being fatigued in a sample of 10 participants. The contraction was divided into five equal epochs.

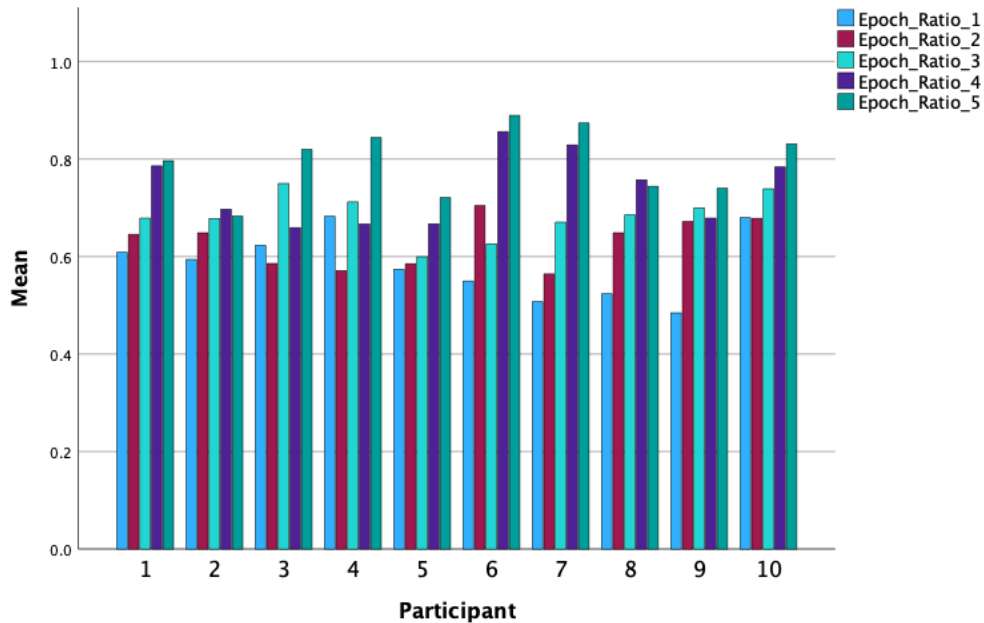


Figure 16. Mean AMG frequency ratios over five epochs while the muscle is being fatigued in a sample of 10 participants. The contraction was divided into five equal epochs.

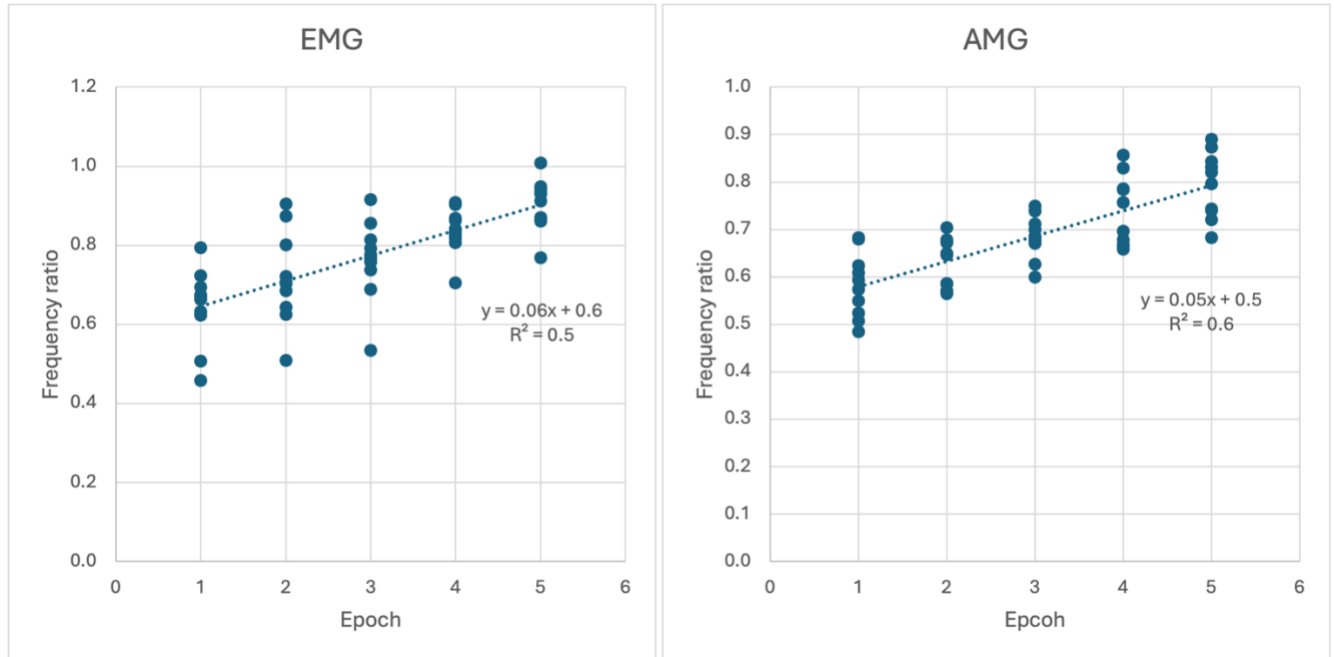


Figure 17. Side-by-side comparison of the linear regression for the frequency ratio change per epoch for the sample of all 10 participants for both the sEMG and AMG sensors.

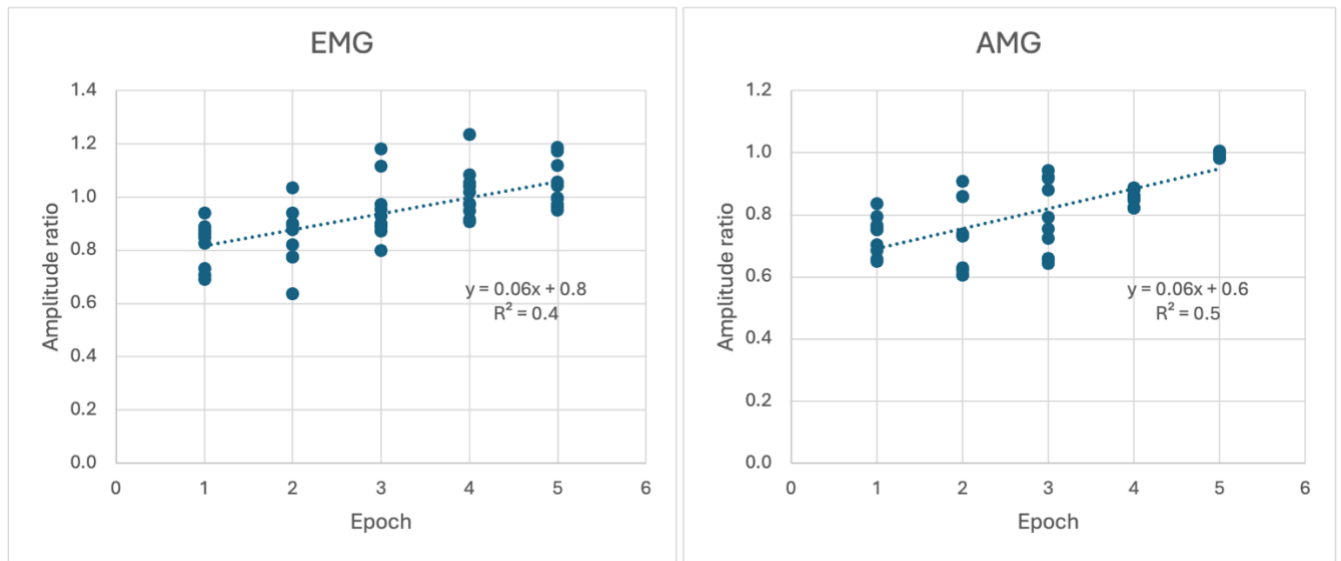


Figure 18. Side-by-side comparison of the linear regression for the amplitude ratio change per epoch for the sample of all 10 participants for both the sEMG and AMG sensors.

4.3.2 Reliability Test

The study included 10 participants, five males and five females. The average age of the studied participants was on average 25 ± 5 years.

The raw data showed that the sEMG slow fibre frequency ranged from 28.3 to 71.8 Hz, and the fast fibre frequency ranged from 45.0 to 95.3 Hz. On the other hand, the AMG slow fibre frequency ranged from 5.0 to 10.1 Hz, and the fast fibre frequency ranged from 8.8 to 18.3 Hz.

A reliability test was done to test the coefficient of variation for both sensors' slow-to-fast fibre ratio amplitudes and frequencies for all five trials between participants. Consequently, this would evaluate the dispersion of the data around the mean. Thus, this would allow us to determine if one sensor has less variability or a lower coefficient of variation and is, therefore, more reliable than the other. It was seen that the coefficient of variation for sEMG and AMG amplitude ratios are relatively the same. The sEMG coefficient of variation was 28.1%, and the AMG coefficient of variation was 27.3% (Table 9).

However, the coefficient of variation for the sEMG frequency ratios is a bit smaller, at 17.7%, whereas the AMG coefficient of variation is 20.2%. This indicates that there may be less variability in how sEMG detects slow and fast fibre frequency ratios compared to AMG (Table 9).

Table 9. Summary of the coefficient of variation for each different test.

Test type	Coefficient of variation (%)
sEMG amplitude ratios	28.1
sEMG frequency ratios	17.7
AMG amplitude ratios	27.3
AMG frequency ratios	20.2

4.3.3 Test on Patients With Post-stroke Spasticity

Three people with upper extremity post-stroke spasticity participated in the study. It consists of one male and two females with a mean age of 68.3 ± 2.9 years, with a mean time since stroke diagnosis of 10.6 ± 8.4 years (Table 10). It is important to note that some participants received Botulinum toxin injections to help decrease joint and muscle stiffness.

Active movement test. A series of active movements were first used to evaluate spasticity characteristics. Results for the isometric movement showed that both sEMG and AMG did not have fast fibres in their arm affected by spasticity for all participants in the study. However, the slow fibre frequency remained present for sEMG and AMG in both the affected and non-affected arms. Mostly, the affected arm in sEMG seemed to have lower slow fibre frequency ratios than the non-affected arm. In contrast, the AMG slow fibre frequency ratio seems consistent for all participants (Table 11, Table 12). Furthermore, the signal-to-noise ratio was used to evaluate a

signal amplitude change. In this case, we saw that for both sEMG and AMG, the signal-to-noise ratio and the signal-to-noise ratio in dB were lower for the affected arm than the non-affected arm across all participants (Table 13, Table 14).

Passive movement test. Second, a passive movement was used to determine spasticity characteristics. The participants were also asked to perform a passive stretch movement, in which the rectified signal was plotted against time in seconds. For the rectified data, in Participant 1, we saw an increase in the amplitude of sEMG data for the affected arm of about 50 mV compared to the non-affected arm, which had an amplitude of around just above 0 mV (Figure 19, Figure 20). Similarly, for the AMG data, there was an increase in the amplitude of the rectified AMG signal for the affected arm with an amplitude of around 10 mV. In contrast, the non-affected arm amplitude remained just above 0 mV (Figure 19, Figure 20). In Participant 2, the sEMG rectified amplitude did not appear to increase for the affected arm, and it seemed as though it remained relatively the same as that of the non-affected arm at around 50 mV (Figure 21, Figure 22). However, the AMG rectified amplitude increased from around 0 mV in the non-affected arm to 10 mV in the affected arm. Lastly, for Participant 3, the sEMG rectified amplitude appeared to increase for the affected arm at around 100 mV from around 0 mV in the non-affected arm. Similarly, for AMG, there seemed to be an increase in amplitude for the affected arm to about 15 mV, compared to the non-affected arm, which remained at around 2 mV (Figure 23, Figure 24).

Table 10. Summary of participant characteristics.

PARTICIPANT NUMBER	SEX (MALE OR FEMALE)	AGE (YEARS)	AFFECTED SIDE (LEFT OR RIGHT)	TIME SINCE STROKE DIAGNOSIS	SEVERITY OF SPASTICITY (MILD, MODERATE OR SEVERE)
1	Male	70	Left	11 months	Moderate
2	Female	70	Right	15 years	Severe
3	Female	65	Right	16 years	Moderate

Table 11. Summary of the slow and fast fiber frequency of sEMG for the affected and non-affected arm of each participant.

<i>PARTICIPANT NUMBER</i>	AFFECTED ARM		NON-AFFECTED ARM	
	<i>Slow fiber frequency (Hz)</i>	<i>Fast fiber frequency (Hz)</i>	<i>Slow fiber frequency (Hz)</i>	<i>Fast fiber frequency (Hz)</i>
<i>1</i>	28.38	Absent	37.5	54.1
<i>2</i>	21.7	Absent	29.2	49.5
<i>3</i>	12.5	Absent	29.8	35.0

Table 12. Summary of the slow and fast fiber frequency of AMG for the affected and non-affected arm of each participant.

<i>PARTICIPANT NUMBER</i>	AFFECTED ARM		NON-AFFECTED ARM	
	<i>Slow fiber frequency (Hz)</i>	<i>Fast fiber frequency (Hz)</i>	<i>Slow fiber frequency (Hz)</i>	<i>Fast fiber frequency (Hz)</i>
<i>1</i>	9.74	Absent	10.9	15.8
<i>2</i>	11.5	Absent	8.0	13.0
<i>3</i>	8.6	Absent	8.8	12.8

Table 13. Summary of the signal to noise ratios of sEMG for the affected and non-affected arm of each participant.

<i>PARTICIPANT NUMBER</i>	AFFECTED ARM		NON-AFFECTED ARM	
	<i>Signal to noise ratio</i>	<i>Signal to noise ratio (DB)</i>	<i>Signal to noise ratio</i>	<i>Signal to noise ratio (DB)</i>
<i>1</i>	1.1	0.5	1.5	3.8
<i>2</i>	1.1	0.8	3.9	11.9
<i>3</i>	1.1	0.5	1.3	3.5

Table 14. Summary of the signal to noise ratios of AMG for the affected and non-affected arm of each participant.

<i>PARTICIPANT NUMBER</i>	AFFECTED ARM		NON-AFFECTED ARM	
	<i>Signal to noise ratio</i>	<i>Signal to noise ratio (DB)</i>	<i>Signal to noise ratio</i>	<i>Signal to noise ratio (DB)</i>
<i>1</i>	1.1	1.1	1.3	2.5
<i>2</i>	1.1	1.2	1.3	2.5
<i>3</i>	1.3	2.9	1.5	3.1

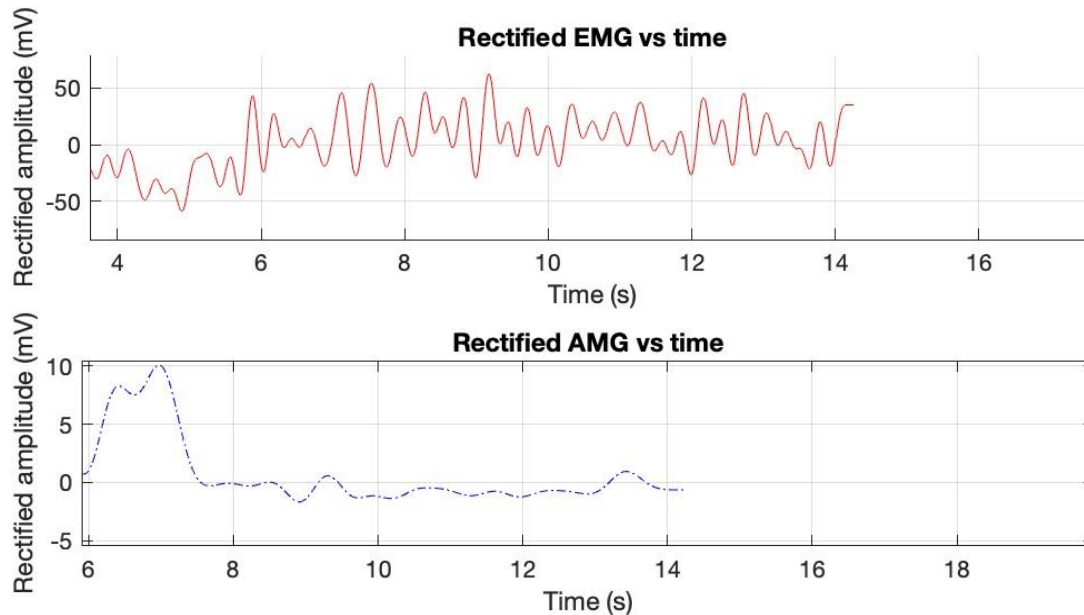


Figure 19. Rectified amplitude of the affected arm of the first participant. The top graph represents the sEMG signal and bottom graph represents the AMG signal.

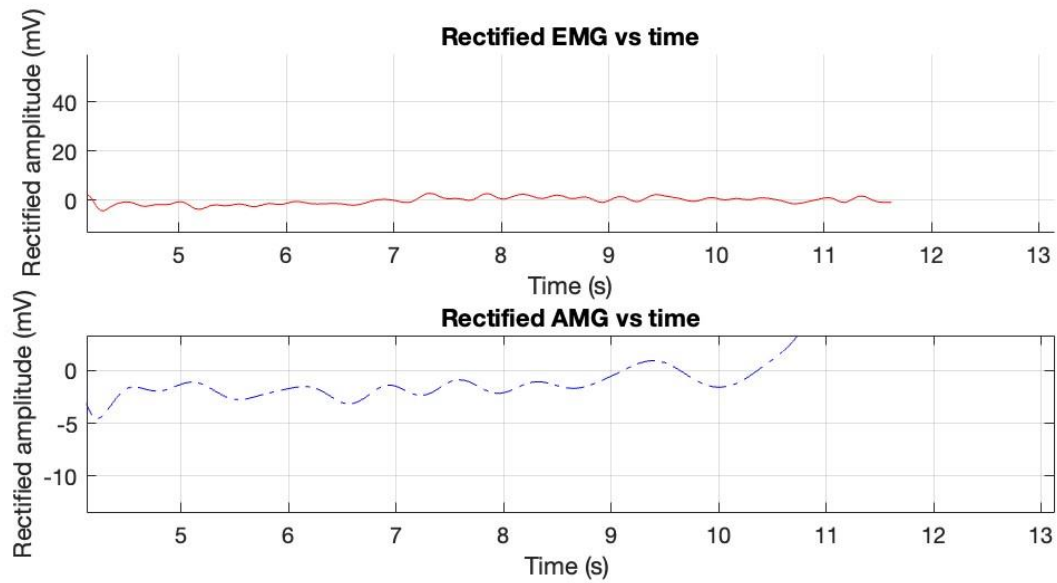


Figure 20. Rectified amplitude of the non-affected arm of the first participant. The top graph represents the sEMG signal and bottom graph represents the AMG signal.

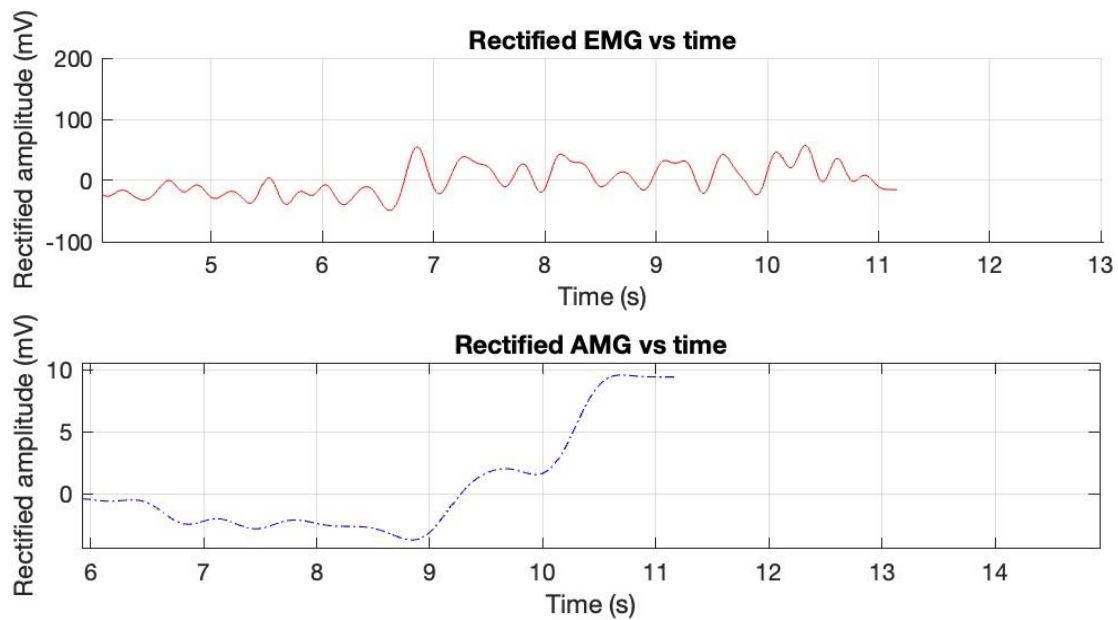


Figure 21. Rectified amplitude of the affected arm of the second participant. The top graph represents the sEMG signal and bottom graph represents the AMG signal.

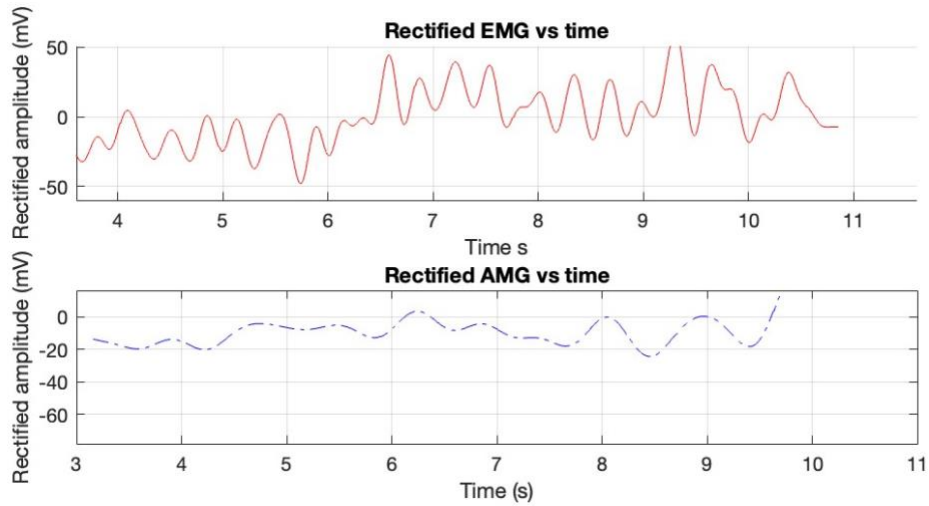


Figure 22. Rectified amplitude of the non-affected arm of the second participant. The top graph represents the sEMG signal and bottom graph represents the AMG signal.

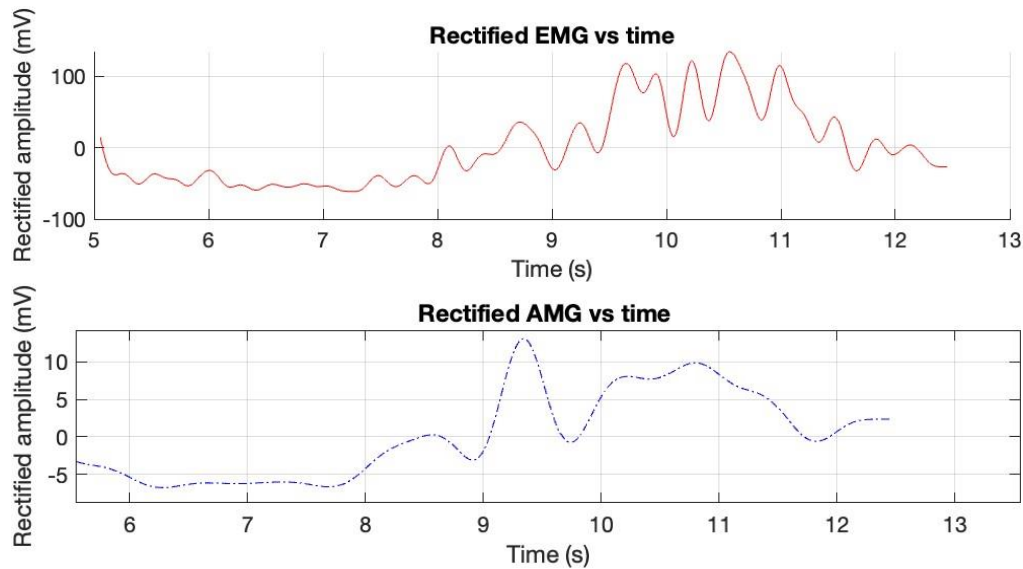


Figure 23. Rectified amplitude of the affected arm of the third participant. The top graph represents the sEMG signal and bottom graph represents the AMG signal.

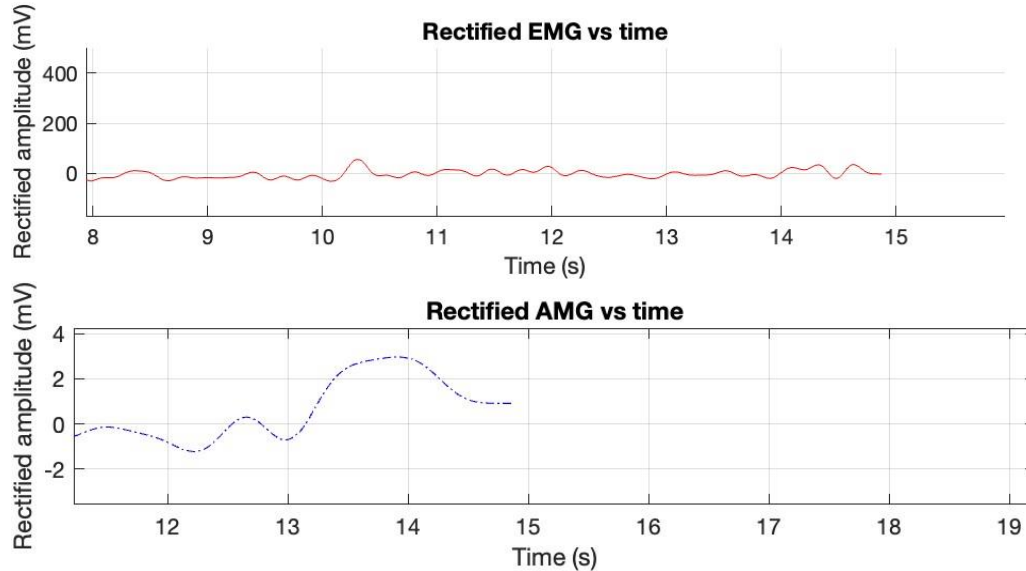


Figure 24. Rectified amplitude of the non-affected arm of the third participant. The top graph represents the sEMG signal and bottom graph represents the AMG signal.

4.4 Discussion

4.4.1 Muscle Fatigue Test

The muscle fatigue test was used to compare sEMG and AMG to see if, similarly to sEMG, AMG can pick slow and fast muscle fibres, which can be detected on power spectrums to evaluate the physiology of muscle contractions. Power spectra may be an excellent way to assess muscle spasticity as they allow clinicians to gain information on motor unit recruitment and muscle fibre types for active and passive contractions in sEMG (Fuglsang-Frederiksen & Rønager, 1988).

Muscle fatigue would allow us to confirm if AMG can detect differences in slow and fast muscle fibre spectral peaks by determining if a similar pattern to sEMG is observed, where the fast fibre frequency content decreases as muscle fatigue progresses. The muscle fatigue contraction burst was divided into five epochs, where the last five epochs would indicate the

most fatigue state. For the purpose of this study, the slow-to-fast fibre frequency and amplitude ratios were used. As fatigue progresses, we expect frequency ratios to be closer to 1 since the fast fibre frequency is shifting to lower frequencies and getting closer to the slow fibre frequencies. In this case, the results showed that sEMG and AMG demonstrated similar trends in which both their mean frequency ratios increased as fatigue (or epoch number) increased for all participants (Figure 13, Figure 14).

A linear regression test was also conducted to determine if there is a correlation between the amplitude or frequency ratio and an increase in epoch value in the sample of 10 participants for both sensors. Based on the interpretation of Chan et al., results demonstrated that sEMG had a moderate correlation between the epoch number and frequency ratio ($R=0.8$). In contrast, AMG had a strong correlation ($R=0.8$) across all participants. For the correlation between the amplitude ratios and epoch number, sEMG ($R=0.7$) and AMG ($R=0.7$) had moderate correlations across all participants (Akoglu, 2018). This indicates a good indication of a strong or moderate relationship between sEMG and AMG sensors as epoch number or fatigue increases from both amplitude and frequency ratios. Therefore, this further allows us to conclude that there is a relationship between muscle fatigue and changes or increases in frequency and amplitude ratios. Furthermore, during the repeated measures ANOVA test, it was determined that the frequency ratios for both tests indicated a significant difference between epochs numbers and ratio for the entire sample of 10 participants for both sensors, with a $p<0.05$ (Table 8). Thus, we can reject the null hypothesis and confirm a change in the frequency ratio of slow to fast muscle fibre spectral peaks with muscle fatigue. This demonstrates a shift to lower frequencies of fast fibres for both sensors during muscle fatigue. This has been established in the literature for sEMG, where researchers have found that fatigue shifts the frequency content of power spectrums to low-

frequency content for fast fibres (Fuglsang-Frederiksen & Rønager, 1988).

Similarly, for the amplitude ratios of sEMG and AMG, we would also expect the slow-to-fast fibre ratio to increase and get to a value closer to 1 as fatigue progresses. The reasoning behind this is that previous studies have found that fast fibre muscles will generate higher power over a short period of time (Lievens et al., 2020). Also, slow-fiber motor units have fewer fibres in the muscle, whereas fast-fiber motor units have more fibres present (Gollapudi et al., 2014). Thus, we expect fast fibre to have a higher amplitude than slow fibre types under non-fatigued conditions as they generate more power. However, as the muscle fatigues, the amplitude of fast fibres on the power spectrum is expected to decrease as fewer fibres will be recruited (Gollapudi et al., 2014). On the graphs plotted, we saw a trend where the mean ratio amplitudes for each epoch in the population tended to increase to a higher ratio, closer to 1, as fatigue progressed (Figure 14, Figure 15). In addition, the repeated measures ANOVA showed that the difference between the epoch number and amplitude ratios for both the sEMG and AMG sensors was significant ($p < 0.05$) (Table 8.) Hence, we can reject the null hypothesis and conclude that there is a change in slow-to-fast fibre amplitude ratios. Consequently, this would mean that the fast fibre amplitudes are generating less power and are generating power closer than what you would typically expect in a slow fibre muscle type. Thus, both sEMG and AMG are comparable in that they show a similar trend to what you would expect based on the muscle's physiology.

In summary, AMG demonstrates the same trends in its ability to recruit slow and fast muscle fibres detected in a power spectrum based on our ability to visually see both peaks and the same trends we expect in the literature for sEMG when the muscle fatigues. This indicates the peaks display characteristics of slow and fast fibres. Hence, this allows us to confirm that AMG is comparable to sEMG in the way it can accurately pick up slow and fast fibres when the

muscle contracts.

4.4.2 Reliability Test

Based on the data obtained in the reliability test, we can confirm what previous researchers have suggested about the frequency components of MMG. Researchers have previously speculated that the high-frequency components of MMG, found between 15 to 60 Hz, give information about fast fibres. Whereas its low-frequency components, below 15 Hz, give information about slow fibres (Beck et al., 2007). The raw data showed that the AMG slow fibre range was below 15 Hz, ranging from 5 to 10 Hz in this study. Furthermore, the fast fibre range was found around the researcher's speculated range, but it was much lower than anticipated, ranging from 8.8 to 18.3 Hz. On the other hand, for sEMG, the literature has stated that its frequency components would be found between 0 to 40 Hz for slow fibres and from 60 to 260 Hz for fast fibres (Hegedus et al., 2020). The raw data showed that the sEMG slow fibre range was from 28.3 to 71.8 Hz, and its fast fibre range was from 45 to 95.3 Hz. Both the fast fibre and slow fibre ranges for sEMG did not correspond to the ranges found in the literature, with a very large range presented in the slow and fast fibre frequencies. These differences observed in the sEMG and AMG sensors could have been because of the type of contraction, muscle type and contraction force. Researchers have found that for sEMG specifically, the power spectrum frequency increases with the force of the contraction due to the fibre type content (Bilodeau et al., 1990). Humans also have different fibre types in their different muscles. Consequently, this leads to the different muscles' force-generating capabilities to vary (Von Tscharnner & Nigg, 2008). A study by Bartuzi et al. also confirmed that the frequency on a power spectrum differs based on the muscle type, which influences the percentage of fast and slow fibres. The researchers found that the frequency and power spectrum shape changes between muscle types

(Bartuzi et al., 2007). Due to the wide range of factors that influence an sEMG power spectrum content, further tests would need to be conducted to determine if this is the adequate fast fibre frequency range for AMG based on various contraction types and muscles used.

A reliability test was conducted to determine whether or not sEMG or AMG appeared to be comparable in their consistency to detect slow-to-fast fibre ratio frequencies and amplitudes through their coefficient of variance. The coefficient of variance determines the dispersion of the data around the mean. If their coefficient of variance differed from each other, this would make one sensor more reliable than the other. The reliability test was conducted for each of the five isometric contraction trials done for the sample of 10 participants. In this case, the conditions of the trials did not vary, but the testing conditions remained the same. The results showed that the sEMG and AMG sensors were relatively similar in detecting amplitude, with a coefficient of variation of 28.1% for sEMG and 27.3% for AMG. However, there was a difference in the sEMG and AMG frequency ratios, where sEMG had a smaller coefficient of variation of 17.7%, and the AMG coefficient of variation was 20.2%. Although more precise statistical tests are required, when comparing the reliability of the frequency ratios between sEMG and AMG, EMG appears to have less dispersion around the mean and may be more reliable in detecting slow and fast fibre frequencies. However, future studies are required to compare these sensors' reliability and the consistency of their measurements. One way this could be done is through test-retest reliability using the intraclass correlation coefficient (ICC) (Weir, 2005). For example, a study by Meagher et al. tested the reliability between changes in MMG signals against sEMG signals during different levels of forces in a test re-test reliability study (Meagher et al., 2020). A similar test could be done to test the reliability of AMG against sEMG during different levels of muscle fatigue to confirm which sensor is more reliable in terms of the measurements it provides.

4.4.3 Test on Patients With Post-stroke Spasticity

The previous tests established that sEMG and AMG seem to be comparable in terms of their ability to pick up slow and fast fibre characteristics in a power spectrum. Although sEMG appeared to be a bit more reliable in its ability to detect power spectrum peak frequency ratios, more studies are required to confirm what this hypothesis suggests and to determine if there is a significant difference between the reliability of sEMG and AMG that would have an effect on the data transmitted to clinicians. Overall, AMG seems like a promising tool for use in a telehealth setting. Thus, a slow and fast fibre test, signal-to-noise ratio test, and change in amplitude test were conducted to see if both sensors could identify and pick up characteristics that could be used to evaluate spasticity. The slow and fast fibre test and the signal-to-noise ratio test would determine if sEMG and AMG are comparable in detecting spasticity characteristics during active movements. On the other hand, the change in amplitude test would determine if they were comparable during passive movements.

Slow and fast fibres. A test was conducted to evaluate whether power spectra would indicate spasticity in sEMG and AMG sensors. In those with spasticity, there is a predominance of slow fibres and a deficiency of fast fibres (Gorgey & Dudley, 2008). Thus, clinicians could use this knowledge to determine if a muscle is spastic by observing if these muscle fibres are in a power spectrum. The study's results showed that sEMG and AMG did not appear to have fast fibre activity based on their power spectra peaks on the arm affected with spasticity. sEMG also demonstrated power spectrum peak frequencies associated with slow fibres and lower frequency ratios on the affected arm compared to the non-affected arm (Table 11, Table 12). AMG may be

an excellent substitution to evaluate muscle spasticity virtually as it can detect slow and fast fibres through power spectra and obtain information on the difference that occurs in a spastic muscle. A future study must determine if these results are consistent across a large sample of participants.

Signal-to-noise ratio. Finding the signal-to-noise ratio could also help evaluate spasticity. A higher signal-to-noise ratio would indicate that the baseline (or noise) value differs greatly from the signal's amplitude. Thus, this measurement may be used to determine if there is a consistent contraction. In spasticity, the muscle constantly contracts, even at rest (Rivelis et al., 2024). Hence, we expect to see a low signal-to-noise ratio if a deliberate contraction is attempted if the muscle displays spasticity, as the constant contraction does not lead to a large difference between the baseline and the amplitude of the force-generated contraction. The results showed that sEMG and AMG had lower signal-to-noise ratios in the arms affected by spasticity (Table 13, Table 14). This is a good indication that a lower signal-to-noise ratio, obtained through RMS values, may detect spasticity characteristics. However, a more robust study that evaluates the range in which you would expect to see these signal-to-ratios for patients with spasticity needs to be conducted. Also, studies would need to determine if the non-affected and affected arm signal-to-noise ratios are statistically different from each other for both the sEMG and AMG. A large sample size would give us a better indication of whether this is an appropriate extraction tool.

Change in amplitude. It has already been established in the literature that sEMG can detect spasticity through the rectified data it picks up during a passive stretch movement. Studies have demonstrated that in sEMG, the amplitude will increase for post-stroke spasticity patients,

indicating an increased stretch reflex response (Xie et al., 2020). Consequently, each participant in this study underwent a passive stretch movement to evaluate if, similarly to sEMG, the AMG rectified data showed an increase in amplitude in the affected arm. The results demonstrated that for Participant 1 and 3, there was an increase in the amplitude of the affected arm for both the sEMG and AMG data. However, for Participant 2, only the AMG sensors appeared to have an increase in the amplitude of the affected arm. Therefore, there was an inconsistency in the results obtained for this test, and sEMG did not always reflect what was stated in the literature. Further testing would be required where multiple tests would be compared per participant in a larger sample size to determine whether or not there is a trend in the data that can be used to evaluate spasticity.

4.5 Limitations

It is essential to consider that there were a number of limitations in this study that may have affected the results obtained.

The most considerable limitation that may have affected the results is sex differences. Studies have found that type I fibres are said to be 19% larger, type IIa fibre types 59% larger and type IIb fibre types 66% larger in male rather than female sexes (Haizlip et al., 2015). Also, there is a large difference between male and female skeletal muscles, which involve different metabolisms and contractile speeds. Males tend to have a higher anaerobic metabolism, allowing them to generate high-power outputs (Glenmark et al., 2004). Thus, researchers have found a significant difference between both sexes and the spectral properties in sEMG during voluntary muscle contractions. It is expected that a larger force or power would be generated in males than in females, leading to higher amplitude in male power spectra. Also, during MVC, a female's power spectrum tends to shift towards lower frequencies than a male's (Cioni et al., 1994).

Lastly, female muscles are more fatigue-resistant than male muscles and may take longer for their frequency content to shift to lower frequencies (Glenmark et al., 2004). Thus, the study's results may have been affected by differences in sex that were not accounted for, which may have caused more variability in the frequency and amplitude ratios for sEMG and AMG.

Furthermore, researchers have found that both MMG and sEMG signals are affected by muscle mass, muscle length and subcutaneous fat (Ibitoye et al., 2014). For subcutaneous tissue fat primarily, researchers have determined that this causes a decrease in the amplitude of the EMG signal. This may indicate that it is also essential to be prudent while using amplitude changes as a measure of spasticity in a patient with higher degrees of subcutaneous fat (Kuiken et al., 2003). Thus, the results may have been impacted by these variations between subjects. While normalization of the data may have accommodated these differences between participants by adjusting the data at a standard scale, some researchers have stated that normalization is insufficient to account for these differences (Ibitoye et al., 2014).

Lastly, data was also not normalized. Typically, data is normalized with sEMG using MVC. However, a considerable challenge for someone with spasticity is that their MVC can be weak, making it harder to normalize using this method (McGibbon et al., 2013). Researchers would have to determine a better way to normalize the data to ensure consistent results and to adequately compare the results in patients with spasticity.

4.6 Conclusion

In conclusion, AMG appears, based on these initial studies, to be a promising alternative to sEMG for virtual spasticity assessments. AMG does not present as many of the barriers as sEMG for ease of use. It can also detect similar information about muscle contraction through its

ability to detect slow and fast fibres, which may be helpful information during spasticity assessments. Furthermore, AMG seems to have around the same measurement reliability as sEMG when the coefficient of variation is used. However, more reliable test measurements are required to confirm this hypothesis. AMG also seems to detect spasticity characteristics, as seen during the ability to detect an absence of fast fibres, lower signal-to-noise ratios and an increase in rectified amplitude in spastic limbs compared to non-affect limbs. Thus, although future studies are required to confirm these hypotheses, AMG seems like a promising tool for virtual spasticity assessments.

Chapter 5. Thesis Discussion and Conclusion

5.1 Summary of Findings

The primary goal of this thesis research was to determine if sEMG could be replaced by the AMG sensor to make virtual spasticity assessments more feasible. Based on previous literature, it has been determined that sEMG may be a useful tool for objective spasticity assessments. Researchers have found that sEMG can detect an increase in rectified amplitude during passive stretch movements to indicate an increase in the stretch reflex response (Xie et al., 2020). Many researchers also use sEMG to investigate the pathophysiology of spasticity (Yu et al., 2020). sEMG has also been used for various other clinical applications. For example, it is used to evaluate temporal changes in gait activity (Fujita et al., 2021). However, sEMG currently

presents many barriers to its use and may not be a suitable candidate for use in a telehealth setting because it often needs a specialist present.

An initial literature review was conducted to see how current sEMG barriers impact telehealth assessments and the solutions researchers have found to overcome them. The most reported barrier in the literature review was the poor reliability of real-time data due to the high amounts of data sEMG requires to be processed with its high bandwidth requirement. Commercial EMG systems use a 1000 Hz sample rate, but clinical data is found in the 10 to 200 Hz range. Higher sampling rates are needed to avoid missing essential data, but the high volume of processed data could cause delays. Other significant barriers included poor user-friendliness and cybersecurity. Few articles proposed solutions to overcome poor real-time data, indicating that no solutions have been successfully implemented. The barriers to patient usability were often overcome in the studies through prior training before virtual assessments. Although the literature does provide some solutions to overcoming barriers to sEMG, AMG does not present these barriers, and it was decided that it should be studied as an alternative to sEMG assessments to make these assessments more accessible virtually.

A portable device to assess spasticity in a telehealth setting was designed and built at the Rehabilitation Robotics Lab at the University of Alberta based on a previous device (TONE device) created by Daniel Gillespie, a former Ph.D. student in Rehabilitation Sciences at the University of Alberta (Gillespie, 2023). The intention of the device is to be further developed into other versions once more research is conducted to find the best portable device to allow clinicians to gain information about biomechanical data for more objective and virtual spasticity assessments. The device was designed based on three essential factors. The first was real-time data to allow clinicians to see a muscle's healthy or excessive tone in real-time through a

dashboard interface. The second was storing the raw data on an SD card to allow researchers or clinicians to see the muscle contraction's spectral composition, post-processing that data as a power spectrum. Power spectra for sEMG sensors relay information on muscle fibre fatigue, motor unit firing rates and slow and fast fibre composition (Fuglsang-Frederiksen & Rønager, 1988). Lastly, an AMG sensor was added to the device to evaluate if there is a more user-friendly alternative to sEMG. Daniel Gillespie has already evaluated how the biomechanical data of force sensors and groomers is affected in spastic muscles. Thus, the device for this thesis intended to be used for research proposes to compare sEMG with AMG specifically by collecting data simultaneously (Gillespie, 2023). Once it had been determined which sensor was the best for virtual assessments, the device was intended to be developed into other versions using the information found for clinical ease of use.

The research in the thesis found that during the muscle fatigue test, AMG demonstrated similar trends to sEMG in its ability to detect the recruitment of slow and fast muscle fibres. This was determined based on our ability to see both the slow and fast fibre peaks in the power spectra and by observing AMG's power spectrum shift to lower frequencies when the muscle fatigues, similar to what would be expected to be seen in sEMG based on the literature. The repeated measures ANOVA tests confirmed that the slow-to-fast frequency and amplitude ratios significantly differed between the epoch numbers for the 10 participants for both sensors. When plotting the mean amplitude and frequency ratios per epoch, it indicated that as the epoch number increased, the level of fatigue also increased across participants. Through this initial test on a population without spasticity, we concluded that AMG is comparable to sEMG because of its ability to pick up both slow and fast fibres during muscle contraction.

A reliability test was also conducted to determine if sEMG and AMG were comparable in terms of their reliability in picking up these slow and fast fibres. The test was evaluated at a MVC without the presence of fatigue in a population without spasticity. The reliability test, using a coefficient of variation, determined that there is a good indication that sEMG and AMG have similar coefficients of variation when detecting amplitude ratios of slow-to-fast fibres. However, it was indicative that there seemed to be a difference between the coefficient of variations for sEMG and AMG slow-to-fast fibre frequency ratios, where sEMG had a smaller coefficient of variation. Although more precise statistical tests are required with a larger sample size, sEMG frequency ratios appear to have less dispersion around the mean, and it is hypothesized that this may lead to sEMG picking up slow and fast fibre frequencies more reliably. More robust studies need to be conducted to confirm the hypothesis in this study. The reliability test also allowed us to evaluate what previous researchers had speculated about the frequency components of MMG. Although it was not yet determined if MMG could detect slow and fast fibres, research had speculations about this due to their knowledge of power spectra and the fact that MMG is distributed at lower frequency ranges. Previous researchers suggested that the high-frequency components of MMG would be found between 15 to 60 Hz. The low-frequency components of MMG were speculated to be found below 15 Hz. Our raw data concluded that the AMG showed a slow fibre frequency between 5 to 10 Hz, below the predicted 15 Hz. However, the predicted higher frequency component was much lower than anticipated, although still around the expected range; it ranged from 8.8 to 18.3 Hz. It was speculated that factors such as the type of muscle used, in our case, the biceps brachii, or the contraction force, may have played a factor as different human muscles have different fibre types, which leads to different force-generating capabilities (Bilodeau et al., 1990; Von Tscherner & Nigg, 2008). Future tests need to be

conducted to determine if this is the accurate fast fibre frequency range by studying AMG under various contraction types using different muscles.

Once it was determined that sEMG and AMG seemed to be comparable in how they can both pick slow and fast fibre characteristics on a power spectrum, it was concluded that AMG seemed like a promising tool for virtual spasticity assessments through the information it can provide us about muscle fibres during a contraction. The last test was conducted on post-stroke spasticity patients to evaluate if sEMG and AMG were comparable in picking up specific characteristics that could be used to assess spasticity and if this differs for passive and active movements. A sample of 3 post-stroke spasticity patients underwent isometric and passive stretch movements to indicate whether or not specific characteristics were apparent when comparing the non-affected arm to the arm affected by spasticity. While observing the slow and fast fibre ratios through an active movement, in this case, an isometric contraction, it was determined that there was an absence of fast fibres in the arm affected by spasticity for both the sEMG and AMG sensors. This aligns with what researchers have found about muscle spasticity, in which the pathophysiology indicates a deficiency in fast fibres (Gorgey & Dudley, 2008). Hence, sEMG and AMG were comparable in detecting the absence of fast fibres during active movements. Furthermore, the signal-to-noise ratio was evaluated as a potential tool for assessing spasticity during active movements. It was found that sEMG and AMG had a lower signal-to-noise ratio in the affected arm compared to the non-affected arm. This fits what was initially hypothesized based on the literature, which indicates that the muscle will be in a constant state of contraction when spasticity is present. Therefore, the baseline sensor value would not vary much from the signal's amplitude during the active contraction. Thus, this indicated that both sEMG and AMG signal-to-noise ratios could be a good way to evaluate the presence of muscle

spasticity. However, more research is needed to see if the signal-to-noise ratio of the affected arm compared to the non-affected arm has a significant difference. Lastly, the literature had previously determined that sEMG can detect spasticity during passive ranges of motion by using its rectified amplitude. The results for the passive stretch test were inconsistent for sEMG, where only two of the three participants showed an increase in amplitude in their arm affected by spasticity for both sensors. In this study, AMG appeared to be able to detect the increase in amplitude more adequately than sEMG, as it also detected the same trend in all participants. Future studies are required to determine if this is an adequate way to detect spasticity for passive movements and if the variety of results in this study is due to potential outliers from the small sample size. Overall, the tests done on the sample of 3 participants with spasticity seemed to indicate that the sEMG and AMG are comparable in their ability to indicate spasticity during active movements.

5.2 Implications of Findings

This thesis aims to provide future researchers with knowledge of sEMG compared to AMG sensors for more feasible and user-friendly virtual spasticity assessments. Indeed, the research intends to serve as a basis for developing protocols and the gold standard for virtual spasticity assessments. Upper limb spasticity has been found to cause pain and socioeconomic burdens due to the inability to perform activities of daily living. Those with post-stroke spasticity must access timely assessments and management (Guo et al., 2022). However, researchers have questioned the validity and reliability of the current assessment tools and their ability to be accessible for those requiring remote assessments. Given the importance of spasticity

assessments for proper management and rehabilitative therapies, there needs to be reliable technological solutions to conduct these assessments (Guo et al., 2022).

By concluding in this research that AMG seems to be a suitable alternative for sEMG, we propose a more user-friendly sensors for clinicians to use not only during remote spasticity assessments but also to allow objective assessments of spasticity without the need to have extensive knowledge on how to use sEMG. Various researchers have suggested objective assessments for a long time to promote more valid and reliable spasticity assessments with better intra-rater reliability, allowing for an improved quality of care and spasticity management.

The research done in this thesis serves as the initial stepping stone towards a proposed solution with a deeper understanding of using an AMG sensor as an alternative to sEMG for virtual spasticity assessments. The developed device, which may include the proposed AMG sensor, is a low-cost, portable device with real-time data capabilities. It can give clinicians quantitative, reliable information on joint angles, muscle activity, and the ability to detect a catch for upper extremity spasticity in stroke patients. The findings in this research may allow for a clinically implemented device that is the easiest to use in a telehealth setting when specialists are at a remote location.

Consequently, quantitative data obtained through AMG sensors and the device's biomechanical data can help create standardized clinical measurement protocols for spasticity assessments, similar to the MAS or MTS, using objective data. Previous researchers have determined that these objective assessments will allow a pathway toward better clinical decision-making and better spasticity management through surgical interventions or medication, preventing unnecessary treatment if not required (Balci, 2018; Harb & Kishner, 2024). However, more research needs to be done to develop a standardized protocol that can be implemented

across patients. While AMG seems promising, research still needs to determine how different degrees of severity to spasticity, similar to grades on the MAS or MTS scale, vary with different quantitative measurements. In other words, we need to ensure it can provide clinicians with information they can adequately interpret during these spasticity assessments. Future researchers could determine if there is a significant difference in the ability of active or passive movements to evaluate spasticity using the quantitative data obtained and if one is more suitable than the other.

The hope is that this research will be adopted into clinical practices. However, as previously mentioned, more research is needed to not only develop protocols to which clinicians can refer for assessing spasticity, but further education needs to be provided to allow clinicians to gain knowledge on how to interpret values from the sensors or other biomechanical data from the portable device. Furthermore, patient- and clinician-oriented research must also be considered to ensure that the methods used in these assessments meet their needs.

5.3 Conclusion

In conclusion, this thesis aimed to find the most convenient and feasible way to conduct spasticity assessments in telehealth by evaluating if AMG was a suitable alternative to sEMG. Previous literature has found many barriers to sEMG use. While some researchers have proposed strategies to overcome some barriers, not all seem easy to overcome. A portable device was designed not only to evaluate and compare these two sensors for research purposes but also with hopes that it may be the basis of a design for a device that can transmit quantitative biomechanical data regarding a patient's spasticity. AMG was found to be comparable to sEMG in the way it detects slow and fast fibres. sEMG and AMG were also both able to detect and

differentiate specific characteristics of spasticity in patients affected by a stroke. These included the deficiency of fast fibres in power spectra and the low signal-to-noise ratio in rectified data during active movements. Thus, the research concludes that AMG is an excellent alternative to sEMG, given its lack of prevalent barriers and its post-processing ability to give information about muscle contractions. Future research is required to allow clinicians to develop a new standardized protocol to conduct these assessments with insight into the severity of spasticity using these measurement tools for proper treatment and management plans.

References

- Agha, Z., Weir, C. R., & Chen, Y. (2013). Usability of Telehealth Technologies. *International Journal of Telemedicine and Applications*, 2013, 1–2.
<https://doi.org/10.1155/2013/834514>
- Ahamed, N. U., Sundaraj, K., & Poo, T. S. (2013). Design and development of an automated, portable and handheld tablet personal computer-based data acquisition system for monitoring electromyography signals during rehabilitation. *Proceedings of the Institution of Mechanical Engineers, Part H: Journal of Engineering in Medicine*, 227(3), 262–274.
<https://doi.org/10.1177/0954411912471493>
- Ahmad Puzi, A., Sidek, S. N., Mat Rosly, H., Daud, N., & Md Yusof, H. (2017). Modified Ashworth Scale (MAS) Model based on Clinical Data Measurement towards Quantitative Evaluation of Upper Limb Spasticity. *IOP Conference Series: Materials Science and Engineering*, 260, 012024. <https://doi.org/10.1088/1757-899X/260/1/012024>
- Akoglu, H. (2018). User's guide to correlation coefficients. *Turkish Journal of Emergency Medicine*, 18(3), 91–93. <https://doi.org/10.1016/j.tjem.2018.08.001>
- Aldekhyyel, R. N., Almulhem, J. A., & Binkheder, S. (2021). Usability of Telemedicine Mobile Applications during COVID-19 in Saudi Arabia: A Heuristic Evaluation of Patient User Interfaces. *Healthcare*, 9(11), 1574. <https://doi.org/10.3390/healthcare9111574>
- AlMohimeed, I., & Ono, Y. (2020). Ultrasound Measurement of Skeletal Muscle Contractile Parameters Using Flexible and Wearable Single-Element Ultrasonic Sensor. *Sensors (Basel, Switzerland)*, 20(13), 3616. <https://doi.org/10.3390/s20133616>

- Arksey, H., & O'Malley, L. (2005). Scoping studies: Towards a methodological framework. *International Journal of Social Research Methodology*, 8(1), 19–32.
<https://doi.org/10.1080/1364557032000119616>
- Badawi, A. A., Al-Kabbany, A., & Shaban, H. A. (2020). Sensor Type, Axis, and Position-Based Fusion and Feature Selection for Multimodal Human Daily Activity Recognition in Wearable Body Sensor Networks. *Journal of Healthcare Engineering*, 2020, 1–14.
<https://doi.org/10.1155/2020/7914649>
- Balci, B. P. (2018). Spasticity Measurement. *Noro Psikiyatri Arsivi*, 55(Suppl 1), S49–S53.
<https://doi.org/10.29399/npa.23339>
- Bartuzi, P., Roman-Liu, D., & Tokarski, T. (2007). A Study of the Influence of Muscle Type and Muscle Force Level on Individual Frequency Bands of the EMG Power Spectrum. *International Journal of Occupational Safety and Ergonomics*, 13(3), 241–254.
<https://doi.org/10.1080/10803548.2007.11076725>
- Beck, T. W., Housh, T. J., Johnson, G. O., Cramer, J. T., Weir, J. P., Coburn, J. W., & Malek, M. H. (2007). Does the frequency content of the surface mechanomyographic signal reflect motor unit firing rates? A brief review. *Journal of Electromyography and Kinesiology: Official Journal of the International Society of Electrophysiological Kinesiology*, 17(1), 1–13. <https://doi.org/10.1016/j.jelekin.2005.12.002>
- Berger, P. D. A., Nascimento, F. A. D. O., Carmo, J. C. D., & Rocha, A. F. D. (2006). Compression of EMG signals with wavelet transform and artificial neural networks. *Physiological Measurement*, 27(6), 457–465. <https://doi.org/10.1088/0967-3334/27/6/003>
- Bilodeau, M., Arsenault, A. B., Gravel, D., & Bourbonnais, D. (1990). The influence of an increase in the level of force on the EMG power spectrum of elbow extensors. *European*

- Journal of Applied Physiology and Occupational Physiology*, 61(5–6), 461–466.
<https://doi.org/10.1007/BF00236068>
- Campbell, N., Egan, T., & Deegan, C. (2017). The application of digital accelerometers for wired and non-wired Mechanomyography. *2017 28th Irish Signals and Systems Conference (ISSC)*, 1–6. <https://doi.org/10.1109/ISSC.2017.7983619>
- Chang, E., Ghosh, N., Yanni, D., Lee, S., Alexandru, D., & Mozaffar, T. (2013). A Review of Spasticity Treatments: Pharmacological and Interventional Approaches. *Critical Reviews in Physical and Rehabilitation Medicine*, 25(1–2), 11–22.
<https://doi.org/10.1615/CritRevPhysRehabilMed.2013007945>
- Cioni, R., Giannini, F., Paradiso, C., Battistini, N., Navona, C., & Starita, A. (1994). Sex differences in surface EMG interference pattern power spectrum. *Journal of Applied Physiology (Bethesda, Md.: 1985)*, 77(5), 2163–2168.
<https://doi.org/10.1152/jappl.1994.77.5.2163>
- Combi, C., Pozzani, G., & Pozzi, G. (2016). Telemedicine for Developing Countries: A Survey and Some Design Issues. *Applied Clinical Informatics*, 07(04), 1025–1050.
<https://doi.org/10.4338/ACI-2016-06-R-0089>
- Constantinescu, G., Kuffel, K., Aalto, D., Hodgetts, W., & Rieger, J. (2018). Evaluation of an Automated Swallow-Detection Algorithm Using Visual Biofeedback in Healthy Adults and Head and Neck Cancer Survivors. *Dysphagia*, 33(3), 345–357.
<https://doi.org/10.1007/s00455-017-9859-2>
- Covidence systematic review software*. (n.d.). [Computer software]. Veritas Health Innovation.

- de-la-Torre, R., Oña, E. D., Victores, J. G., & Jardón, A. (2024). SpasticSim: A synthetic data generation method for upper limb spasticity modelling in neurorehabilitation. *Scientific Reports*, *14*(1), 1646. <https://doi.org/10.1038/s41598-024-51993-w>
- Dinashi, K., Ameri, A., Akhaee, M. A., Englehart, K., & Scheme, E. (2022). Compression of EMG Signals Using Deep Convolutional Autoencoders. *IEEE Journal of Biomedical and Health Informatics*, *26*(7), 2888–2897. <https://doi.org/10.1109/JBHI.2022.3142034>
- Elbaz, S., Cinalioglu, K., Sekhon, K., Gruber, J., Rigas, C., Bodenstein, K., Naghi, K., Lavin, P., Greenway, K. T., Vahia, I., Rej, S., & Sekhon, H. (2021). A Systematic Review of Telemedicine for Older Adults With Dementia During COVID-19: An Alternative to In-person Health Services? *Frontiers in Neurology*, *12*, 761965. <https://doi.org/10.3389/fneur.2021.761965>
- Francisco, G. E., Wissel, J., Platz, T., & Li, S. (2021). Post-Stroke Spasticity. In T. Platz (Ed.), *Clinical Pathways in Stroke Rehabilitation* (pp. 149–173). Springer International Publishing. https://doi.org/10.1007/978-3-030-58505-1_9
- Fuglsang-Frederiksen, A., & Rønager, J. (1988). The motor unit firing rate and the power spectrum of EMG in humans. *Electroencephalography and Clinical Neurophysiology*, *70*(1), 68–72. [https://doi.org/10.1016/0013-4694\(88\)90196-4](https://doi.org/10.1016/0013-4694(88)90196-4)
- Fujimura, K., Mukaino, M., Itoh, S., Miwa, H., Itoh, R., Narukawa, D., Tanikawa, H., Kanada, Y., Saitoh, E., & Otaka, Y. (2022). Requirements for Eliciting a Spastic Response With Passive Joint Movements and the Influence of Velocity on Response Patterns: An Experimental Study of Velocity-Response Relationships in Mild Spasticity With Repeated-Measures Analysis. *Frontiers in Neurology*, *13*, 854125. <https://doi.org/10.3389/fneur.2022.854125>

- Fujita, K., Kobayashi, Y., & Hitosugi, M. (2021). Temporal Changes in Electromyographic Activity and Gait Ability during Extended Walking in Individuals Post-Stroke: A Pilot Study. *Healthcare (Basel, Switzerland)*, 9(4), 444.
<https://doi.org/10.3390/healthcare9040444>
- Ganesh, A., Stang, J. M., McAlister, F. A., Shlakter, O., Holodinsky, J. K., Mann, B., Hill, M. D., & Smith, E. E. (2022). Changes in ischemic stroke presentations, management and outcomes during the first year of the COVID-19 pandemic in Alberta: A population study. *CMAJ: Canadian Medical Association Journal = Journal de l'Association Medicale Canadienne*, 194(12), E444–E455. <https://doi.org/10.1503/cmaj.211003>
- GBD 2019 Stroke Collaborators. (2021). Global, regional, and national burden of stroke and its risk factors, 1990-2019: A systematic analysis for the Global Burden of Disease Study 2019. *The Lancet. Neurology*, 20(10), 795–820. [https://doi.org/10.1016/S1474-4422\(21\)00252-0](https://doi.org/10.1016/S1474-4422(21)00252-0)
- Gillespie, D. (2023). *Setting the Tone for Virtual Spasticity Assessment: Planning Development and Testing of the Telerehabilitation-Objective-Neuromuscular- Evaluation (TONE) Device*. University of Alberta.
- Glenmark, B., Nilsson, M., Gao, H., Gustafsson, J.-Å., Dahlman-Wright, K., & Westerblad, H. (2004). Difference in skeletal muscle function in males vs. females: Role of estrogen receptor- β . *American Journal of Physiology-Endocrinology and Metabolism*, 287(6), E1125–E1131. <https://doi.org/10.1152/ajpendo.00098.2004>
- Gorgey, A. S., & Dudley, G. A. (2008). Spasticity may defend skeletal muscle size and composition after incomplete spinal cord injury. *Spinal Cord*, 46(2), 96–102.
<https://doi.org/10.1038/sj.sc.3102087>

- Guo, X., Wallace, R., Tan, Y., Oetomo, D., Klaic, M., & Crocher, V. (2022). Technology-assisted assessment of spasticity: A systematic review. *Journal of NeuroEngineering and Rehabilitation*, *19*(1), 138. <https://doi.org/10.1186/s12984-022-01115-2>
- Haizlip, K. M., Harrison, B. C., & Leinwand, L. A. (2015). Sex-based differences in skeletal muscle kinetics and fiber-type composition. *Physiology (Bethesda, Md.)*, *30*(1), 30–39. <https://doi.org/10.1152/physiol.00024.2014>
- Haleem, A., Javaid, M., Singh, R. P., & Suman, R. (2021). Telemedicine for healthcare: Capabilities, features, barriers, and applications. *Sensors International*, *2*, 100117. <https://doi.org/10.1016/j.sintl.2021.100117>
- Harb, A., & Kishner, S. (2024). Modified Ashworth Scale. In *StatPearls*. StatPearls Publishing. <http://www.ncbi.nlm.nih.gov/books/NBK554572/>
- Hassan, S. R., Ahmad, I., Ahmad, S., Alfaiy, A., & Shafiq, M. (2020). Remote Pain Monitoring Using Fog Computing for e-Healthcare: An Efficient Architecture. *Sensors*, *20*(22), 6574. <https://doi.org/10.3390/s20226574>
- Heaffey, J., Koutsos, E., & Georgiou, P. (2015). Live demonstration: Wearable device for remote EMG and muscle fatigue monitoring. *2015 IEEE Biomedical Circuits and Systems Conference (BioCAS)*, 1–5. <https://doi.org/10.1109/BioCAS.2015.7348324>
- Holzgreve, F., Maurer-Grubinger, C., Isaak, J., Kokott, P., Mörl-Kreitschmann, M., Polte, L., Solimann, A., Wessler, L., Filmann, N., Van Mark, A., Maltry, L., Groneberg, D. A., & Ohlendorf, D. (2020). The acute effect in performing common range of motion tests in healthy young adults: A prospective study. *Scientific Reports*, *10*(1), 21722. <https://doi.org/10.1038/s41598-020-78846-6>

- Hryvniak, D., Wilder, R. P., Jenkins, J., & Statuta, S. M. (2021). Therapeutic Exercise. In *Braddom's Physical Medicine and Rehabilitation* (pp. 291-315.e4). Elsevier.
<https://doi.org/10.1016/B978-0-323-62539-5.00015-1>
- Huber, J., Kaczmarek, K., Leszczyńska, K., & Daroszewski, P. (2022). Post-Stroke Treatment with Neuromuscular Functional Electrostimulation of Antagonistic Muscles and Kinesiotherapy Evaluated with Electromyography and Clinical Studies in a Two-Month Follow-Up. *International Journal of Environmental Research and Public Health*, *19*(2), 964. <https://doi.org/10.3390/ijerph19020964>
- Ibitoye, M. O., Hamzaid, N. A., Zuniga, J. M., Hasnan, N., & Wahab, A. K. A. (2014). Mechanomyographic parameter extraction methods: An appraisal for clinical applications. *Sensors (Basel, Switzerland)*, *14*(12), 22940–22970.
<https://doi.org/10.3390/s141222940>
- Ingvaldsen, S. H., Tronvik, E., Brenner, E., Winnberg, I., Olsen, A., Gravdahl, G. B., & Stubberud, A. (2021). A Biofeedback App for Migraine: Development and Usability Study. *JMIR Formative Research*, *5*(7), e23229. <https://doi.org/10.2196/23229>
- Ito, J., Araki, A., Tanaka, H., Tasaki, T., Cho, K., & Yamazaki, R. (1996). Muscle histopathology in spastic cerebral palsy. *Brain and Development*, *18*(4), 299–303.
[https://doi.org/10.1016/0387-7604\(96\)00006-X](https://doi.org/10.1016/0387-7604(96)00006-X)
- Jarque-Bou, N. J., Sancho-Bru, J. L., & Vergara, M. (2021). A Systematic Review of EMG Applications for the Characterization of Forearm and Hand Muscle Activity during Activities of Daily Living: Results, Challenges, and Open Issues. *Sensors (Basel, Switzerland)*, *21*(9), 3035. <https://doi.org/10.3390/s21093035>

- Kantarcigil, C., Kim, M. K., Chang, T., Craig, B. A., Smith, A., Lee, C. H., & Malandraki, G. A. (2020). Validation of a Novel Wearable Electromyography Patch for Monitoring Submental Muscle Activity During Swallowing: A Randomized Crossover Trial. *Journal of Speech, Language, and Hearing Research, 63*(10), 3293–3310.
https://doi.org/10.1044/2020_JSLHR-20-00171
- Kishimoto, M., Yoshida, T., Hayasaka, T., Mori, D., Imai, Y., Matsuki, N., Ishikawa, T., & Yamaguchi, T. (2009). An internet-based wearable watch-over system for elderly and disabled utilizing EMG and accelerometer. *Technology and Health Care, 17*(2), 121–131.
<https://doi.org/10.3233/THC-2009-0538>
- Krueger, E., Scheeren, E. M., Nogueira-Neto, G. N., Button, V. L. D. S. N., & Nohama, P. (2014). Advances and perspectives of mechanomyography. *Revista Brasileira de Engenharia Biomédica, 30*(4), 384–401. <https://doi.org/10.1590/1517-3151.0541>
- Kuiken, T. A., Lowery, M. M., & Stoykov, N. S. (2003). The effect of subcutaneous fat on myoelectric signal amplitude and cross-talk. *Prosthetics and Orthotics International, 27*(1), 48–54. <https://doi.org/10.3109/03093640309167976>
- Kuo, C.-L., & Hu, G.-C. (2018). Post-stroke Spasticity: A Review of Epidemiology, Pathophysiology, and Treatments. *International Journal of Gerontology, 12*(4), 280–284.
<https://doi.org/10.1016/j.ijge.2018.05.005>
- Ladegaard, J. (2002). Story of electromyography equipment. *Muscle & Nerve, 999*(S11), S128–S133. <https://doi.org/10.1002/mus.10176>
- Lance, J. W. (1990). What is spasticity? *Lancet (London, England), 335*(8689), 606.
[https://doi.org/10.1016/0140-6736\(90\)90389-m](https://doi.org/10.1016/0140-6736(90)90389-m)

- Lee, D., Van Holsbeeck, M. T., Janevski, P. K., Ganos, D. L., Ditmars, D. M., & Darian, V. B. (1999). DIAGNOSIS OF CARPAL TUNNEL SYNDROME. *Radiologic Clinics of North America*, 37(4), 859–872. [https://doi.org/10.1016/S0033-8389\(05\)70132-9](https://doi.org/10.1016/S0033-8389(05)70132-9)
- Levy, J., Karam, P., Forestier, A., Loze, J.-Y., & Bensmail, D. (2023). Botulinum toxin use in patients with post-stroke spasticity: A nationwide retrospective study from France. *Frontiers in Neurology*, 14, 1245228. <https://doi.org/10.3389/fneur.2023.1245228>
- Li, S., & Francisco, G. E. (2015). New insights into the pathophysiology of post-stroke spasticity. *Frontiers in Human Neuroscience*, 9. <https://doi.org/10.3389/fnhum.2015.00192>
- Lievens, E., Klass, M., Bex, T., & Derave, W. (2020). Muscle fiber typology substantially influences time to recover from high-intensity exercise. *Journal of Applied Physiology*, 128(3), 648–659. <https://doi.org/10.1152/jappphysiol.00636.2019>
- Man, J. P., Weinkauff, J. G., Tsang, M., & Sin, J. H. D. D. (2003). Why do Some Countries Publish More Than Others? An International Comparison of Research Funding, English Proficiency and Publication Output in Highly Ranked General Medical Journals. *European Journal of Epidemiology*, 19(8), 811–817. <https://doi.org/10.1023/B:EJEP.0000036571.00320.b8>
- Marin-Pardo, O., Phanord, C., Donnelly, M. R., Laine, C. M., & Liew, S.-L. (2021). Development of a Low-Cost, Modular Muscle–Computer Interface for At-Home Telerehabilitation for Chronic Stroke. *Sensors*, 21(5), 1806. <https://doi.org/10.3390/s21051806>
- Marshall, A., Kalteniece, A., Ferdousi, M., Azmi, S., Jude, E. B., Adamson, C., D’Onofrio, L., Dhage, S., Soran, H., Campbell, J., Lee-Kubli, C. A., Hamdy, S., Malik, R. A., Calcutt,

- N. A., & Marshall, A. G. (2023). Spinal disinhibition: Evidence for a hyperpathia phenotype in painful diabetic neuropathy. *Brain Communications*, 5(2), fcad051. <https://doi.org/10.1093/braincomms/fcad051>
- Matsunaga, F., Kokubu, S., Tortos Vinocour, P. E., Ke, M.-T., Hsueh, Y.-H., Huang, S. Y., Gomez-Tames, J., & Yu, W. (2023). Finger Joint Stiffness Estimation with Joint Modular Soft Actuators for Hand Telerehabilitation. *Robotics*, 12(3), 83. <https://doi.org/10.3390/robotics12030083>
- McGibbon, C. A., Sexton, A., Jones, M., & O'Connell, C. (2013). Elbow spasticity during passive stretch-reflex: Clinical evaluation using a wearable sensor system. *Journal of NeuroEngineering and Rehabilitation*, 10(1), 61. <https://doi.org/10.1186/1743-0003-10-61>
- Meagher, C., Franco, E., Turk, R., Wilson, S., Steadman, N., McNicholas, L., Vaidyanathan, R., Burridge, J., & Stokes, M. (2020). New advances in mechanomyography sensor technology and signal processing: Validity and intrarater reliability of recordings from muscle. *Journal of Rehabilitation and Assistive Technologies Engineering*, 7, 205566832091611. <https://doi.org/10.1177/2055668320916116>
- Merletti, R., & Farina, D. (2009). Analysis of intramuscular electromyogram signals. *Philosophical Transactions. Series A, Mathematical, Physical, and Engineering Sciences*, 367(1887), 357–368. <https://doi.org/10.1098/rsta.2008.0235>
- Milligan, J., Ryan, K., & Lee, J. (2019). Demystifying spasticity in primary care. *Canadian Family Physician Medecin De Famille Canadien*, 65(10), 697–703.
- Mills, K. R. (2005). The basics of electromyography. *Journal of Neurology, Neurosurgery, and Psychiatry*, 76 Suppl 2(Suppl 2), ii32-35. <https://doi.org/10.1136/jnnp.2005.069211>

- Murphy, S. J., & Werring, D. J. (2020). Stroke: Causes and clinical features. *Medicine (Abingdon, England: UK Ed.)*, 48(9), 561–566.
<https://doi.org/10.1016/j.mpmed.2020.06.002>
- Nazmi, N., Abdul Rahman, M. A., Yamamoto, S.-I., Ahmad, S. A., Zamzuri, H., & Mazlan, S. A. (2016). A Review of Classification Techniques of EMG Signals during Isotonic and Isometric Contractions. *Sensors (Basel, Switzerland)*, 16(8), 1304.
<https://doi.org/10.3390/s16081304>
- Olsson, M. C., Krüger, M., Meyer, L.-H., Ahnlund, L., Gransberg, L., Linke, W. A., & Larsson, L. (2006). Fibre type-specific increase in passive muscle tension in spinal cord-injured subjects with spasticity. *The Journal of Physiology*, 577(Pt 1), 339–352.
<https://doi.org/10.1113/jphysiol.2006.116749>
- Padulo, J., Laffaye, G., Chamari, K., & Concu, A. (2013). Concentric and eccentric: Muscle contraction or exercise? *Sports Health*, 5(4), 306.
<https://doi.org/10.1177/1941738113491386>
- Palumbo, A., Ielpo, N., Calabrese, B., Corchiola, D., Garropoli, R., Gramigna, V., & Perri, G. (2021). SIMpLE: A Mobile Cloud-Based System for Health Monitoring of People with ALS. *Sensors*, 21(21), 7239. <https://doi.org/10.3390/s21217239>
- Palumbo, A., Vizza, P., Calabrese, B., & Ielpo, N. (2021). Biopotential Signal Monitoring Systems in Rehabilitation: A Review. *Sensors*, 21(21), 7172.
<https://doi.org/10.3390/s21217172>
- Peng, Q., Park, H.-S., Shah, P., Wilson, N., Ren, Y., Wu, Y.-N., Liu, J., Gaebler-Spira, D. J., & Zhang, L.-Q. (2011). Quantitative evaluations of ankle spasticity and stiffness in

- neurological disorders using manual spasticity evaluator. *Journal of Rehabilitation Research and Development*, 48(4), 473–481. <https://doi.org/10.1682/jrrd.2010.04.0053>
- Pham, S., & Puckett, Y. (2024). Physiology, Skeletal Muscle Contraction. In *StatPearls*. StatPearls Publishing. <http://www.ncbi.nlm.nih.gov/books/NBK559006/>
- Puzi, A. A., Sidek, S. N., Khairuddin, I. M., & Yusof, H. Md. (2020). Objective Assessment for Classification of Muscle Spasticity Level. *Proceedings of the 2020 4th International Symposium on Computer Science and Intelligent Control*, 1–6. <https://doi.org/10.1145/3440084.3441181>
- Rajashekar, D., & Liang, J. W. (2024). Intracerebral Hemorrhage. In *StatPearls*. StatPearls Publishing. <http://www.ncbi.nlm.nih.gov/books/NBK553103/>
- Rivelis, Y., Zafar, N., & Morice, K. (2024). Spasticity. In *StatPearls*. StatPearls Publishing. <http://www.ncbi.nlm.nih.gov/books/NBK507869/>
- Roberts, T. J., & Gabaldón, A. M. (2008). Interpreting muscle function from EMG: Lessons learned from direct measurements of muscle force. *Integrative and Comparative Biology*, 48(2), 312–320. <https://doi.org/10.1093/icb/icn056>
- Rogante, M., Silvestri, S., Grigioni, M., & Zampolini, M. (2010). Electromyographic audio biofeedback for telerehabilitation in hospital. *Journal of Telemedicine and Telecare*, 16(4), 204–206. <https://doi.org/10.1258/jtt.2010.004012>
- Rosales, R. L., Kanovsky, P., & Fernandez, H. H. (2011). What’s the “catch” in upper-limb post-stroke spasticity: Expanding the role of botulinum toxin applications. *Parkinsonism & Related Disorders*, 17 Suppl 1, S3-10. <https://doi.org/10.1016/j.parkreldis.2011.06.019>
- Sethi, A., Ting, J., Allen, M., Clark, W., & Weber, D. (2020). Advances in motion and electromyography based wearable technology for upper extremity function rehabilitation:

A review. *Journal of Hand Therapy*, 33(2), 180–187.

<https://doi.org/10.1016/j.jht.2019.12.021>

- Shah, K., & Tomljenovic-Berube, A. (2021). A New Dimension of Health Care: The Benefits, Limitations and Implications of Virtual Medicine. *Journal of Undergraduate Life Sciences*, 15(1), 10. <https://doi.org/10.33137/juls.v15i1.37034>
- Shaw, L. C., Price, C. I. M., Van Wijck, F. M. J., Shackley, P., Steen, N., Barnes, M. P., Ford, G. A., Graham, L. A., & Rodgers, H. (2011). Botulinum Toxin for the Upper Limb After Stroke (BoTULS) Trial: Effect on Impairment, Activity Limitation, and Pain. *Stroke*, 42(5), 1371–1379. <https://doi.org/10.1161/STROKEAHA.110.582197>
- Skalsky, A. (2017). Spasticity: The need for objective assessment. *Developmental Medicine & Child Neurology*, 59(2), 114–114. <https://doi.org/10.1111/dmcn.13219>
- Sommerfeld, D. K., Eek, E. U.-B., Svensson, A.-K., Holmqvist, L. W., & Von Arbin, M. H. (2004). Spasticity After Stroke: Its Occurrence and Association With Motor Impairments and Activity Limitations. *Stroke*, 35(1), 134–139. <https://doi.org/10.1161/01.STR.0000105386.05173.5E>
- Talib, I., Sundaraj, K., & Lam, C. K. (2018). Choice of Mechanomyography Sensors for Diverse Types of Muscle Activities. *Journal of Telecommunication, Electronic and Computer Engineering (JTEC)*, 10(1–13), 79–82.
- Teasell, R., Salbach, N. M., Foley, N., Mountain, A., Cameron, J. I., Jong, A. de, Acerra, N. E., Bastasi, D., Carter, S. L., Fung, J., Halabi, M.-L., Iruthayarajah, J., Harris, J., Kim, E., Noland, A., Pooyania, S., Rochette, A., Stack, B. D., Symcox, E., ... Lindsay, M. P. (2020). Canadian Stroke Best Practice Recommendations: Rehabilitation, Recovery, and Community Participation following Stroke. Part One: Rehabilitation and Recovery

- Following Stroke; 6th Edition Update 2019. *International Journal of Stroke: Official Journal of the International Stroke Society*, 15(7), 763–788.
<https://doi.org/10.1177/1747493019897843>
- Tricco, A. C., Lillie, E., Zarin, W., O'Brien, K. K., Colquhoun, H., Levac, D., Moher, D., Peters, M. D. J., Horsley, T., Weeks, L., Hempel, S., Akl, E. A., Chang, C., McGowan, J., Stewart, L., Hartling, L., Aldcroft, A., Wilson, M. G., Garritty, C., ... Straus, S. E. (2018). PRISMA Extension for Scoping Reviews (PRISMA-ScR): Checklist and Explanation. *Annals of Internal Medicine*, 169(7), 467–473. <https://doi.org/10.7326/M18-0850>
- Trinity, J. D., & Richardson, R. S. (2019). Physiological Impact and Clinical Relevance of Passive Exercise/Movement. *Sports Medicine (Auckland, N.Z.)*, 49(9), 1365–1381.
<https://doi.org/10.1007/s40279-019-01146-1>
- Trompetto, C., Marinelli, L., Mori, L., Pelosin, E., Currà, A., Molfetta, L., & Abbruzzese, G. (2014). Pathophysiology of spasticity: Implications for neurorehabilitation. *BioMed Research International*, 2014, 354906. <https://doi.org/10.1155/2014/354906>
- Turker, H., & Sze, H. (2013). Surface Electromyography in Sports and Exercise. In Dr. H. Turker (Ed.), *Electrodiagnosis in New Frontiers of Clinical Research*. InTech.
<https://doi.org/10.5772/56167>
- Türker, K. S. (1993). Electromyography: Some methodological problems and issues. *Physical Therapy*, 73(10), 698–710. <https://doi.org/10.1093/ptj/73.10.698>
- United Nation. (2014). *Country Classification*.
- Valdez, R. S., Rogers, C. C., Claypool, H., Triesmann, L., Frye, O., Wellbeloved-Stone, C., & Kushalnagar, P. (2021). Ensuring full participation of people with disabilities in an era of

- telehealth. *Journal of the American Medical Informatics Association*, 28(2), 389–392.
<https://doi.org/10.1093/jamia/ocaa297>
- van den Noort, J. C., Scholtes, V. A., & Harlaar, J. (2009). Evaluation of clinical spasticity assessment in cerebral palsy using inertial sensors. *Gait & Posture*, 30(2), 138–143.
<https://doi.org/10.1016/j.gaitpost.2009.05.011>
- Verduzco-Gutierrez, M., Romanoski, N. L., Capizzi, A. N., Reebye, R. N., Kotteduwa Jayawarden, S., Ketchum, N. C., & O’Dell, M. (2020). Spasticity Outpatient Evaluation via Telemedicine: A Practical Framework. *American Journal of Physical Medicine & Rehabilitation*, 99(12), 1086–1091. <https://doi.org/10.1097/PHM.0000000000001594>
- Von Tscherner, V., & Nigg, B. M. (2008). Point:Counterpoint: Spectral properties of the surface EMG can characterize/do not provide information about motor unit recruitment strategies and muscle fiber type. *Journal of Applied Physiology*, 105(5), 1671–1673.
<https://doi.org/10.1152/jappphysiol.90598.2008>
- Vukova, T., Vydevska-Chichova, M., & Radicheva, N. (2008). Fatigue-induced changes in muscle fiber action potentials estimated by wavelet analysis. *Journal of Electromyography and Kinesiology*, 18(3), 397–409.
<https://doi.org/10.1016/j.jelekin.2006.09.014>
- Weir, J. P. (2005). Quantifying test-retest reliability using the intraclass correlation coefficient and the SEM. *Journal of Strength and Conditioning Research*, 19(1), 231–240.
<https://doi.org/10.1519/15184.1>
- Woodward, R. B., Stokes, M. J., Shefelbine, S. J., & Vaidyanathan, R. (2019). Segmenting Mechanomyography Measures of Muscle Activity Phases Using Inertial Data. *Scientific Reports*, 9(1), 5569. <https://doi.org/10.1038/s41598-019-41860-4>

- Xie, T., Leng, Y., Zhi, Y., Jiang, C., Tian, N., Luo, Z., Yu, H., & Song, R. (2020). Increased Muscle Activity Accompanying With Decreased Complexity as Spasticity Appears: High-Density EMG-Based Case Studies on Stroke Patients. *Frontiers in Bioengineering and Biotechnology*, 8, 589321. <https://doi.org/10.3389/fbioe.2020.589321>
- Xu, J., Hamadi, H., Hicks-Roof, K., Zeglin, R., Bailey, C., & Zhao, M. (2021). Healthcare Professionals and Telehealth Usability During COVID-19. *Telehealth and Medicine Today*. <https://doi.org/10.30953/tmt.v6.270>
- Yee, J., Low, C. Y., Mohamad Hashim, N., Che Zakaria, N. A., Johar, K., Othman, N. A., Chieng, H. H., & Hanapiah, F. A. (2023). Clinical Spasticity Assessment Assisted by Machine Learning Methods and Rule-Based Decision. *Diagnostics (Basel, Switzerland)*, 13(4), 739. <https://doi.org/10.3390/diagnostics13040739>
- Yi, C., Jiang, F., Yang, C., Chen, Z., Ding, Z., & Liu, J. (2021). Reference Frame Unification of IMU-Based Joint Angle Estimation: The Experimental Investigation and a Novel Method. *Sensors*, 21(5), 1813. <https://doi.org/10.3390/s21051813>
- Yu, S., Chen, Y., Cai, Q., Ma, K., Zheng, H., & Xie, L. (2020). A Novel Quantitative Spasticity Evaluation Method Based on Surface Electromyogram Signals and Adaptive Neuro Fuzzy Inference System. *Frontiers in Neuroscience*, 14, 462. <https://doi.org/10.3389/fnins.2020.00462>
- Zayia, L. C., & Tadi, P. (2024). Neuroanatomy, Motor Neuron. In *StatPearls*. StatPearls Publishing. <http://www.ncbi.nlm.nih.gov/books/NBK554616/>
- Zeng, H., Chen, J., Guo, Y., & Tan, S. (2020). Prevalence and Risk Factors for Spasticity After Stroke: A Systematic Review and Meta-Analysis. *Frontiers in Neurology*, 11, 616097. <https://doi.org/10.3389/fneur.2020.616097>

Zhao, S., Liu, J., Gong, Z., Lei, Y., OuYang, X., Chan, C. C., & Ruan, S. (2020). Wearable Physiological Monitoring System Based on Electrocardiography and Electromyography for Upper Limb Rehabilitation Training. *Sensors*, 20(17), 4861.
<https://doi.org/10.3390/s20174861>

Appendices

Appendix 1. Ethics Approval



RESEARCH ETHICS OFFICE
Health Research Ethics Board
 2-01 North Power Plant (NPP)
 11312 - 89 Ave NW
 Edmonton, Alberta, Canada T6G 2N2
 Tel: 780.492.0459
 www.uab.ca/reo

Approval Form

Date: April 11, 2023
 Study ID: Pro00129191
 Principal Investigator: Martin Ferguson-Pell
 Study Title: A comparison between surface EMG and AMG for virtual health assessments during static muscle contraction in the biceps brachii
 Approval Expiry Date: April 9, 2024
 Sponsor/Funding Agency: NSERC - Natural Sciences And Engineering Research Council

NSERC

Project ID	Title	Grant Status	Sponsor	Project Start Date	Project End Date	Purpose	Other Information
View RES0059942	NSERC CREATE in Sensory-Motor Adaptive Rehabilitation Technologies (SMART) - subgrant for Dr. Martin Ferguson-Pell	Awarded		2022-09-01	2024-08-31	Grant	

Thank you for submitting the above study to the Health Research Ethics Board - Health Panel. Your application has been reviewed and approved on behalf of the committee.

Approved Documents:

Recruitment Materials
Recruitment Letter_v3_clean.docx
Consent Forms
Combined Information Letter and Consent Form_18 years of age_15-17 years of age with decision-making capacity v2_clean.docx
Combined Information Letter and Consent Form_parental consent form v2_clean.docx
Assent Forms
Assent form for older children v2_clean.docx.docx
Questionnaires, Cover Letters, Surveys, Tests, Interview Scripts, etc.
PatientExperienceMeasure_TeleR_clean.docx
Protocol/Research Proposal
Research Protocol.docx

Any proposed changes to the study must be submitted to the REB for approval prior to implementation. A renewal report must be submitted next year prior to the expiry of this approval if your study still requires ethics approval. If you do not renew on or before the renewal expiry date, you will have to re-submit an ethics application.

Approval by the REB does not constitute authorization to initiate the conduct of this research. The Principal Investigator is responsible for ensuring required approvals from other involved organizations (e.g., Alberta Health Services, Covenant Health, community organizations, school boards) are obtained, before the research begins.

Sincerely,

Anthony S. Joyce, PhD
 Chair, Health Research Ethics Board - Health Panel

Note: This correspondence includes an electronic signature (validation and approval via an online system).



Appendix 2. Search Strategy

#	Searches
1	Electromyography/
2	(electromyogra* or EMG).mp.
3	1 or 2
4	Telemedicine/ or remote consultation/ or Videoconferencing/
5	((Online or virtual or remote* or video or digital or telephone or phone or tele) adj4 (treatment* or intervention* or program* or diagnos* or assessment or evaluation or follow-up or care or health or consult* or communicat* or medicine)).mp.
6	((remote or online or virtual* or electronic* or digital* or distan*) adj2 deliver*).mp.
7	(telehealth or tele-health or telemedicine or tele-medicine or telerehab* or tele-rehab* or teleconsult* or tele-consult* or mobile-health* or mhealth or m-health or distance health* or electronic-health* or ehealth or e-health or virtual health or Remote delivery or electronic-delivery or digital health or video conferenc* or videoconferenc* or teleconferenc* or tele-conferen* or video-to-home or video-visit* or video-technology).mp.
8	4 or 5 or 6 or 7

9	3 and 8
10	limit 9 to english language
11	limit 10 to (address or autobiography or bibliography or biography or clinical trial, veterinary or clinical trials, veterinary as topic or comment or congress or dictionary or editorial or lecture or legal case or news or newspaper article or observational study, veterinary)
12	10 not 11

Appendix 3. Component Parts of Designed Portable Device

- 2 GND Electrodes
- 2 Circular EMG 5 pin connectors (EPG.0B.305.HLN)
- 1 On/Off Switch
- 1 Powerboost
- 2 RP-0505D
- 1 Battery
- 1 wireless charging pad
- 4 1k resistors
- 2 10k resistors
- 2 Rectifier Diodes
- 2 Slide Switches
- 2 OP277
- 9 Pin VGA connector (for the ribbon cable connection)
- 2 Feather Adaloggers
- 1 Xbee Explorer
- 1 Xbee Series 1 Pro
- Red, Green, Yellow LEDs

Appendix 4. Arduino Firmware Code for Designed Portable Device

```
// PIN    FUNCTION
/* 1      ENABLE FOR SD FEATHER
* 2      EMG 1 From SD Feather board to AD 3 now
* 3      NC
* 4      NC
* 5      NC
* 6      EMG 2 From SD Feather board to AD 1 now
* 7      NC
* 8      NC
* 9      NC
* 10     NC
* 11     NC
* 12     AD 3 OLD EMG 1
* 13     NC
* 14     AD 4 AMG 1
* 15     NC
* 16     NC
* 17     AD 2 GONIOMETER
* 18     NC
* 19     NC
* 20     GND FOR SD FEATHER
*
* AD 0   FORCE INTERNAL CONNECTION
* AD 5   MVC POTENTIOMETER INTERNAL
*
* AMG 2 needs another AD input
*
* DIGITAL I/O
* 5 BODY SIDE SWITCH
* 6 GREEN LED
* 10 BUTTON SWITCH
* 12 BUZZER
```

```

*/
//
+++++
+++++
//          INCLUDE THE DEFINITIONS OF LIBRARIES AND VARIABLE DECLARATIONS
//
+++++
+++++

/*
MAKE SURE ALL LIBRARY FILES ARE SAVED IN THE LIBRARY DIRECTORY OF C:/ PROGRAM FILES (X86)
ARDUINO ....
OR IN MAC DOCUMENTS ARDUINO LIBRARY

*/

#include <SD.h>           // include the SD library:
#include <SPI.h>          // include the SPI library for SD card management
#include <elapsedMillis.h> // To estimate the time elapsed since start of test
#include <math.h>
#include <Average.h>
#include <Arduino.h>
#include <Adafruit_Sensor.h>
#include <Wire.h>
#include <XBee.h>
//#include <MovingAverage.h>
#define ERROR_NOERROR    (0x00)
#define cardSelect 4      // For Logger SD card
#define SAMPLE_PERIOD_US (1000 * 10)
#define VBATPIN A7        // To monitor as the battery voltage
#define STATE_IDLE      (0x00)
#define STATE_ACTIVE    (0x01)

// General public variables declarations *****

```

/* NOTE BASIC RULE OF C++ IS THAT THE FOLLOWING VARIABLES ARE DECLARED GLOBAL AND ARE "KNOWN" AND CAN BE CHANGED

THROUGHOUT THE PROGRAM. TRY TO USE PASS BY REFERENCE FOR VARIABLES THAT ARE SPECIFIC TO CERTAIN FUNCTIONS

IF A VARIABLE IS DECLARED WITHIN { } IT IS A LOCAL VARIABLE. THIS INCLUDES WITHING IF OR FOR LOOPS.

TO REFERENCE A LOCAL VARIABLE OUT OF A FUNCTION PLACE & IN FRONT OF THE VARIABLE IN THE LIST OF VARIABLES

PASSED TO THE FUNCTION (THIS IS NOT THE SAME USE OF & AS YOU WOULD USE IT FOR GETTING THE ADDRESS OF

A VARIABLE WHICH WOULD ONLY HAPPEN IN THE BODY OF THE FUNCTION.*/

```
elapsedMillis timeElapsed;           //declare global if you don't want it reset every time loop runs
uint32_t lastTime;                  // unsigned 32 bit integer measures number of microseconds in loop
uint32_t currentTime;               // Current time in micro secs since start of program
long runTime;                       // elapsed time
uint32_t startTime;                 // Time at start of loop in microseconds
uint32_t procTime;                  // time spent saving and processing
uint32_t currentTimegon = millis(); // Current time in micro secs of the goniometer measurements
uint32_t runTimegon ;               // gives a measure of sampling rate in micros
uint32_t lastTimegon;
uint32_t buttpresstime;             // time when button is pressed
uint32_t buttduration;             // duration button is being pressed
uint32_t buttnowtime;              // Obtaining the time during button press

// COUNTERS
long i = 0;                          // Large Counter
long j = 0;                          // Loop counter used for spefic purpose on RMS header
int r = 0;                            // Return state of file save in Loop
int k = 0;                            // Counter used to empty the array to sd card
int contraction=0;                   // Is there a contraction (=1) or not (0) Start assuming there is to avoid blank saves in
loop
int ii;                              // Counter used for goniometer

// DATA ARRAYS
char inData[20];                     // Allocate some space for string
char inChar = -1;                    // Where to store the character read
```

```

int mvcData[200];           // An array to put 20s of force readings
bool on = false;           // Use for LED p13 monitor

// ***** Adjustables *****

const long contrnumReadings = 800;
const int numReadings = 10;
const int precontrnumReadings = 250; // Number of readings to put in front and behind the contraction
float sdthresh = 10;        // Set the standard deviation threshold to avoid noise triggering a burst
// *****

int val = 0;                // General purpose variable
int contrast = 0;          // The value to trigger sd card reading
Average<int> ave1(200);     // Defines the array averaged for Analog Input CH4
Average<long> aversemp(200); // Defines the array for runtime to give estimated sampling rate
static int dataset[contrnumReadings]; // Array for raw data 6000 rows, 1 cols @ 1000Hz = 6s per contraction
int *pntrdataset = &dataset[0]; // The compiler will only accept max of ~6000 values in this array
// We therefore have the capacity to store 6K of raw int value

int readings1[numReadings]; // Sets up an array for the circular array
int scratch1[numReadings]; // scratch array for smoothed data
static int contrscratch[precontrnumReadings]; // scratch array for pre-post contraction trace
int *pntcontrscratch = &contrscratch[0]; // Associated pointer
static int contrreadings[precontrnumReadings]; // Sets up array for the pre contraction circular array
int *pntcontrreadings = &contrreadings[precontrnumReadings]; // Associated pointer

int readIndex = 0;        // The index of the current reading
long total1 = 0;          // The running total
long total2 = 0;          // The running total
int avevalue1 = 1610;     // Average defining the baseline, start with 1650/1024 which is roughly half ref value
of Feather
int averagecom = 20;      // Average for threshold that defines contraction with baseline removed start
nominal
int average1;
int average2;
int average3;
int aboutzerovalue1 = 0; // The EMG value with baseline removed
int absvalue1 = 0;       // Absolute value of EMG signal
float sdval1;           // Standard deviation of baseline data
int maxForce;           // The maximum force generated during the MVC test

```

```

int forcethresh;
int potvalue;
float sdvalcom;

// LOOP COUNTING
int loopcount = 0;           // Loop counter must be an integer for Switch to work properly
uint32_t looplong = 0;      // Loop counter to count number of loops for contraction
int loopforave = 0;         // Loop counter to determine when to send sampled values to XBee

const uint8_t headerch = 0x7F; // This is the headercharacter used by the Dashboard to identify start of packet
const uint8_t headerchend = 0x7E; // This stops the receiver
int run;                     // Controls start or stop of loop
uint8_t errno;              // error number for sd card
char filename[25];          // Sets up a character array to enable filename to be incremented
float estsamplingRate;      // Frequency during baseline measurement (runtime for first 200 samples / 200)
long estsamplingInterval;   // Interval that includes the delay in case 1

float measuredvbat = analogRead(VBATPIN); // Variable for the battery voltage

float JointAnglemeas=analogRead(2);
float JointAngle;          // Measure the voltage from the potentiometer of the goniometer starting with zeros
int JointAnglePacket;     // Convert to int so that it can be put in packet
float JointAngleVelocity;
float JointAngleArray[30];
int JointAngleVelocityPacket; // Convert to int so that it can be put in packet

// ***** Assign pins *****

const int buttonPin = 10; // Stop and Start data collection ... active low hardware pin 5
// Since we are powered from BAT we need a pull up resistor (10k)

const int greenLED = 6; // General purpose green LED normally off
const int redLED = 13; // Red Led used for error status
const int bodySIDE = 5; // Slider switch to indicate left or right measurement
const int greenBUILTIN=8; // Green builtin led next to SD card
const int buzzer = 12;

String SIDE;

```

```

// YELLOW LED IS DIRECTLY WIRED TO INDUCTION COIL OUTPUT TO INDICATE CHARGING
// RED LARGE LED IS DIRECTLY WIRED TO THE POWER SUPPLY OF THE SYSTEM

int runbuttonstatus;      // Stop and Start data collection
int sidebuttonstatus;     // Left or right arm

// General public variables declarations for ADC XBEE LIMITED BY DASHBOARD *****

int value0=0; // Force AD0
int value1=0; // EMG1 AD1 Then rectified to create valuetry
int value2=0; // Goniometer AD2
int value3=0; // NOT CONNECTED
int value4=0; // AMG1 Z AXIS
int value5=0; // MVC POT

int valuetry=0;
float ZeroForce=0.0;

/* Note the A-REF pin is set to default 3.3 volts on Feather linked to supply which defines range 0 - 3.3V */

/* Setting up the XBee */

/* ***** COMMUNICATION ***** */
uint8_t payload_1[16];

XBee xbee_1 = XBee();
// Set up XBee 1 = Channel 1 DASHBOARD
XBeeResponse response_1 = XBeeResponse();
Rx16Response rx16_1 = Rx16Response();

// use this to reply to TX
uint8_t payload_response1[1];

// create an open request object targeting address 0x8888 on the Rx XBee with the given payload
Tx16Request tx_response1 = Tx16Request(0x8888, payload_response1, sizeof(payload_response1)); // Channel 1
DASHBOARD

```

```

// (overwrite the payload later to modify it)
// PAYLOAD SET UP

Tx16Request tx_1 = Tx16Request(0x8888, payload_1, sizeof(payload_1)); // To the Feather that relays to the
Dashboard Xbee

// state control
// state control
uint8_t state = STATE_ACTIVE;
// If you don't get a reply from the RX XB then the system hangs at this point

void flashLED(uint8_t LED, uint8_t times) {
    while(times > 0) {
        digitalWrite(redLED, HIGH);
        delay(100);
        digitalWrite(redLED, LOW);
        delay(100);

        times--;
    }
}

//***** CREATE THE SETUP FUNCTION
*****

void setup() {

    pinMode(13, OUTPUT);           // Sets up the Red LED pin next to USB port
    pinMode(13, LOW);
    pinMode(8, OUTPUT);           // Green LED on Feather next to SD Card
    pinMode(8, LOW);
    pinMode(6, OUTPUT);           // GREEN LARGE LED
    pinMode(12,OUTPUT);
    pinMode(12, LOW);             // Buzzer
    pinMode(10,INPUT_PULLUP);
    pinMode(5,INPUT_PULLUP);      // High = Right LOW = Left
}

```

```

i = 0;

Serial.begin(57600);
delay(100);

/* ONLY USE IF YOU MUST HAVE THE SERIAL PORT CONNECTION FOR THE APPLICATION TO FUNCTION
 * OTHERWISE THE PROGRAM WILL HALT WAITING FOR THE SERIAL TO BE CONNECTED
 */

{
#ifdef ESP8266
while (!Serial); // will pause Feather Adafruit Adalogger M0 until Serial Port opens
#endif
}

Serial1.begin(57600); // Starts the serial channel for XBee

xbee_1.setSerial(Serial1);
delay(100);

{
#ifdef ESP8266
while (!Serial1); // will pause Feather Adafruit Adalogger M0 until Xbee opens
#endif
}
Serial.println("XBEE Has responded");

// Get the battery voltage before changing AD resolution

measuredvbat = analogRead(VBATPIN);

// Serial.print("RAW Battery Voltage "); Serial.println(measuredvbat);

measuredvbat *= 2; // We divide by 2 in the hardware so multiply back
measuredvbat *= 3.3; // Multiply by our reference voltage

```

```

    measuredvbat /= 1024; // Convert to voltage

    Serial.print("Battery Voltage "); Serial.println(measuredvbat);

    analogReadResolution(16);

    digitalWrite(greenLED, HIGH);
    delay(500);
    digitalWrite(greenLED, LOW);

    delay(1000);

    /***** Set all the loop counters, elapsed time and arrays to zero *****/

    readIndex = 0;           // Just to make sure that the index in smoothing array starts at zero
    run = 0;                 // Sets the start condition of loop starter
    total1 = 0;
    total2 = 0;
    loopcount = 0;
    lastTime = micros();    // record the start time just before the end of "setup"

    loopcount = 0;
    looplong = 0;
    loopforave = 0;
    startTime = micros();
    runTime = 0;

    Serial.println("Starting to sample data:"); // Only on monitor
    Serial.println("Press Button to Start Sampling:");

    digitalWrite(greenLED, HIGH); // Green LED on lid to indicate starting to transmit
    digitalWrite(redLED, LOW); // We are going into the loop and green is HIGH red comes on when we save raw EMG

    /* ***** ZERO FORCE SENSOR ***** */

    value0 = analogRead(0);

```

```

ZeroForce = 42.67*log(value0) -360.9; // Make sure the force sensor is not loaded

} // END OF SETUP

// ***** THE LOOP FUNCTION *****
*****

void loop() {

// ***** Button Press to Start Loop *****

// THERE ARE TWO CONDITIONS. IF THE MVC IS TO BE SET THEN BUTTON MUST BE PRESSED FOR 5s
// Otherwise if the button is released before 5s the normal data collection process occurs.

while(digitalRead(buttonPin) == HIGH){
digitalWrite(LED_BUILTIN, HIGH);
digitalWrite(greenLED, HIGH);
digitalWrite(greenBUILTIN, HIGH);
runbuttonstatus = digitalRead(buttonPin);

    delay(300); // Flashing the LEDs
    digitalWrite(LED_BUILTIN, LOW);
digitalWrite(greenLED, LOW);
digitalWrite(greenBUILTIN, LOW);
delay(300); // Flashing the LEDs

}

// Button has been pressed so get the time
buttpresstime=millis();
Serial.print("Button Status: "); Serial.println(runbuttonstatus);
Serial.print("Button Press Time: "); Serial.println(buttpresstime);

//for (;;) {
while (digitalRead(buttonPin) == LOW){

```

```

Serial.print("Button Status in WHILE Loop: "); Serial.println(runbuttonstatus);

buttnowtime = millis();
buttduration = buttnowtime - buttpresstime;
Serial.print("Button Duration: "); Serial.println(buttduration);
delay(200);

if (buttduration >= 5000 && runbuttonstatus == HIGH) {
  Serial.println("Going to the POT ADJ ROUTINE: ");
  setMVCpot(); // Go to the set the pot function
}

} // End of button check WHILE loop

delay(2000); // Give time to fully let go

/*
#####
##### */
// ##### THIS IS THE START OF THE MAIN LOOP
#####
/*
#####
##### */

for(;;){ // Infinite loop flashing red LED when button pressed

  runbuttonstatus = digitalRead(buttonPin); // Stop and Start data collection status digitalRead(10)
  //Serial.print("Button Status: "); Serial.println(runbuttonstatus);

  // ***** This stops the acquisition on button press

  //if (runbuttonstatus == LOW) { // OLD DEVICE The button to stop run is on pin 10
  if (runbuttonstatus == LOW) { // The button to stop run is on pin 10
    //stopsendoutpackets(); // Stops the receiver

```

```

Flash_Led();
//logfile.println("Button stopped at start of loop"); // Print if the logfile is closed
//logfile.close();
digitalWrite(greenLED, LOW);
Serial.print("Button stopped at end of loop");

for(;;){                                     // Infinite loop flashing red LED when button pressed
    digitalWrite(redLED, LOW);

    Flash_Led();
}

}

// ***** Now the Acquisition Functions Start

digitalWrite(greenLED, HIGH);
digitalWrite(greenBUILTIN, HIGH);

if (loopcount <= 200) {
    //logfile.println(loopcount);
    baseline();                               // Collects baseline values as moving average
}

else if (loopcount == 201) {
    baselineaverage();                         // Calculates the average and sd of baseline
    //baselinedata();                          // Saves the baseline data to SD card and sets up Header for rest of data
}

else if (loopcount > 202) {
    loopcount = 203;                           // We reset loopcount to a fixed value now to stop it getting too large
                                                // Setting it above 202 makes sure we don't repeat the baseline next pass

    collect_force_data();                       // collects one sample of FORCE data

    Goniometer();                              // Get joint angle data

```

```

collect_emg_data();           // Collect data from analog channel once every loop

collect_amg_data();           // Collect data from analog channel once every loop

smoothanalogchan();           // Each time we go around the loop from now on we smooth the value
                               // with the previous (numReadings) reading. This gives us the rectified
                               // data array that can be sent out in real time by XBee with IMU data

sendoutpackets_Xbee1();       // Send out the payload to XBee receiver and dashboard system

buzzercheck();                // Sounds the buzzer if force exceeds 80% MVC

}

contraction=0;                // If the contraction was saved reset and keep zero if no contraction last time

loopcount++;                  // This loopcount is just used to determine if we are getting baseline data

loopforave++;                 // This integer loop counter is to determine when 10 values have been collected

                               // and their average needs to be sent out on XBee

delay(10);                    // Set sampling rate here to about 100 Hz if possible

} // End of the Main While Loop

//logfile.close();

digitalWrite(greenLED, LOW);

// End of sampling
}

/* ===== END OF THE LOOP ===== */

```

```

//
*****

// ***** FUNCTIONS
*****

//
*****

// ***** SETMVC POT()
*****

// ***** FUNCTION TO SET THE MVC POT
*****

//
*****

void setMVCpot() {
Serial.println("Starting the POT ADJUST ROUTINE");

// APPLY THE MVC FORCE, ADJUST THE POT
for(i=1; i=100; i++) {
value5 = analogRead(5);
mvcData[i] = value5;
// the led flashing delay determines duration of the time to collect force array
digitalWrite(LED_BUILTIN, HIGH);
digitalWrite(greenLED, HIGH);
digitalWrite(greenBUILTIN, HIGH);
delay(100); // FAST Flashing the LEDs
digitalWrite(LED_BUILTIN, LOW);
digitalWrite(greenLED, LOW);
digitalWrite(greenBUILTIN, LOW);
delay(100); // FAST Flashing the LEDs

// APPLY THE MVC FORCE IN A 20S TIME WINDOW GATHER FORCE VALUES INTO ARRAY
maxForce= max(maxForce,mvcData[i]);
return;
}

```

```

digitalWrite(LED_BUILTIN, LOW);
digitalWrite(greenLED, LOW);
digitalWrite(greenBUILTIN, LOW);

delay(2000); // Pause before adjusting the pot

for (i=1;i=200;i++) {
if (value5 >= 0.8*maxForce) {
    digitalWrite(buzzer, HIGH);
    delay(1000); // ADJUST THE POT TO TURN IT OFF
}
if (value5 < 0.8*maxForce) {
    digitalWrite(buzzer, LOW);
}
}

// NOW THE POT IS SET TO 80% MVC
}

// ***** BASELINE()
*****

// ***** FUNCTION TO COLLECT EMG BASELINE
*****/

//
*****

void baseline() {
    //Serial.println("In baseline measuring RAW EMG");

    value3 = analogRead(3);           // Read Channel 3 of Adalogger M0 ADC Raw EMG

    ave1.push(value3);               // Calls the average function from math/h
    // and the value is assigned to (value3) bucket
}
// End of function

```

```

// ***** BASELINEAVERAGE()
*****

// ***** FUNCTION TO CALCULATE THE MEAN AND STDEV OF
BASELINE DATA *****

//
*****

void baselineaverage() {
//Serial.println("In baseline average");

avevalue1 = ave1.mean();           // Calculates baseline value and assigns mean and SD

sdval1 = ave1.stddev();           // SD gives us a measure of the resting activity noise level

}
// End of Function

// ***** COLLECT_FORCE_DATA()
*****

// ***** FUNCTION TO COLLECT FORCE DATA EACH PASS OF THE LOOP
*****

//
*****

void collect_force_data(){

// THIS IS THE CALIBRATION APRIL 18 2023

//y = 42.672ln(x) - 360.9 with r^s of 0.98

value0= (analogRead(0));
valuetry = 42.67*log(value0) -360.9 - ZeroForce;

//valuetry = (analogRead(0)*0.0018 + 15.216) - ZeroForce; // Cal in Newtons

```

```

Serial.print("Force: "); Serial.print("\t"); Serial.println(value0);
} // End of function

// ***** COLLECT_EMG_DATA
*****

// ***** FUNCTION TO COLLECT EMG DATA EACH PASS OF THE LOOP
*****

//
*****

void collect_emg_data() { // Function to collect the emg data

    currentTime = millis(); // Update current time ready for timestamp
    timeElapsed = currentTime - startTime; // Time Stamp in microseconds as global in micros now
    procTime = currentTime - lastTime; // procTime gives a measure of sampling rate in micros
    lastTime = currentTime;
    runTime = timeElapsed; // Time Stamp in milliseconds

// Serial.print("Loop Time micros: "); Serial.println(procTime); // With serial port running this is about 2ms or 500Hz

    value3 = analogRead(3); // Read Channel 3 of Adalogger M0 ADC Raw EMG
    // NOTE: value3 is used by baseline() to get the average for the first
    // 200 passes before we get to this function. From here value1 is being read
    // just to collect the raw EMG from 201 onwards. This works OK as we don't
    // go back to baseline() but be aware. value3 is global.

    aboutzerovalue1 = value3 - (avevalue1); // Remove the offset We are leaving aboutzerovalue1 and
    avevalue1 as 1 not 3
/*
// Make the Raw EMG mV about the baseline
    aboutzerovalue1 *= 3.3; // Multiply by our reference voltage
    aboutzerovalue1 /= 65536; // Convert to voltage as we set AD converter to 16 bit
    aboutzerovalue1 *=1000; // To make the value mV
*/

//Serial.print("AD CH 3: ");

```

```

//Serial.println(aboutzerovalue1); // The raw value

}
// End of function

// ***** COLLECT_AMG_DATA *****
// *****
// ***** FUNCTION TO COLLECT EMG DATA EACH PASS OF THE LOOP *****
// *****
//
// *****

void collect_amg_data() { // Function to collect the emg data

    currentTime = micros(); // Update current time ready for timestamp
    timeElapsed = currentTime - startTime; // Time Stamp in microseconds as global in micros now
    procTime = currentTime - lastTime; // procTime gives a measure of sampling rate in micros
    lastTime = currentTime;
    runTime = timeElapsed; // Time Stamp in milliseconds

// Serial.print("Loop Time micros: "); Serial.println(procTime); // With serial port running this is about 2ms or 500Hz

    value4 = analogRead(4); // Read Channel 4 of Adalogger M0 ADC Raw Z AMG1
    //value5 = analogRead(5); // Read Channel 4 of Adalogger M0 ADC Raw Z AMG2
}
// End of function

// ***** SMOOTHANALOGCHAN() *****
// *****
// ***** FUNCTION FOR SMOOTHING IN REAL TIME *****
// *****/
//
// *****

/* This smoothing function enables us to get a smoothed value to identify and keep running a contraction
   An alternative approach would be to use the rectified signal and set an amplitude threshold on the rectified signal.
*/

```

```

void smoothanalogchan() {

    // We are using the milli second elapsed time count

    // First we will create a scratch array with (numReadings) of raw EMG with baseline removed (aboutzerovalue1)
    // We also rectify by taking the abs value
    // We nominally set numReadings to 10 which is the data block we are averaging
    // First few times around the loop creates a false average (~10ms)

    i = 0;
    for (i = 0; i < numReadings - 1; i++) {          // Shift all the readings up the array by 1
        readings1[i] = scratch1[i + 1];             // The nth element of scratch is n-1th of readings
    }

    // Put the new value at the bottom of the readings1 array

    readings1[numReadings - 1] = abs(aboutzerovalue1); // At this point i is equal to 1-numreadings so we are adding
new readings
                                                    // to bottom of array readings1[]

    i = 0;                                          // Now reset i

    // Add up all the readings in the scratch array
    for (i = 0; i < numReadings; i++) {
        total1 = (total1 + readings1[i]);
    }

    // total1 is now the sum of readings up to i readings

    average1 = total1 / numReadings;

    /*
    // To convert Rectified EMG signal to mV
        average1 *= 3.3; // Multiply by our reference voltage
        average1 /= 65536; // Convert to voltage as we set AD converter to 16 bit
        average1 *=1000; // To make the value mV
    */
}

```

```

*/
//Serial.print("Rect Values: ");
Serial.print("EMG Averaged"); Serial.print("\t");Serial.println(average1);

//logfile.print("Smoothed Rectified EMG values: ");logfile.print(",");logfile.println(average1);

total1 = 0; // Reset total1
i = 0;

for (i = 0; i < numReadings; i++) { // Set scratch up for next time round loop

    scratch1[i] = readings1[i]; // The nth element of scratch is now nth of new readings arrays are the
same now
}

//return;
}
// End of function

// ***** SENDOUTPACKETS() TO DASHBOARD
*****
// ***** FUNCTION TO TRANSMIT XBEE DATA
*****
//
*****

void sendoutpackets_Xbee1() {
Serial.println("In sendout packets");
digitalWrite(greenLED, HIGH);

// Note the rectified EMG values are averaged but the rest are not

// Make sure your Tx and Rx XBees are in API=1 or dashboard will not work due to spurious characters in header.

```

```

// NOTE: There are four special characters used by XBee. They are 7E 7D 0x11 and 0x13. So when you send for
example 0x11 the receiving XBee
// will add a flag (7D) and then XOR the value with 0x20 so what you see transmitted appears to be 7D 31
// To resolve this when you have received the data you will need code to look for the 7D flag and then OR the byte
after it to revert the
// value back to what was transmitted. So... 0x11 is seen on the Rx side as 7D 31 . When you see the 7D ignore that
flag and then XOR the next
// byte with 0x20 and you will get back to 0x11 again as the inverse of XOR is XOR. The operator for XOR is ^ in c
and in python.

```

```

//value0 = analogRead(0); // FORCE
//value1 = analogRead(1); // EMG But we want to send the averaged data not raw
//value2 = analogRead(2); // Goniometer
//value3 = analogRead(3); // NOT USED
//value4 = analogRead(4); // AMG1
//value5 = analogRead(5); // MVC POT

```

```

//Serial.print("FORCE:");Serial.println(value0);
//Serial.print("EMG1 RAW:");Serial.println(value1);
//Serial.print("GONIOMETER ANGLE:");Serial.println(value2);
//Serial.println(average1); // The EMG rectified signal
//Serial.print("AMG1:");Serial.println(value4);
//Serial.print("MVC POT:");Serial.println(value5);

```

```

// convert the timestamp (long)

```

```

payload_1[ 0] = (headerch   ) & 0xff; // The header character used by Dashboard to identify start of
packet

```

```

payload_1[ 1] = (headerch   ) & 0xff;
payload_1[ 2] = (runTime >> 24) & 0xff;
payload_1[ 3] = (runTime >> 16) & 0xff;
payload_1[ 4] = (runTime >> 8) & 0xff;
payload_1[ 5] = (runTime   ) & 0xff;

```

```

payload_1[ 6] = (average1 >> 8) & 0xff; // EMG (H byte) (would normally be EMG) now in mV
payload_1[ 7] = (average1   ) & 0xff; // EMG (L byte)
payload_1[ 8] = (valuetry >> 8) & 0xff; // Force Sensor Calibrated Value (H byte)

```

```

payload_1[ 9] = (value1 >> 8) & 0xff; // Force Sensor Calibrated Value (L byte)
payload_1[10] = (value2 >> 8) & 0xff; // Elbow Angle (H byte)
payload_1[11] = (value2 >> 0) & 0xff; // Elbow Angle (L byte)
payload_1[12] = (0x0 >> 8) & 0xff; // blank not sending AMG or MVC pot
payload_1[13] = (0x0 >> 0) & 0xff; // blank
payload_1[14] = (0x0 >> 8) & 0xff; // blank
payload_1[15] = (0x0 >> 0) & 0xff; // blank

// send it along
xbee_1.send(tx_1);

digitalWrite(greenLED, LOW);
//return;

} // End of Function

//
*****
// ***** FUNCTION TO READ THE POTENTIOMETER GONIOMETER *****
//
*****

void Goniometer() {
//Serial.println("In goniometer");

// Establish Left or Right Arm

sidebuttonstatus=digitalRead(bodySIDE);

// Calibration April 1 2023
// LEFT: Degrees = -0.0043* Computer Units + 141.62

// RIGHT: Degrees = 0.0038* Computer Units - 124.6

```

```

if (sidebuttonstatus == LOW) {
  SIDE = "LEFT";
  JointAngle = ((analogRead(2))*-0.0043 + 141.62); // The value is sent to XBee
}
else
{
  SIDE = "RIGHT";
  JointAngle = ((analogRead(2))*0.0038 - 124.6); // The value is sent to XBee
}
//Serial.print("Which Body Side? "); Serial.println(SIDE);
value2= JointAngle; // Comment out to get the raw values for calibration
//value2=analogRead(2); // Use this to get raw values for calibration then comment out
Serial.print("Joint Angle"); Serial.print("\t"); Serial.println(value2);

// ***** To measure the joint angle from goniometer *****

  JointAnglemeas = analogRead(2); // Measure the voltage from the potentiometer of the goniometer

  // Measure the goniometer voltage and provide value in volts

  JointAnglemeas *= 3.3; // Multiply by our reference volatage *= and /= is shorthand way to multiply/divide one
variable by another
  JointAnglemeas /= 1024; // Convert to voltage

/* OLD CALIBRATION DAN's DEVICE
// CHECK THIS CALIBRATION
  JointAngle = 0.0787*JointAnglemeas*1000 - 52.418; // Convert volts to degrees degrees where 0 degrees = 180
(clinical protocol)
  JointAnglePacket = JointAngle; // Convert to integer to transmit
*/

ii++; // increments each time we go around the main while loop

// ***** To calculate joint angle velocity *****

if (ii<30) {
  JointAngleArray[ii]=JointAngle;

```

```

}

else {
  ii=0;
}

if (ii==29) {

  currentTimegon = millis();          // Current time in millisecs since start of program
  runTimegon = currentTimegon - lastTimegon;          // runTime gives a measure of sampling rate in micros
  lastTimegon = currentTimegon;

  JointAngleVelocity = (abs(JointAngleArray[29] - JointAngleArray[1])/runTimegon)*1000000; // To convert degrees
per micor second to per second. NOTE UNSIGNED INTEGER FOR THE ANGLE MEASURES
  JointAngleVelocityPacket = JointAngleVelocity;

  //Serial.print("Joint Angle Goniometer 1: "); Serial.print(JointAngleArray[29]);Serial.print("  Joint Angle Goniometer
2: "); Serial.print(JointAngleArray[1]);Serial.print("  Joint Angle Packet  ");
  Serial.print(JointAnglePacket);Serial.print("  Joint Angle Velocity Packet Goniometer:  ");
  Serial.print(JointAngleVelocityPacket);Serial.print("  Elapsed Time:  "); Serial.print(runTimegon);Serial.print("
Counter:  "); Serial.println(ii);
}

//          return;
}

//
*****
// ***** FUNCTION TO SOUND BUZZER IF FORCE EXCEED 80 MVC*****
*****
//
*****

void buzzercheck() {

```

```

// The pot voltage on A5 is the threshold for the buzzer
value5 = analogRead(5); // Pot value
value0 = analogRead(0); // Force value
forcethresh = k*potvalue;
// We have cross-calibrated by determining k the force value based on the pot value forcethresh = potvalue*k
if (value5>= forcethresh) {
  digitalWrite(buzzer, HIGH);
}

// The participant should be asked to ease of their applied force is the buzzer sounds and increase
// force if it has not sounded. They can try and hold in an on-off-on condition.
}

//
*****
// ***** FUNCTION TO FLASH RED LED TO INDICATE ERROR OR TERMINATION OF
PROGRAM *****
//
*****

void Flash_Led() {
  digitalWrite(redLED, HIGH);
  delay(200);
  digitalWrite(redLED, LOW);
  delay(200);
}
// End of function

//
*****
// ***** SD CARD ERROR STATUS
*****
//
*****

// blink out an error code for SD card status

```

```

void error(uint8_t errno) {
    while (1) {
        uint8_t i;
        for (i = 0; i < errno; i++) {
            digitalWrite(13, HIGH);
            delay(150);
            digitalWrite(13, LOW);
            delay(150);
        }
        for (i = errno; i < 10; i++) {
            delay(100);
        }
    }
}
//
*****
// ***** END OF FUNCTIONS SECTION *****
*****
//
*****

```

Appendix 5. MATLAB Code for Power Spectra

```

%%%%%%%%%% EMG CALIBRATION" %%%%%%%%%%%

```

```

% *****

```

```

% READING THE DATA AND SETTING UP THE ARRAYS

```

```

% *****

```

```

% Clear the Command Window

```

```

clc;

```

```

clearvars;

```

```

sampinterval = 1258.1;% this value is taken from the runtime vs sample number plot in micros

```

```

sampfr = 1000000/1258.1;
Fnyq = sampfr/2; % The Nyquist frequency is half sampling frequency
% https://en.wikipedia.org/wiki/Nyquist\_frequency

[stroke_input_data,sourcepath] = uigetfile('*.xlsx');
stroke_input_data = strcat(sourcepath,stroke_input_data);
output_dir = sourcepath; % Used for outputting the figures at the end

%Read data into table from Excel
dataTable = readtable(stroke_input_data,'RANGE','A:D');

%dataTable = dataTable(1:end,:); % Removing header info

muscle = "Biceps Dominant Arm";

% We fill a 1 dimensional array for each column

TimeofSampleDEL = dataTable(1:end,4); % Reads the values from dataTable into the Time Stamp vector

valRawEmg = dataTable(1:end,2); % Reads the values from dataTable into the Delsys EMG vector

TimeofSampleDEL = table2array(TimeofSampleDEL(1:end,1));
TimeofSampleDEL = TimeofSampleDEL(~isnan(TimeofSampleDEL));

valRawEmgvec = table2array(valRawEmg);
valRawEmgvec = valRawEmgvec(~isnan(valRawEmgvec));

% *****
% OBTAINING THE RECTIFIED VALUES OF EMG
% *****

```

```
absemg = abs(valRawEmgvec-mean(valRawEmgvec)); % we subtract the mean in case it is not perfectly  
at zero
```

```
valRawEmg = valRawEmgvec-mean(valRawEmgvec);
```

```
% We will now apply a low pass Butterworth 2nd order filter
```

```
% cutoff frequency fco to obtain envelope
```

```
fco = 1; % Edit to setup the cutoff frequency in Hz depending on detail required Change this for AMG  
from 5 to 1 Hz
```

```
% in the envelope trace
```

```
% We apply an adjustment factor of 25% to correct for 2nd order Butterworth
```

```
% as the filter is applied twice, forward and backward.
```

```
[b,a]=butter(2,fco*1.0/Fnyq); % change the cut off frequency as necessary to produce outline of EMG  
envelope
```

```
zEMG=filtfilt(b,a,absemg); % so zEMG is an array of the filtered data
```

```
%% ***** NOTE ON FUNCTION TO TRIM ZEROS *****
```

```
% We created a custom function called trimzeros so that we removed trailing zeros and made the two  
% vectors the same length (time and EMG).
```

```
% You need to have this function called trimzeros.m in the same folder that you are running this code  
from.
```

```
% The is the code for the function:
```

```
% function [ varargout ] = trimzeros( varargin )
```

```
% %TRIMZEROS Removes trailing "zero" datapoints from the input vectors
```

```
% % At the end of the `emg` array are expected to be a series of 0.0 values which
```

```
% % cause problems for data analysis. This function will remove those zeros from the
```

```

%% input columns. Call this function using either:
%% >> [ t, emg ] = trimzeros(t, emg);
%% or:
%% >> [ t, emg, force ] = trimzeros(t, emg, force);
%
%   if (nargin < 2) || (nargin > 3)
%       error('Please call this function with 2 or 3 arguments in the order: t, emg, force!');
%   end
%
%   if nargin ~= narginout
%       error('Please call this function with the same number of outputs as inputs!');
%   end
%
%   % find the first ending 0
%   i = length(varargin{2});
%   for k = i:-1:1
%       if varargin{2}(k) ~= 0
%           i = k;
%           break;
%       end
%   end
%
%   % found the first starting 0, it's at index: i + 1

%% *****

% *****

%% OBTAIN THE FREQUENCY SPECTRUM FOR DELSYS USING FFT ANALYSIS STORE AS JPEG
% *****

%% POWER SPECTRUM

```

```
%%%%%%%%%% POWER SPECTRUM OF SIGNAL
```

```
%%%%%%%%%%
```

```
L = length(valRawEmgvec);
```

```
f = sampfr*(0:(L/2))/L;
```

```
Y = fft(valRawEmgvec);
```

```
P2 = abs(Y/L);
```

```
P1 = P2(1:L/2+1);
```

```
P1(2:end-1) = 2*P1(2:end-1);
```

```
P1MoveAve = movmean(P1,25); % Moving mean for a window of 20 points (out of over 4300)
```

```
f=f.'; % Make into vertical vector
```

```
maxplotfr = 100; % We only need 10-100 Hz range for AMG
```

```
fmax = f(f<maxplotfr);
```

```
maxloc=length(fmax);
```

```
% We need to avoid the DC level and so consider eliminating frequencies lower than
```

```
% a frequency of 10Hz
```

```
fmin = f(f<5); % Cut off below 5 Hz
```

```
minloc=length(fmin);
```

```
figure(1)
```

```
plot(f(minloc:maxloc,1),P1MoveAve(minloc:maxloc,1))
```

```
title("Single-Sided Amplitude Spectrum of S(t)")
```

```
xlabel("f (Hz)")
```

```
ylabel("|P1(f)|")
```

```
axis ([5 100 0 inf])
```

```
% %%%%%%%%% Save figures %%%%%%%%%
```

```
saveas(figure(1), strcat(output_dir, 'Power Spectrum DELSYS EMG.jpg'));
```

Appendix 6. MATLAB Code for Rectified Data

```
%sampfr = 2000;
```

```
sampfr = 1123; % Obtain this from plotting elapsed time vs number of samples
```

```
Fnyq = sampfr/2; % The Nyquist frequency is half sampling frequency
```

```
fn = Fnyq;
```

```
[passive_stretch_input_data,sourcepath] = uigetfile('*.xlsx');
```

```
passive_stretch_input_data = strcat(sourcepath,passive_stretch_input_data);
```

```
output_dir = sourcepath; % Need for output tables
```

```
%Read data into table from Excel
```

```
dataTable = readtable(passive_stretch_input_data, 'RANGE', 'A:AZ');
```

```
% NOTE: REMOVE ANY TRAILING ZEROS AT END OF XLSX DATA FILE BEFORE PROCESSING
```

```
temg = dataTable{50:end,1};
```

```
valemg =dataTable{50:end,3};
```

```
valamg1 =dataTable{50:end,4};
```

```
valamg2 =dataTable{50:end,5};
```

```
temg=temg/1000000; % Convert time from microseconds to seconds
```

```
% Firstly obtain the absolute values of the raw data
```

```
absemg = abs(valemg-mean(valemg)); % we subtract the mean in case it is not perfectly at zero
```

```
absamg1 = abs(valamg1-mean(valamg1));
```

```
absamg2 = abs(valamg2-mean(valamg2));
```

```
% We will now apply a low pass Butterworth 2nd order filter
% cutoff frequency fco to obtain envelope
```

```
%% Filter Characteristics for EMG
```

```
fc1=5;% cut off frequency
order = 6; %6th order filter, high pass
[b1 a1]=butter(order,(fc1/fn),'low');
```

```
fc2=.05;% cut off frequency
order = 6; %6th order filter, high pass
[b2 a2]=butter(order,(fc2/fn),'high');
```

```
%filtered EMG data
```

```
zemg=filfilt(b2,a2,absemg);
zemg=filfilt(b1,a1,absemg);
```

```
%% Filter Characteristics for AMG
```

```
fc3=2;% cut off frequency
order = 6; %6th order filter, high pass
[b3 a3]=butter(order,(fc3/fn),'low');
```

```
fc4=.1;% cut off frequency
order = 6; %6th order filter, high pass
[b4 a4]=butter(order,(fc4/fn),'high');
```

```
%filtered AMG data
```

```
zamg1=filfilt(b4,a4,absamg1);
zamg1=filfilt(b3,a3,absamg1);
```

```
zamg2=filfilt(b4,a4,absamg2);
zamg2=filfilt(b3,a3,absamg2);
```

```
zamgbase1=mean(zamg1);
```

```
zamgbase2=mean(zamg2);
```

```
zemgbase=mean(zemg);
```

```
zemg=zemg-zemgbase;
```

```
zamg1=zamg1-zamgbase1;
```

```
zamg2=zamg2-zamgbase2;
```

```
figure(1)
```

```
subplot(3,1,1)
```

```
hold on
```

```
p=plot(temg,absemg,'-b');
```

```
title('Raw EMG vs Time:');
```

```
xlabel('Time (s)'); ylabel('EMG (V)');
```

```
subplot(3,1,2)
```

```
hold on
```

```
plot(temg,absamg1,'-g');
```

```
title('Raw AMG1 vs Time:');
```

```
grid on;
```

```
xlabel('Time s '); ylabel('Filtered EMG Amplitude')
```

```
axis auto;
```

```
subplot(3,1,3)
```

```
hold on
```

```

plot(temg,absamg2,'-.g');

title('Raw AMG2 vs Time:');

grid on;

xlabel('Time s '); ylabel('Filtered EMG2 Amplitude')
axis auto;

hold off

figure (2)
subplot(3,1,1)
hold on
plot(temg,zemg,'-r');

title('Rectified EMG vs Time s:');

grid on;

xlabel('Time s'); ylabel('Rectified EMG Amplitude')

subplot(3,1,2)

plot(temg,zamg1,'-.b'); % Filtered High and Low Pass

title('Rectified AMG1');

grid on;

xlabel('Time s '); ylabel('Rectified AMG1 Amplitude')
axis auto;

```

```

subplot(3,1,3)

plot(temg,zamg2,'-b'); % Filtered High and Low Pass

title('Rectified AMG2 vs Time:');

grid on;

xlabel('Time s '); ylabel('Rectified AMG2 Amplitude')
axis auto;
hold off

saveas(figure(1), strcat(sourcepath,'Raw EMG and AMG1,2 vs Time.jpg'));
saveas(figure(2), strcat(sourcepath,'Filtered EMG and AMG1,2 vs Time.jpg'));

```

Appendix 7. MATLAB Code for Signal-to-noise Ratio

```

sampinterval = 1330.7 % this value is taken from the runtime vs sample number plot in micros
sampfr = 1000000/1330.7;
Fnyq = sampfr/2; % The Nyquist frequency is half sampling frequency
% https://en.wikipedia.org/wiki/Nyquist\_frequency

[stroke_input_data,sourcepath] = uigetfile('*.*xlsx');
stroke_input_data = strcat(sourcepath,stroke_input_data);
output_dir = sourcepath; % Used for outputting the figures at the end

%Read data into table from Excel
dataTable = readtable(stroke_input_data,'RANGE','A:D');

%dataTable = dataTable(1:end,:); % Removing header info

```

```

muscle = "Biceps Dominant Arm";

TimeofSampleDEL = dataTable(1:end,4); % Reads the values from dataTable into the Time Stamp vector

valRawEmg = dataTable(1:end,2); % Reads the values from dataTable into the Delsys EMG vector

TimeofSampleDEL = table2array(TimeofSampleDEL(1:end,1));
TimeofSampleDEL = TimeofSampleDEL(~isnan(TimeofSampleDEL));

valRawEmgvec = table2array(valRawEmg);
valRawEmgvec = valRawEmgvec(~isnan(valRawEmgvec));

% *****
% OBTAINING THE RECTIFIED VALUES OF EMG
% *****

absemg = abs(valRawEmgvec-mean(valRawEmgvec)); % we subtract the mean in case it is not perfectly
at zero

valRawEmg = valRawEmgvec-mean(valRawEmgvec);

% We will now apply a low pass Butterworth 2nd order filter
% cutoff frequency fco to obtain envelope

fco = 5; % Edit to setup the cutoff frequency in Hz depending on detail required
% in the envelope trace

% We apply an adjustment factor of 25% to correct for 2nd order Butterworth
% as the filter is applied twice, forward and backward.

```

```
[b,a]=butter(2,fco*1.0/Fnyq); % change the cut off frequency as necessary to produce outline of EMG envelope
```

```
zEMG=filtfilt(b,a,absemg); % so zEMG is an array of the filtered data
```

```
rms_zEMG_baseline = rms(zEMG(200:5000,1));
```

```
rms_zEMG_contraction = rms(zEMG(5001:end,1));
```

```
signal_to_noise_ratio = (rms_zEMG_contraction)/(rms_zEMG_baseline); % Result in dB
```

```
signal_to_noise_dB = 20*log10(signal_to_noise_ratio); %power of the signal
```

```
%% ***** NOTE ON FUNCTION TO TRIM ZEROS *****
```

```
% We created a custom function called trimzeros so that we removed trailing zeros and made the two  
% vectors the same length (time and EMG).
```

```
% You need to have this function called trimzeros.m in the same folder that you are running this code  
from.
```

```
% The is the code for the function:
```

```
% function [ varargout ] = trimzeros( varargin )
```

```
% %TRIMZEROS Removes trailing "zero" datapoints from the input vectors
```

```
% % At the end of the `emg` array are expected to be a series of 0.0 values which
```

```
% % cause problems for data analysis. This function will remove those zeros from the
```

```
% % input columns. Call this function using either:
```

```
% % >> [ t, emg ] = trimzeros(t, emg);
```

```
% % or:
```

```
% % >> [ t, emg, force ] = trimzeros(t, emg, force);
```

```
%
```

```
% if (nargin < 2) || (nargin > 3)
```

```
% error('Please call this function with 2 or 3 arguments in the order: t, emg, force!');
```

```
% end
```

```
%
```

```
% if nargin ~= nargout
```

```

%           error('Please call this function with the same number of outputs as inputs!');
%   end
%
%   % find the first ending 0
%   i = length(varargin{2});
%   for k = i:-1:1
%       if varargin{2}(k) ~= 0
%           i = k;
%           break;
%       end
%   end
%
%   end
%
%   % found the first starting 0, it's at index: i + 1

%% *****

% *****

%% OBTAIN THE FREQUENCY SPECTRUM FOR DELSYS USING FFT ANALYSIS STORE AS JPEG
% *****

%% POWER SPECTRUM

%%%%%%%%%% POWER SPECTRUM OF SIGNAL
%%%%%%%%%%

L = length(valRawEmgvec);
f = sampfr*(0:(L/2))/L;
Y = fft(valRawEmgvec);
P2 = abs(Y/L);
P1 = P2(1:L/2+1);
P1(2:end-1) = 2*P1(2:end-1);

```

